12-2018

Understanding and Predicting Nematode Damage on Soybean using Spatially Weighted Analysis

Barry Boney
University of Arkansas, Fayetteville

Understanding and Predicting Nematode Damage on Soybean using Spatially Weighted Analysis

A thesis submitted in partial fulfillment
of the requirements for the degree of
Master of Science in Plant Pathology

by

Barry Boney
University of Arkansas at Monticello
Bachelor of Business Administration in Accounting, 2014
University of Arkansas at Monticello
Bachelor of Science in Agriculture, 2016

December 2018
University of Arkansas

This thesis is approved for recommendation to the Graduate Council.

_____
Terry Spurlock, Ph.D.
Thesis Director

_____
John Rupe, Ph.D.
Committee Member

_____
Terry Griffin, Ph.D.
Committee Member

_____
Terry Kirkpatrick, Ph.D.
Committee Member

Abstract

Aerial imagery offers great potential as a predictive scouting method and could allow growers to better understand crop performance over time. Evidence suggests that the seed treatments fluopyram and abamectin result in decreased reproduction and root galling by *Meloidogyne incognita*, but yield protection in fields with higher or different nematode pressure is unclear. The objective of this work was to determine the efficacy of these seed treatments compared to 1,3-dichloropropene (1,3-D) applied site-specifically and then predict where these might best be applied to other fields. In a soybean field infested with *M. incognita*, apparent electrical conductivity was highly correlated with sand content, and treatments were applied the total length of the field, across two soil textural zones. Fluopyram and abamectin seed treatments were compared to seeds without a nematicide seed treatment (control) and seeds without a nematicide seed treatment but planted within 1,3-D treated areas. Historical satellite images, normalized difference vegetation index (NDVI) and near infrared (NIR), from Sentinel-2 at 10-meter resolutions were compared to yield to determine if correlations with crop performance were evident over time. In 2016, treatment yields were not significant by zone, but yield was greater in the 1,3-D strips than all other treatments, while fluopyram and abamectin were not different than strips lacking nematicide (P=0.001). In 2017, 1,3-D strips had higher yield than all other treatments in both zones except for residual 1,3-D treatments that were applied in 2016 in Zone 2 (P=0.01). Fluopyram, abamectin, and the control treatments were not significantly different in Zone 1. Treatment effects for all treatments differed between the two textural zones (P=0.01). The distribution of *M. incognita* at harvest was uniformly distributed by treatments (P=0.08), suggesting that 1,3-D could be used as a two-year control and would be economically beneficial as a whole-field application when a susceptible soybean is planted. In 2017, NDVI and NIR observations were clustered, meaning that data are significantly positive for local spatial

autocorrelation (P<0.05). Seven surrounding fields were further observed and 100% of analyses were clustered using NDVI and NIR images from multiple snapshots throughout the 2017 growing season. Initial analyses indicated correlations with yield, suggesting opportunities for prediction and that site-specific application of 1,3-D in these fields might be beneficial when susceptible soybean varieties are planted.

Acknowledgements

This work would not have been possible without the financial support of the Arkansas Soybean Promotion Board and the USDA CARE program. I am especially indebted to my major advisor Dr. Terry Spurlock, who has been supportive of my career goals and who worked actively to provide me with the experience and academia needed to pursue those goals. He was always available whenever I ran into a problem or had a question about my research, and he consistently steered me in the right the direction. As my teacher and mentor, he has taught me more than I could ever give him credit for here. He has shown me, by his example, what a good scientist (and person) should be.

I am grateful for all of those that work at the Southeast Research and Extension Center (SEREC) whom I have had the pleasure to work with during this and other projects, which includes but is not limited to Mandy Tolbert, Robert Hoyle, Justin Bailey, Ben Fish, Kristina Cook, and Sydney Pennington. Without their participation and input, this research could not have been successfully conducted. Also, I would like to thank each of the members on my Thesis Committee. They have provided me with extensive personal and professional guidance by improving my knowledge of both research and science.

Finally, I wish to thank my loving and supportive wife, Kaley, for providing me with unfailing support and continuous encouragement throughout the duration of this study and through the process of researching and writing this thesis, as well as in my personal life. Nobody has been more supportive and uplifting in the pursuit of this project than she has.

This accomplishment would not have been possible without all these people.

Thank you.

Table of Contents

Chapter 1: Literature Review

Soybean Production in Arkansas

Soybean was first introduced in Arkansas during the 1920's and gained popularity among growers around the mid-1900s. From 1960 to 1979, harvested hectares increased dramatically, with soybean peaking in Arkansas during the 1979 growing season at 2.08 million hectares (Coats & Ashlock 2000). Although somewhat lower than in 1979, soybean are still grown on more hectares today than any other production crop in Arkansas, and account for fifty-one percent of all principle crops planted in Arkansas; with 1.27 million hectares grown in 2016 (Arkansas Acreage Report 2016).

Common Tillage Practices

Tillage practices have intensely shifted from conventional tillage to conservation tillage in the past three decades. Regardless of the tillage system used, the goal on the farm level is to promote adequate root and crop development that results in profitable production (Huitink & Tacker 2000). Conservation tillage (CT) is a production system where at least 30% of crop residue remains on the soil surface (Evans et al. 2000) and varies with specific field operations that may include stubble mulch tillage, reduced tillage, or no-till systems. Furthermore, improved planting equipment and effective herbicides make CT economical and practical for soybean production (Kulkarni 2002). Stale seedbeds are an aspect of a reduced tillage system, that save time, conserve moisture, and can result in higher soybean yields (Kulkarni 2002). Implementing stale seedbeds in a tillage system will allow growers to re-form old seedbeds in the fall and let them settle (undisturbed) over the winter to "mellow" clods (Spradley 2005). Herbicides are applied in early spring to kill winter vegetation, and then the tops of the seedbeds are flattened and (or) packed

before planting. Stale seedbeds are most effective in clay soils that often form clods after being tilled, resulting in increased planting difficulties (Huitink & Tacker 2000).

No-till systems (NT) are commonly recommended for increasing soil organic matter and decreasing soil erosion, but they require proper use of herbicides and heavy-duty no-till seeding equipment that are long-term investments for growers (Huitink & Tacker 2000). In many cases, growers are hesitant to switch to NT from CT because of the expense involved in acquiring more precise equipment, which can be substantially higher. Because much of the land that is farmed in Arkansas is leased, growers may be hesitant to make the investments that are required, because of the uncertainty of access to the land from season to season. Many growers are given a verbal lease agreement that could change anytime, based on discretions of the land owner.

Fertilization Practices

As with other legumes, soybean roots are associated symbiotically with the bacteria *Bradyrhizobium japonicum*. The soybean plant supplies nutrients and energy for the bacteria to fix nitrogen in nodules, which in turn is beneficial for the plant. Since soybean plants have a high demand for nitrogen and most of the nitrogen is provided via biological fixation, producers should evaluate plants to determine if they are activity fixing nitrogen. In fields with poor nodulation, soybean seeds should be inoculated with *B. japonicum*, especially where soybean have not been grown in the past three to five years (Slaton et al. 2013). In row crops, phosphorous and potassium are generally the most yield limiting nutrients and are normally applied before planting (Spradley 2005). Micronutrient deficiencies are rare but can occur in soils with low cation exchange capacity (CEC). Every 100 kg of soybean requires 1.5 kg of phosphorus (P_2O_5), and 6.2 kg of potassium (K_2O.), which is 150% to 300% more per bushel than that of other row crops, such as corn or rice (Slaton et al. 2013).

The University of Arkansas Division of Agriculture recommends that soil samples (collected at a ten-centimeter depth) should be used to guide fertilizer inputs. Samples should be collected following the same crop in a rotation and at approximately the same time of year; soil test results should be calculated based on an anticipated average field yield of 3362.55 kg hectare^{-1} (Slaton et al. 2013). Potassium-depleted soils, which are mostly silt loam or sandy soils, commonly contain 0-90 ppm of potassium. These soils should be amended with an additional application of 135 to 179 kg of K_2O hectare^{-1} (Slaton et al. 2013). The most common source of potassium used in Arkansas is muriate of potash (0-0-60). Growers generally apply potassium during the fall or early spring, but before seedbeds are re-formed in order to incorporate the nutrients into the soils. Phosphorous is recommended by the University of Arkansas Division of Agriculture when soil test levels are ≤ 26 ppm. Phosphorus is generally not expected to increase soybean yields but is applied to replace the phosphorus that was removed with the harvested grain (Slaton et al. 2013). The two most commonly used fertilizers supplying phosphorus in Arkansas are triple superphosphate (0-46-0) and diammonium phosphate (18-46-0). Poultry liter can also be applied as a phosphorus and potassium source, but nutrient contents can vary. So, every load of litter that is applied should be subsampled individually. Slaton et al. (2013) suggests that spring fertilizer applications may be best on soils soil test levels below ≤ 60 ppm of potassium and ≤ 15 ppm of phosphorus, because as soil test index values decrease, the soil's capacity to rapidly fix nutrients into unavailable forms increase.

Pest Management

Insects

The University of Arkansas Division of Agriculture reports research-based economic threshold levels for most problematic insects, and control applications that should be triggered when threshold levels are reached (on a field by field basis). Pests in Arkansas soybean are extremely variable from year to year, due to environmental conditions (Lorenz et al. 2000). Agricultural practices also have a huge impact on the occurrence of pests in soybean. Row width, planting date, tillage systems, adjacent crops, and soybean monoculture all can impact pest incidence and pressure. Sweep nets and drop cloths are the most efficient methods for determining insect thresholds in soybean (Zehnder 2014).

The most common insect pests of soybean grown in Arkansas are *Helicoverpa zea* (corn earworm*), Halyomorpha halys* (brown mamorated stink bug), *Chinavia hilaris* (green stink bug), *Nezara viridula* (southern green stink bug), *Piezodorus guildinii* (redbanded stink bug), and *Pseudoplusia includens* (soybean looper). *Helicoverpa zea* is considered the most devastating insect to soybean plants in Arkansas, because larvae feed on pods and seeds, directly decreasing yield. This pest also has an extremely wide host range, resulting in exponential opportunities throughout the season for reproduction to occur. Although young larvae do not cause significant injury, the last two instars account for 96% of the damage (Spradley 2005). According to Lorenz et al. (2000), fields that do not have canopy closure by the time soybean plants start to bloom are more susceptible to *H. zea*. An "Early Soybean Production System," which became popular in the Mid-South several years ago involves planting MG III and IV soybean in late March or early April to enhance canopy closure before the first *H. zea* flight, which should reduce the number of insecticide applications (Lorenz et al. 2000).

Weeds

Weeds in soybean production must be properly identified to get effective control. The most common weeds in Arkansas soybean are *Amaranthus palmeri* (palmer amaranth), *Echinochloa crus-galli* (barnyard grass), *Ipomoea spp.* (morningglory species), *Digitaria sanguinalis* (hairy crabgrass), *Urochloa platyphylla* (broadleaf signalgrass), *Euphorbia maculate* (spotted sandmat), *Sesbania herbacea* (hemp sesbania), and *Lolium multiflorum* (perennial ryegrass). Herbicide-resistant weeds are currently the most crucial issue in soybean production systems. *Amaranthus palmeri* is the number one herbicide-resistant weed for growers to manage. Populations of *A. palmeri* at 5, 10, 20, and 40 weeds per 6 row meters reduced soybean yield by 26%, 40%, 64%, and 66%, respectively (Baldwin et al. 2000). One female *A. palmeri* plant can contain up to 1.5 million seeds (Scott & Smith 2011), which is why a "Zero Tolerance" program is being practiced by many Arkansas growers to help eliminate pigweed seed production and reduce the soil seed-bank. Seed-bank management is critical with respect to herbicide resistant species, because even with a 99.9% effective herbicide program, an estimated 54 to 1,020 *A. palmeri* plants will likely escape and be present in the first and second years after is a "Zero Tolerance" program is not adopted (Barber et al. 2015). *Amaranthus palmeri* has been confirmed to be resistant to several chemical classes of herbicides, including microtubule inhibitors, acetolactate synthase (ALS) inhibitors, 5-enolpyruvylshikimate-3-phosphate (EPSP) synthase inhibitors, and protoporphyrinogen oxidase (PPO) inhibitors in Arkansas (Barber et al. 2015).

Glyphosate and PPO inhibitor resistant *A. palmeri* continue to be a major concern for soybean producers. New herbicide classes and strategies for controlling resistant pigweed are limited. New herbicide resistant lines of soybean have been introduced into the Arkansas production system. Cultivars with traits that resist glufosinate and dicamba are becoming

increasingly available commercially, but a concern with the introduction of this technology is that soybean plants without the glufosinate (Liberty-Link®) or dicamba-resistance genes are highly susceptible to these herbicides. As of the 2016 growing season, glufosinate was the only labeled post-emergence herbicide on soybean that was recommended for control of glyphosate-resistant *A. palmeri*. In 2017, dicamba (Engenia®) was approved by the Arkansas Plant Board to be used as a post-emergence control for this weed. Although the new dicamba formulation can be used as a control throughout the growing season, there are still certain limitations that include buffer zones and specific spray nozzle types. Research shows that the first growth stage of reproduction in soybean is one of the most sensitive stages to dicamba drift, and a ten percent yield loss was observed from an over-the-top application of 1/1024X the labeled rate (Barber 2016). By the end of the 2017 growing season, the Arkansas State Plant Board had received 985 complaints about dicamba drift, and effective 2018 February 1 applications of dicamba cannot be applied between April 16 and October 31. Even with timing and buffer restrictions, growers are swiftly adopting this technology into production fields due to the concern of dicamba drift from on and off label applications.

Diseases

For growers, many important decisions are made before seeds are planted. Some of these include the type of crop and appropriate cultivar selection. Pathogens have caused severe yield suppression on crops, and management methods are constantly being revised and improved. The most common disease management practices include tillage, crop rotation, burning, and chemical control. Each of these management methods have benefits and drawbacks for both growers and the environment. For many growers today, the overall farming objective includes selecting the highest yielding variety for production, with little concern for disease resistance. Disease control

using fungicides has been the most popular method for disease management in Arkansas. Many variables have required growers to use chemicals to control diseases, rather than using cultural practices and disease-resistant plants. Soybean diseases are a significant consideration in both soybean production and cultivar selection, and the University of Arkansas Division of Agriculture tests numerous soybean cultivars annually for yield, maturity date, lodging, and nematode and disease resistance (University of Arkansas Division of Argriculture 2017). Fungi, bacteria, nematodes, and viruses all may impact soybean yield performance in the state.

Plant-parasitic Nematodes

Root-knot Nematode

Meloidogyne incognita, southern root-knot nematode, overwinters in the soil as eggs in masses attached to the roots of the previous crop. Juveniles may also survive in the soil all winter, during favorable environments (Evans & Perry 2009). As the egg develops, cells differentiate and the first stage juvenile (J1) forms inside the egg. When temperatures reach 25°-30°C, *M. incognita* eggs hatch and emerging second-stage juveniles (J2) move to soybean roots, targeting the root tip where cells are undifferentiated in the zone of root elongation. Upon root penetration, the nematode stylet secretes proteins and other compounds that allow the nematode to evade host defense response pathways and oxidative reactions. These secretions also help degrade the cell wall and allow for manipulation of cellular functions for nematode benefit (Hussey 1989). Cells are signaled to initiate cell division but do not complete the last stage, resulting in multi-nucleate cells called "giant-cells" (Favery et al. 2016). Once the giant-cell is formed, the nematode remains sedentary at the site and relies on the cell as the sole source of nutrients for the remainder of life (Choi et al. 2017). These structures along with the growing nematode result in the formation of visible galls or "knots" on the roots (Mitkowski & Abawi 2003). The juvenile molts through J3 and J4 stages

and then becomes an adult, either male or female. Adult females begin to produce eggs in an exterior, gelatinous mass that can contain up to a thousand eggs. The J1 forms completely within the egg shell, molts, then hatches into the J2 stage, completing the lifecycle (Chitwood & Perry 2009).

Galls can be observed visually on infected roots, and some above ground symptoms may include stunted and yellowed plants. Also, foliar symptoms of nutrient deficiencies are commonly observed and associated with *M. incognita* infected plants because of the reduced uptake of soil nutrients. Although nutrient levels could be optimum in the soil, root damage and galling caused by nematodes may prevent uptake for plant growth, therefore reducing yield. Management strategies for *M. incognita* are limited in soybean production, which includes the availability of a few resistant cultivars, crop rotation, and nematicidal seed treatments.

Three *Meloidogyne* spp. (*M. incognita*, *M. javanica*, and *M. arenaria*) have been identified in the Mississippi Alluvial Plain and throughout the southern parts of Alabama, Georgia, South Carolina, and North Carolina, as well as in parts of California, Arizona, New Mexico, Texas, and Florida. However, in Arkansas *M. incognita* is by far the most predominant species, particularly in crop production (Kirkpatrick, personal communication). *Meloidogyne incognita* has a broad host range that includes cotton, tomato, okra, banana, sunflower, tobacco, and several other crops including soybean. *Meloidogyne incognita* estimated to reduce soybean yield in Arkansas by 40, 142, and 181 million kilograms during the 2013, 2014, and 2016 growing seasons, respectively (Koenning 2014; Allen et al. 2015; Allen et al. 2017).

The distribution of *M. incognita* within a field is associated with noticeable areas called “hot spots,” which result in significant yield losses in sandy soils within the field (Monfort et al. 2007). Because nematodes are clustered, soil sampling using the grid sampling method may be

effective in determining nematode populations but can be labor-intensive and cost-prohibitive (Wheeler et al. 2000; Wrather et al. 2002). Another sampling method is referred to as zone sampling. This method identifies areas (or zones) in a field with similar characteristics, such as crop yield, soil fertility or soil texture for targeted sampling. Zone sampling could be an effective method to characterize the spatial distribution of nematode populations. Soils with a ≥ 86% sand content showed a significantly higher level of migration of *M. incognita* than soils between 75% and 86% (Prot & Van Gundy 1981). Also, Monfort et al. (2007) found that fewer *M. incognita* in population are required to suppress yield in soil with a higher sand content. Therefore, soil texture is crucial in determining the damage potential of *M. incognita*, and percent sand is directly related to the migration and penetration of roots by the J2.

Because classical soil texture analysis can be laborious, extensive research has been performed to identify other field characteristics that are less formidable to sample. Mueller et al. (2003) indicated that soil electric conductivity was correlated with soil texture, and based on research conducted in eleven cotton fields during 2005 and 2006, Ortiz et al. (2011) reported areas within a field that are likely to have high levels of *M. incognita* could be predicted using relative field changes in apparent EC.

Stunt Nematode

Stunt nematodes, including *Tylenchorhynchus spp*. (*T. annulatus*, *T. canalis*, *T. claytoni*, *T. dubius*, *T. ewingi*, *T. goffarti*, *T. maximus*, *T. nudus*), *Merlinius brevidens*, and *Quinisulcius spp*. (*Q. acti* and *Q. acutus*), are another common nematode found in Arkansas. Of these species, four are commonly found in soybean production: *T. canalis*, *T. ewingi*, *T. goffarti*, and *Q. acutus* (Robbins et al. 1987; Wehunt et atl. 1989). Robbins et al. (1987) sampled 134 fields in 1985 and 1986, and they found that 52% and 34% of those fields, respectively, showed the presence of stunt

nematode (*Tylenchorhynchus spp*. and *Q. actus*). Furthermore, of the fields sampled in 1985 and 1986, *Q. acutus* and *T. ewingi* were the most common (Robbins et al. 1987). Unlike *M. incognita*, stunt nematodes reproduce well across a variety of soil types from sandy to loamy clay soils (Bond et al. 2000) and have a wide host range. Population densities are reduced in saturated soils, such as flooded rice fields (Rodriguez-Kabana 1965). Stunt nematodes are usually deemed a minor pest in row crops, although in corn, populations can cause damage in conjunction with other nematodes.

Spatial Analysis

Why Use Spatial Analysis

Spatial analysis is the process of answering important questions, explaining patterns, and enhancing decision making with spatial data, which is information that identifies a geographic location by relying on both exploratory and confirmatory techniques (Grubesic & Nelson 2016). Exploratory data analysis looks for patterns while confirmatory data analysis tests the proposed models. For example, understanding distributions of pathogens in production fields could explain the dynamics of how the disease is dispersed by showing where it was initially, where it spread, and how fast it spread. Answering these questions could lead to discoveries of more effective control strategies.

Significant Distributions

There are three main types of distinctions of spatial association: uniform, clustered, and random. Uniform distribution, or even distribution, is a distribution that has constant probability. These values are equally spaced apart and are usually describable by rectangular patterns or lines in nature. Samples that are consistent and equally spaced throughout the field are often man-made in one way or another. These can occur due to malfunctioning equipment, cultivation, or pesticide or fertilizer applications. Clustered distributions occur when data points show a relationship due

to location (likely spatial dependence). Diseases or fertility issues often correlate with soil texture and are the main causes of clustered distributions in production fields.

Fields that are variable in soil texture may fluctuate in soil nutrient levels, and potassium-deficient plants may be more susceptible to pathogens (Wang et al. 2013). Plant available soil potassium is in an ionic, electrically charged, form. This is a positive charge, making potassium a cation. Cations are attracted to, and held by negatively charged colloids, (clay and organic matter) that make up the cation exchange capacity (CEC) of the soil. The higher the CEC values, the more potassium that can remain in the soil. Areas with low CEC values within in a field can be leached of potassium due to excessive rainfall or irrigation, while soil potassium levels can remain adequate in more clay areas. Random distributions occur when data points show no correlation in location between each other. Foliar diseases caused by pathogens with secondary cycles can be randomly distributed initially. Secondary infections can be repeated many times during a growing season from the spread of asexual spores. These infections result in exponential growth of the pathogen so that the disease may spread to become clustered.

Of the three distribution patterns, only two of them are relevant: values that are clustered (positive spatial autocorrelations) or dispersed (negative spatial autocorrelation). Problematic areas within a field that are either clustered or uniform tend to have an identifying cause or association, while random patterns are unpredictably formed. With an identifying cause, aggravating agent(s) can be discovered and diagnosed for proper management methods. Without properly identifying the causal agent, a solution can only be generated by trial and error. Uniform distributions are likely caused by man or objects that are man-made, while clustering patterns may not have such an obvious contagion causing the distribution.

Modifiable Areal Unit Problem

Geographical space can either be composed of boundaries or locations of objects and features (Wong 2008). The Modifiable Areal Unit Problem (MAUP) impacts the results of univariate and multivariate regressions and arises from errors that are created when data are grouped together for analysis (Openshaw 1984). The Modifiable Areal Unit Problem is associated with the use of scaling or zoning data related to geographical areas (Ervin 2012). The scale effect refers to how changing the number of areal units on a map can influence the interpretation, and the zoning effect refers to how changing the space within a map, while maintaining the same number of areal units, can also influence the interpretation (Jones 2011). An example would be looking at the average number of kilograms per hectare of soybean grown in Arkansas. The scale of this analysis could be changed to look at kilograms per hectare on a regional, county, farm, or field level scale. Each level would provide different quantitative values. This could be due to many things, for example, certain fields or areas in the state might be irrigated while other parts are non-irrigated. Also, some growers practice a high input production system, which usually means both higher input costs and higher yields. Changing the volume or shape of the observation area within the same study would be a zonal problem. To satisfy MAUP all solutions must be consciously and logically attempted to minimize negative effects of grouping (Ervin 2012).

Spatial Regression

Spatial regression examines, explores, and models geographical data. Also, it explains the factors that contribute to clustered distributions. Predictive modeling can be derived from spatial regressions. Ordinary least squares (OLS) linear regression can be used to estimate the relationship between a dependent variable (y) and one or more independent variables (x) (Brusilovskiy 2010). Ordinary least squares generates predictions or models a dependent variable in terms of its

relationships to a set of explanatory variables. The closer the data points are to the line, the more the variables are correlated with each other. Correlation is a statistical technique that can show if and how strongly variables are related. Probability values (p-values) and coefficients in a regression analysis demonstrate which relationships in the model are statistically significant and the nature of those relationships. The coefficients describe the mathematical relationship between each independent variable and the dependent variable. The p-values for the coefficients indicate whether these relationships are statistically significant (Frost 2014). Recently these techniques have been used for more practical application in pest management and understanding losses, specifically for *M. incognita* (Liu et al. 2014).

Geographically weighted regression (GWR) should be used when modeling spatial heterogeneity or uneven distributions across a study area. Unlike other regression models, GWR produces a separate equation for every feature and generates a set of location-specific parameters that can be mapped and analyzed (Matthews & Yang 2012).

Designing a Spatial Test

A test that can be analyzed spatially must have observations collected at fixed points in an area. The points where data are collected cannot change and data should be collected at a given point in time so as not to introduce temporal variability. Typically, experimental units are lacking when spatial design is implemented, creating issues with analysis. For example, Anselin (2006) indicated a minimum of 50 observations were needed to perform an accurate Moran's I analysis and approximately 100 observations were necessary to reliably analyze a spatial dependence model. When numbers of points of observations are satisfied, determining spatial dependence and correlation across points in space between a dependent and explanatory variable is accomplished using measures of aggregation (Moran's I) and correlation using spatial regression. Spatial

dependence is a phenomenon that occurs when the values of a variable at a point in space are related to nearby values of the same variable. Spatial models can be used to adjust for spatial dependence by exploiting the relationship of the data set.

Recently, a "strips and anchors" (Spurlock 2017) method of spatial analysis was proposed, and it will be used for one objective in this project. With this approach, treatments are applied in strips across the area. Observations are made within and adjacent to each treatment, exhausting logical space and satisfying MAUP. Quantitative variables that correlate to the desired dependent variable are kriged (Oliver 1990) and aggregated areas of different values are used as qualitative zones for analysis of treatment means (within zones). This method of spatial analysis allows the use of fewer observations to collect data while still relating it to important changes in disease pressure and treatment efficacy.

Precision Agriculture

Equipment and Remote Sensing

Precision agriculture, or site-specific farming, is a farm management concept where growers focus on different variables within each field to optimize inputs and maximize outputs. The technology that makes precision agriculture available are global navigation satellite system (GNSS) that allow georeferencing of specific data. For example, yield monitors on harvest equipment may record the yield for thousands of points per hectare and the data are georeferenced so that a spatial data layer can be created. Other factors that might be measured include soil texture and (or) fertility, presence and density of pests, crop growth, etc. Although currently very few growers fully utilize site-specific/georeferenced practices in their production systems, yield maps, soil texture maps, aerial imagery all could improve efficiency and accuracy in making management decisions. As one example, evidence suggests that more economical and environmentally

appropriate control of nematodes, such as *M. incognita*, could be achieved by use of site-specific techniques (Monfort et al. 2007; Overstreet et al. 2014).

Big Data

Precision agriculture can generate a tremendous amount of data, and each site-specific practice can have thousands of associated data points with many different properties for each one (Griffin et al. 2016). Manipulation and analysis of this huge quantity of data requires the use of complex software and high computation power. Most often synthesis and analysis of these data are beyond the capabilities of farmers, consultants, and retail agriculture professionals. In addition, outputs from many applications may not be universally compatible due to software proprietary concerns, making it impossible to exchange data. Because the concepts and technology that are associated with precision agriculture are relatively recent developments, not enough data has been collected to determine exactly what the results mean in certain scenarios. The adoption of precision agriculture and site-specific management will be reliant on trained agronomists and will require more data to determine its true value.

Farming of the Future

The Food and Agriculture Organization predicts that there will be 9.6 billion people in the world to feed by 2050, which means food production needs to increase by 70% despite the limited availability of arable land (Guerrini 2015). To resolve the issue of future food demands, current production systems need to increase yields per hectare, requiring implementation of new production systems. The goal of precision agriculture is to maximize outputs (yield), while optimizing inputs (costs). Computer programs will soon be able to tell growers exactly what applications to make on every hectare, or less, of their farm with few or no diagnosis being

performed by humans. On the other hand, new types of production systems have been created in other areas of agriculture, such as vegetable production.

Literature Cited

2016. *Arkansas Acreage Report.* National Agricultural Statistics Service. Little Rock, Arkansas: United States Department of Agriculture.

University of Arkansas Division of Argriculture. 2017. *Soybean Variety Testing Program*. Retrieved from Arkansas Variety Testing: http://www.arkansasvarietytesting.com/home/soybean/

Allen, T. W., Bradley, C. A., Damicone, J. P., Dufault, N. S., Faske, T. R., Hollier, C. A., . . . Young, H. 2017. Southern United States Soybean Disease Loss Estimates for 2016. *Proceedings of the Southern Soybean Disease Workers, forty-fourth Annual Meeting.* Pensacola, FL: Southern Soybean Disease Workers.

Allen, T. W., Damicone, J. P., Dufault, N. S., Faske, T. R., Hershman, D. E., Hollier, C. A., . . . Young, H. 2015. Southern United States Soybean Disease Loss Estimates for 2014. *Proceedings of the Southern Soybean Disease Workers, forty-second Annual Meeting.* Pensacola Beach, FL: Southern Soybean Disease Workers.

Anselin, L. 2005. *Exploring spatial data with GeoDa: A workbook.* Retrieved from Spatial Analysis Laboratory, Department of Geography, University of Illinois: http://www.unc.edu/~emch/gisph/geodaworkbook.pdf

Baldwin, F., Oliver, D., & Smith, K. 2000. Weed Control. *Arkansas Soybean Production Handbook*, 50-63.

Barber, T. 2016. *Arkansas Soybeans: Dicamba Dift and Potential Effects on Yields.* Little Rock, AR: Univeristy of Arkansas Cooperative Extension Service Printing Services.

Barber, T., Smith, K., Scott, R., Norsworthy, J., & Vangilder, A. 2015. *Zero Tolerance: A Community-Based Program for Glyphosate-Resistant Palmer Amaranth Management.* Little Rock, AR: Univeristy of Arkansas Cooperative Extension Service Printing Services.

Bond, J. P., McGawley, E. C., & Hoy, J. W. 2000. Distribution of Plant-Parasitic Nematodes on Sugarcane in Louisiana and Efficacy of Nematicides. *Supplement to the Journal of Nematology 32(4S)*, 493-501.

Brusilovskiy, E. 2010. *Spatial Regression: A Brief Introduciton.* Philadelphia, PA: Business Intelligence Solutions. Retrieved from http://www.bisolutions.us/A-Brief-Introduction-to-Spatial-Regression.php

Chitwood, D. J., & Perry, R. N. 2009. Reproduction, Physiology and Biochemistry. In R. N. Perry, M. Moens, & J. L. Starr, *Root-knot Nematodes* (pp. 182-200). Cambridge, MA: CABI.

Choi, I., Subramanian, P., Shim, D., Oh, B.-J., & Hahn, B.-S. 2017. RNA-Seq of Plant-Parasitic Nematode Meloidogyne incognita at Various Stages of Its Development. *Frontiers in Genetics*, https://doi.org/10.3389/fgene.2017.00190.

Coats, R., & Ashlock, L. 2000. The Arkansas Soybean Industry. *Arkansas Soybean Handbook*, 1-6.

Ervin, D. 2012. *MAUP.* Santa Barbara, CA: Advanced Spatial Analysis in the Population Sciences and Spatial Demography. Retrieved from http://gispopsci.org/maup/

Evans, A., & Perry, R. N. 2009. Survival Mechanisms. In R. Perry, M. Moens, & J. L. Starr, *Root-knot Nematodes* (pp. 201-222). Cambridge, MA: CABI.

Evans, M. G., Eck, K. J., Gauck, B., Krejci, J. M., Lake, J. E., & Matzat, E. A. 2000. *Conservation tillage update: Keeping soil covered and water clean in the new millennium.* West Lafayette, IN: Purdue University Agronomy.

Favery, B., Quentin, M., Jaubert-Possamai, S., & Abad, P. 2016. Gall-forming root-knot nematodes hijack key plant cellular functions to induce multinucleate and hypertrophied feeding cells. *Journal of Insect Physiology*, 60-69.

Frost, J. 2014. *How to Correctly Interpret P Values.* The Minitab Blog. Retrieved from http://blog.minitab.com/blog/adventures-in-statistics-2/how-to-correctly-interpret-p-values

Griffin, T. W., Mark, T. B., Ferrell, S., Janzen, T., Ibendahl, G., Bennett, J. D., . . . Shanoyan, A. 2016. Big Data Considerations for Rural Property Professionals. *Journal of American Society of Farm Managers and Rural Appraisers*, 167-180.

Grubesic, T., & Nelson, J. 2016. *Spatial Analysis.* Oxford Bibliographies.

Guerrini, F. 2015. *The Future of Agiculture? Smart Famring.* Forbes. Retrieved from https://www.forbes.com/sites/federicoguerrini/2015/02/18/the-future-of-agriculture-smart-farming/#3ef960053c42

Huitink, G., & Tacker, P. 2000. Drainage and Tillage. *Arkansas Soybean Handbook*, 27-34.

Hussey, R. S. 1989. Disease-inducing secretions of plant-parasitic nematodes. *Annual Review of Phytopathology*, 123-141.

Jones, R. 2011. *The Modifiable Areal Unit Problem in GIS.* Cartographica. Retrieved from https://blog.cartographica.com/blog/2011/5/19/the-modifiable-areal-unit-problem-in-gis.html

Koenning, S. R. 2014. Southern United States Soybean Disease Loss Estimate For 2013. *Proceedings of the Southern Soybean Disease Workers, forty-first Annual Meeting.* Pensacola Beach, FL: Southern Soybean Disease Workers.

Kulkarni, S. 2002. *Planting Reduced-Tillage Soybeans.* Little Rock, AR: Univeristy of Arkansas Cooperative Extension Service Printing Services.

Liu, Z., Griffin, T., & Kirkpatrick, T. L. 2014. Statistical and Economic Techniques for Site-specific Nematode Managment. *Journal of Nematology, 46*, 12-17.

Lorenz, G., Johnson, D., Studebaker, G., Allen, C., & Young, III, S. 2000. Insect Pest Management in Soybeans. *Arkansas Soybean Production Handbook*, 84-94.

Matthews, S., & Yang, T.-C. 2012. Mapping the results of local statistics: Using geographically weighted regression. *Demographic Research*, 151-166.

Mitkowski, N. A., & Abawi, G. S. 2003. Root-knot nematodes. *The Plant Health Instructor*, doi: 10.1094/PHI-I-2003-0917-01.

Monfort, W. S., Kirkpatrick, T. L., Rothrock, C. S., & Mauromoustakos, A. 2007. Potential for site-specific management of Meloidogyne incognita in cotton using soil textural zones. *Journal of Nematology, 39*, 1-8.

Mueller, T. G., Hartsock, N. J., Stombaugh, T. S., Shearer, S. A., Cornelius, P. L., & Barnhisel, R. I. 2003. Soil electrical conductivity map variability in limestone soils overlain by loess. *Agronomy Journal*, 496-507.

Oliver, M. A. 1990. Kriging: A Method of Interpolation for Geographical Information Systems. *International Journal of Geographic Information Systems 4*, 313-332.

Openshaw, S. 1984. The Modifiable Areal Unit Problem. *Geo Books*.

Ortiz, B. V., Sullivan, D. G., Perry, C., & Vellidis, G. 2011. Delineation of Management Zones for Southern Root-Knot Nematode using Fuzzy Clustering of Terrain and Edaphic Field Characteristics. *Communications in Soil Science and Plant Analysis 42*, 1972–1994.

Overstreet, C., McGawley, E. C., Khalilian, A., Kirkpatrick, T. L., Monfort, W. S., Henderson, W., & Mueller, J. D. 2014. Site specific nematode managment-development and success in cotton production in the United States. *Journal of Nematology, 46*, 309-320.

Prot, J.-C., & Van Gundy, S. D. 1981. Effect of Soil Texture and the Clay Component on Migration of Meloidogyne incognita Second-stage Juveniles. *Jouranl of Nematology*, 213-217.

Robbins, R. T., Riggs, R. D., & Von Steen, D. 1987. Results of annual phytoparasitic nematode surveys of Arkansas soybean fields, 1978-1986. *Annals of Applied Nematology*, 50-55.

Rodriguez-Kabana, R. 1965. *Chemical antibiosis to nematodes in rice fields.* Baton Rouge, LA: Louisiana State University.

Scott, R., & Smith, K. 2011. *Prevention and control of glyphosate-resistant pigweed in soybean and cotton.* Little Rock, AR: Univeristy of Arkansas Cooperative Extension Service Printing Services.

Slaton, N., Roberts, T., & Ross, J. 2013. Fertilization and Liming Practicies. *Arkansas Soybean Production Handbook*, 21-26.

Spradley, P. 2005. *Crop Profile for Soybeans in Arkansas.* Little Rock, AR: Southern IPM Center.

Spurlock, T. 2017. Proceedings of the Southern Soybean Disease Workers 44th Annual Meeting. *Southern Soybean Disease Workers.* Pensacola, FL: Southern Soybean Disease Workers.

Wang, M., Zheng, Q., Shen, Q., & Guo, S. 2013. The Critical Role of Potassium in Plant Stress Response. *International Jouranl of Molecular Sciences, 14(4)*, 7370-7390.

Wehunt, E. J., Golden, A. M., & Robbins, R. T. 1989. *Plant nematodes occurring in Arkansas.* 677-681: Supplement to Journal of Nematology.

Wheeler, T. A., Baugh, B., Kaufman, H., Schuster, G., & Siders, K. 2000. Variability in Time and Space of Meloidogyne incognita Fall Population Density in Cotton Fields. *Journal of Nematology 32(3)*, 258–264.

Wong, D. 2008. The Modifiable Areal Unit Problem (MAUP). In A. S. Fotheringham, & P. A. Rogerson, *The SAGE Handbook of Spatial Analysis* (pp. 105-124).

Wrather, J. A., Stevens, W. E., Kirkpatrick, T. L., & Kitchen, N. R. 2002. Effects of Site-specific Application of Aldicarb on Cotton in a Meloidogyne incognita-infested Field. *Journal of Nematology 34(2)*, 115–119.

Zehnder, G. 2014. *Overview of Monitoring and Identification Techniques for Insect Pests.* Retrieved from eXtension: http://articles.extension.org/pages/19198/overview-of-monitoring-and-identification-techniques-for-insect-pests

Chapter 2: Site-specific management of plant pathogenic nematodes on soybean

Abstract

The southern root-knot nematode, *Meloidogyne incognita*, is responsible for substantial yield losses on soybean grown in the Mississippi Alluvial Plain. Evidence suggests that the seed treatment nematicides fluopyram and abamectin may suppress reproduction and root galling by *M. incognita*, but yield protection in fields with higher nematode pressure is less obvious. The objective of this work was to determine the efficacy of these seed treatment nematicides compared to 1,3-dichloropropene (1,3-D) applied site-specifically. In a production field infested with *M. incognita,* shallow (0 to 0.3 m) and deep (0 to 0.91 m) apparent electrical conductivity (ECa) readings were highly correlated with sand content, and treatments were applied the total length of the field (verification strips), across two soil textural zones. Fluopyram and abamectin treated seeds were compared to seeds without nematicide seed treatment (control) and seeds without nematicide seed treatment but planted within 1,3-D treated soil. In 2016, yields were not improved by the seed treatments in either of the zones. Fumigation with 1,3-D improved yield in comparison to all other treatments, while fluopyram and abamectin were not effective in improving yields (P=0.001). In 2017, 1,3-D strips had significantly higher yield than all other treatments in all other zones except for residual 1,3-D treatments that were applied in 2016 in Zone 2 (P=0.01). Fluopyram, abamectin, and the control treatments were not significantly different in Zone 1, but treatment effects were significantly different between textural zones for all treatments (P=0.01). The distribution of *M. incognita* at harvest was uniformly distributed by treatments (P=0.08) suggesting that 1,3-D could be used as a two-year control and would be economically beneficial as a whole-field application (across both soil textural zones) when a susceptible soybean is planted.

Introduction

Nematodes are microscopic roundworms, many of which are soil-dwelling and plant-parasitic. Plant-parasitic nematodes feed on root cells with a stylet. They can also utilize the plant roots for reproductive activity (Mitkowski & Abawi 2003). Root dysfunction and damage caused by nematodes produce above-ground symptoms that are similar to soil nutrient deficiencies (Mitkowski & Abawi 2003). Plant-parasitic nematodes are economically important pests that affect many row crops in the Mid-South. Nematodes are host-specific organisms and strategies for management of these pests will vary by crop. Chemical control options for nematodes are limited, so often crop rotation to a non-host is the best solution (Hurd & Faske 2017). However, with fluctuating commodity prices, rotational options are also limited because some crops are not economically beneficial to growers (Starr et al. 2007). For this reason, seed treatments are being marketed for crop protection, but their efficacy is questionable in fields with high nematode pressure.

Soybean were first introduced in Arkansas during the 1920's and gained popularity among growers around the mid-1900s. From 1960 to 1979, harvested hectares increased dramatically, and peaked in 1979 at 2.08 million hectares (Coats & Ashlock 2000). Although somewhat lower than in 1979, soybean are still grown on more hectares today than any other production crop in Arkansas, and account for fifty-one percent of all principle crops planted in Arkansas; with 1.27 million hectares grown in 2016 (Arkansas Acreage Report 2016). Three *Meloidogyne* spp. (*M. incognita*, *M. javanica*, and *M. arenaria*) have been identified in the Mississippi Alluvial Plain and throughout the southern parts of Alabama, Georgia, South Carolina, and North Carolina, as well as in parts of California, Arizona, New Mexico, Texas, and Florida. However, in Arkansas *Meloidogyne incognita* is by far the most predominant species, particularly in crop production

(Kirkpatrick, personal communication), and were estimated to reduce soybean yield in Arkansas by 40, 142, and 175 million kilograms during the 2013, 2014, and 2016 growing seasons, respectively (Koenning 2014; Allen et al. 2015; Allen et al. 2017). *Meloidogyne incognita* has a broad host range that includes cotton, tomato, okra, banana, sunflower, tobacco, and several other crops including soybean. Infected roots result in the formation of galls or "knots" that can be observed visually. Some above-ground symptoms may include stunted and yellowed plants and foliar symptoms of nutrient deficiencies, because of the reduced uptake of soil nutrients. Although nutrient levels could be optimum in the soil, root damage and galling caused by nematodes may prevent uptake for plant growth, therefore reducing yield. Management strategies for *M. incognita* are limited in soybean production, and include the availability of a few resistant cultivars, crop rotation, and nematicidal seed treatments.

Meloidogyne incognita overwinters in the soil as eggs in egg masses attached to the roots of the previous crop; juveniles may survive in the soil all winter under favorable environments (Evans & Perry 2009). As the egg develops, cells differentiate and the first-stage juvenile (J1) forms inside the egg shell. At temperatures of 25°-30°C, *M. incognita* eggs hatch and emerging second-stage juveniles (J2) migrate to soybean roots, targeting the root tip where cells are undifferentiated in the zone of root elongation. During the penetration process, the nematode stylet secretes proteins and other compounds that allow the nematode to evade host defense response pathways and oxidative reactions. These secretions also help degrade the cell wall and allow for manipulation of cellular functions for nematode benefit (Hussey 1989). Cells are signaled to initiate cell division but do not complete the last stage, resulting in multi-nucleate cells called "giant-cells" (Favery et al. 2016). Once the giant-cell is initiated, the nematode remains sedentary at the site and relies on the cell as the sole source of nutrients for the remainder of its life (Choi et

al. 2017). These breeding sites along with the nematode result in the formation of visible galls on infection site of the roots (Mitkowski & Abawi 2003). The juvenile molts twice after the third and fourth stage and then becomes an adult male or female. Adult females will begin to produce eggs in an exterior, gelatinous mass that can contain up to a thousand eggs. The J1 forms completely within the egg shell, molts, then hatches into the J2 stage, completing the lifecycle (Chitwood & Perry 2009).

Within fields, *M. incognita* are associated with noticeable areas called "hot spots", which may result in significant yield losses in sandy soils within the field (Monfort et al. 2007). Because nematodes are clustered in distribution, soil sampling using the grid sampling method may be effective in determining nematode populations but can be labor-intensive and cost-prohibitive (Wheeler et al. 2000; Wrather et al. 2002). Another sampling method is referred to as zone sampling. This method defines areas (or zones) in a field with similar characteristics, such as crop yield, soil fertility or soil texture. Zone sampling could be an effective method to characterize the spatial distribution of nematode populations because soils with a ≥ 86% sand content showed a significantly higher level of migration of *M. incognita* than soils between 75% and 86% (Prot & Van Gundy 1981). Also, Monfort et al. (2007) found that fewer *M.* incognita in population are required to suppress yield in soil with a higher sand content. Therefore, soil texture is crucial in determining the infectivity of *M. incognita*, and percent sand is directly related to the migration in the soil and penetration of roots by the J2. Because classical soil texture analysis can be laborious, identifying other field characteristics that are less formidable to sample may be beneficial. Mueller et al. (2003) indicated that soil electrical conductivity was correlated with soil texture. Based on research conducted in eleven cotton fields during 2005 and 2006, Ortiz et al. (2011) reported areas

within a field that are likely to have high levels of *M. incognita* could be predicted using relative field changes in apparent EC.

Precision agriculture, or site-specific management, is a farm management concept where growers focus on field variability to optimize inputs (seed, fertilizer, pesticides, etc.) and maximize outputs (yield). The technology that makes precision agriculture available is global navigation satellite systems (GNSS) that allow georeferencing of data. Computers on harvest equipment may record data, such as yield, grain moisture, elevation, etc., by georeferencing thousands of specific points in every hectare, thus creating a spatial data layer. A spatial data layer is a set of features that are symbolized and labeled to represent a geographic dataset. Variables that can be measured include (but are not limited to) soil texture, fertility, presence and density of pests, crop growth, crop health. Evidence suggests that more economical and environmentally appropriate control of nematodes, such as *M. incognita*, could be achieved by use of site-specific techniques (Monfort et al. 2007; Overstreet et al. 2014). Although very few growers are currently utilizing site-specific practices in their production system, spatial data layers could improve farm efficiency, aid in management decisions, and help create a more profitable and sustainable industry.

The objectives of this work were to determine the value in site-specific management of *M. incognita* in soybean, and to generate teaching materials explaining how and when to apply nematicides site-specifically.

Materials and Methods

A field near Backgate, Arkansas, with a center point coordinate of -91.399318° and 33.946616° (longitude and latitude, respectively), was determined to have severe *M. incognita* based on nematode density, poor plant growth, and yield loss in 2015 (Figure 1). Soybean plants were yellowed and stunted (Figure 2), and roots were damaged from severe galling (Figure 3).

Leaf tissue and soil samples were collected and analyzed; indicating low potassium and manganese levels in the plants. A two-year study (2016 and 2017) was created in this field with treatments arranged in a randomized complete block design, with each treatment covering 12 rows wide and extending the length of the field (verification strips), replicated three times. In 2017, a second location was added in a field near Meroney, Arkansas, with a center point coordinate of -91.727073° and 33.971782° (longitude and latitude, respectively), which had previously been diagnosed as severely damaged by *M. incognita* in 2016 (Figure 4). Aerial imagery was captured by the Sentinel-2 satellite at 10-meter resolution and from an airplane mounted with a visual (RGB) and near infrared (NIR) sensor at 20-centimeter resolution throughout the growing season for observation of field variability and treatment effects. Historical aerial imagery (2015 to present) was also recovered with the Sentinel-2 satellite for comparison of normalized difference vegetation index (NDVI) and NIR variability within the fields.

Yield data of the verification strips were collected by a John Deere GreenStar™ 3 2630 Display (Deere & Company, Moline, IL) and averaged in ArcMap 10.4 (Esri, Redlands, CA). Other spatial analysis of variables, where appropriate, were completed in GeoDa 1.12 (GeoDa Center, University of Illinois-Chicago). ArcMap 10.4 was used to perform geographically weighted regression (GWR), which models spatial heterogeneity or uneven distributions across a study area. Unlike other regression models, GWR produces a separate equation for every feature and generates a set of location-specific parameters that can be mapped and analyzed (Matthews & Yang 2012). Data were also subjected to analysis of variance (ANOVA) and means of treatment effects were separated using Fischer's least significant difference test in ARM 2016 (Gylling Data Management, INC., Brookings, SD).

Backgate, Arkansas

In 2016, verification strips of 1,3-dichloropropene (1,3-D) were applied with a modified liquid manure applicator three weeks prior to planting, 12 rows wide with a spacing of 96.52 cm per row, that extended the length of the field. Armor DK4744 soybean with fluopyram (56.19 ml/140,000 seeds) and abamectin (41.99 ml/140,000 seeds) seed treatments were compared to seeds without a nematicide seed treatment (control) and seeds without a nematicide seed treatment but planted within the 1,3-D treated soil. All soybean seeds were standard treated with CruiserMaxx® seed treatment, while fluopyram and abamectin seeds were treated over the top of the standard CruiserMaxx®. Ten sampling points within each of the 12 verification strips were designated by dividing the field length equally and marked with a Yuma 2 (Trimble Inc., Sunnyvale, CA), which data was collected throughout the duration of the trial. Soil fertility and nematode samples were extracted at plant emergence and plant harvest and then divided proportionally for analysis at the Arkansas Nematode Diagnostic Laboratory in Hope, Arkansas and the Soil Testing and Research Laboratory in Marianna, Arkansas. During the growing season, an application of Quadris Top® SBX at 548.08 milliliters hectare^{-1} was applied and suppressed *C. sojina* (southern stem canker) from further escalating in the field. Prior to harvest, ten random plants at each of the 120 sampling points were extracted with a shovel and rated for incidence and severity of root galling, and other potentially yield limiting diseases. The trial was harvested on 22 September 2016 by a John Deere 9770 combine (Deere & Company, Moline, IL), using a John Deere 635F draper header (Deere & Company, Moline, IL), with John Deere GreenStar™ 3 2630 Display (Deere & Company, Moline, IL). Soil texture was estimated using the Veris 3150 Soil EC Mapping System (Veris Technologies, Salina, KS) on 4 November 2016 (Figure 5).

In 2017, treatments were placed in a randomized complete block design similar to the year before. Verification strips of 1,3-D were applied with a modified liquid manure applicator two weeks prior to planting, 11 rows wide with a spacing of 96.52 cm per row, that extended the length of the field. Armor 46-D08 soybean with fluopyram (56.19 ml/140,000 seeds) and abamectin (41.99 ml/140,000 seeds) seed treatments were compared to seeds without a nematicide seed treatment (control), seeds without a nematicide seed treatment but planted within the 1,3-D treated soil, and seeds without a nematicide seed treatment but planted within the residual of 1,3-D treated soil from the previous year. All soybean seeds were treated with CruiserMaxx® seed treatment as the standard, while fluopyram and abamectin seeds were treated over the top of the standard CruiserMaxx®. Each treatment was planted in adjacent verification strips of equal size and replicated three times. Ten sampling points within each of the 15 verification strips were designated by equal spacing, marked with a Yuma 2, and data was collected throughout the duration of the trial. Nematode samples were extracted and at the start of plant reproduction and at plant harvest. Fertility samples were also extracted at plant harvest. Samples were divided proportionally for analysis at the Arkansas Nematode Diagnostic Laboratory in Hope, Arkansas and the Soil Testing and Research Laboratory in Marianna, Arkansas. Prior to harvest, ten random plants at each of the 150 sampling points were extracted with a shovel and rated for incidence and severity of root galling and other yield limiting diseases. The trial was harvested on 19 September 2017 by a John Deere 9770 combine, using a John Deere 635F draper header, with John Deere GreenStar™ 3 2630 Display.

Meroney, Arkansas

In 2017, treatments were arranged in a randomized complete block with verification strips of 1,3-D applied with a modified liquid manure two weeks prior to planting, 12 rows wide with a

spacing of 96.52 cm per row, that extended the length of the field. Pioneer 46T59 soybean with abamectin (41.99 ml/140,000 seeds) seed treatment was compared to seeds without a nematicide seed treatment (control) and seeds without a nematicide seed treatment but planted within the 1,3-D treated soil. All soybean seeds were treated with CruiserMaxx® as a standard, while abamectin seeds were treated over the top of the standard CruiserMaxx®. Furthermore, Pioneer 46T59 is rated as resistant cultivar to *M. incognita*, according to company data. Ten sampling points within each of the 9 verification strips were designated by dividing the field length equally and marked with a Yuma 2, which data was collected throughout the duration of the trial. Nematode samples were extracted and at the start of plant reproduction and at plant harvest. Fertility samples were also extracted at plant harvest. Samples were divided proportionally for analysis at the Arkansas Nematode Diagnostic Laboratory in Hope, Arkansas and the Soil Testing and Research Laboratory in Marianna, Arkansas. Prior to harvest, ten random plants at each of the 90 sampling points were extracted with a shovel and rated for *M. incognita* severity and incidence. The trial was harvest on 14 September 2017 by a John Deere S680 combine (Deere & Company, Moline, IL) with a John Deere GreenStar™ 3 2630 Display.

Results

Backgate, Arkansas

Apparent soil electrical conductivity (ECa) varied within the field from 3 to 114 millisiemens meter^{-1} and ranged from sand to silty loam, respectively, with an average cation exchange capacity (CEC) of 8.05 meq/100g. Although ECa was dynamic across the field, only two soil textural zones were derived for data comparison, because of the minimal change in soil texture (Figure 6).

In 2016, nematode samples taken at planting showed no difference in *M. incognita* levels across treatments. Population densities were significantly lower at harvest in the 1,3-D verification strips than in the fluopyram treated strips, and verification strips lacking nematicide (Table 1). Consistent June, July and August average daily high temperatures remained from 30 to 35° C, with total monthly rainfall higher in July and August (Figure 7). During the growing season *C. sojina* was observed in the field and treated when lesions covered eight percent total leaf area index in the top one third of the plant canopy (average of the entire field). On 3 September 2016, visual differences in canopy densities were noticed between verification strips (Figure 8). Furthermore, treatment effects were noticeable with NDVI and CIR maps at 20-centimeter resolution, (Figures 9 and 10, respectively). Harvest data indicated 1,3-D averaged 3,485.3 kilograms hectare^{-1}, which was a significantly greater yield than the other treatments (Table 1, Figures 11 and 12). Fluopyram, abamectin, and the control treatments were not different from each other, and effects were not different among any of the treatments when compared by zone (P=0.01) (Figure 13). Additionally, the distribution of *M. incognita* at harvest was aligned with the treatments (P=0.08), suggesting that 1,3-D would be economically beneficial as a whole-field application across both soil textural zones when a susceptible soybean is planted.

In 2017, nematode samples taken at the beginning of plant reproduction did not differ in *M. incognita* population density, while populations were significantly greater at harvest in the abamectin verification strips than all other treatments (P=0.10) (Table 2). During the growing season, temperatures were slightly cooler than the previous year (Figure 14) with the monthly high temperatures remained from 21°C to 31°C. Monthly average precipitation ranged from 5 to 20 centimeters, with the lowest amount in July. On 17 August 2017, visual differences in canopy densities were noticed between verification strips (Figure 15). Treatment effects were detectable

with NDVI and NIR maps from the Sentinel-2 satellite at 10-meter resolution, (Figures 16 and 17, respectively). Harvest data indicated that 1,3-D verification strips applied in 2017 averaged 6,699 kilogram hectare^{-1} in Zone 2, which was significantly greater than all other treatments in all other zones except the residual 1,3-D verification strips in Zone 2 that were applied in 2016 (Figures 18 and 19). Fluopyram, abamectin, and the control treatments did not differ in Zone 1, but all treatments were significantly different from each other when compared by zones (Figure 19). The distribution of *M. incognita* across the field at harvest was consistent with the treatments (P=0.10). These results suggest that 1,3-D fumigation could be used as a two-year control of *M. incognita* and would be economically beneficial as a whole-field application (across both soil textural zones) when a susceptible soybean is planted.

Meroney, Arkansas

In 2017, nematode samples taken at the beginning of plant reproduction showed no difference in *M. incognita* population density (P=0.10) (Table 3). On 21 May 2017, treatments effects were detectable with a NDVI map from the Sentinel-2 satellite at 10-meter resolution (Figure 20). Treatment effects progressed further throughout the growing season and harvest data indicated that 1,3-D verification strips averaged 4,722 kilogram hectare^{-1}, which was significantly greater than all other (Table 3 and Figure 21). The population of *M. incognita* across the field at harvest was uniform (matching the treatments, P=0.10). These results suggest that 1,3-D fumigation could be used to control *M. incognita*, even when a nematode-resistant variety is planted.

Discussion

Site-specific management of *Meloidogyne incognita* using management zones and predicting crop damage areas using EC may offer grower and environmental, as well as economic,

benefits when compared to field-wide 1,3-D fumigation applications. *Meloidogyne incognita* management strategies are limited for crop protection. Therefore, site-specific management strategies may be crucial for sustained and profitable soybean production in the Mid-South. With the average size of farms growing in the United states (MacDonald et al. 2013), field sampling may not adequately characterize spatial distributions of *M. incognita* in individual fields, because sampling can be labor-intensive and (or) cost-prohibitive. Accurate spatial and temporal detection of *M. incognita* can be questionable with classical sampling methods, while soil textural variability within fields can be estimated relatively accurately and easily by calculating EC with soil mapping equipment (Monfort et al. 2007). This study is in agreement with recent research investigating site-specific nematicide applications as a management tool for producers in the Mid-South (Overstreet et al. 2014). By utilizing this technology along with other spatial data layers, such as yield and aerial imagery, growers can make more economical and efficient management decisions.

In the field near Backgate, Arkansas, soil EC was variable throughout the field with soil textures ranging from sand to silty loam. In both years of this study, *M. incognita* populations at harvest throughout the field correlated with treatments ($P=0.08$). Soybean yield was lower in 2016, a year that was moderately warm and received timely precipitation throughout the growing season (Figures 7 and 14). These environmental factors were conducive to *D. merdionalis*, as well as *M. incognita*, resulting in yield suppression across the entire field. Weather patterns in 2017 were similar to the previous year, except rainfall was less frequent during the month of July (Figure 7). Regardless of year, the relationship between *M. incognita* populations and soil texture was similar. Treatments differed significantly by zone in 2017; a year where rainfall was lower during reproduction and grain-fill stages, likely resulting in greater drought stress in the higher sand content soil texture. The uniformity of *M. incognita* populations during both years and under

different environmental factors implies that it may be possible to develop management strategies on a field-by-field basis that include site-specific nematicide applications based on soil textural zones.

This research showed that EC can be employed as an indicator of where nematicides will be most effective. Moreover, this trial highlighted that the soil fumigant 1,3-D protected yield in both zones during both years. In this study, nematode populations across the field remained uniform during both years, but yield reduction was significantly greater in the higher sand content soil texture during the second year. Similarly, Monfort et al. (2007) found that *M. incognita* damage to cotton was more closely tied to soil texture than to population density. This challenges some of the classical thoughts relating plant damage with *M. incognita* quantity (population densities) regardless of soil texture (Seinhorst 1965). All treatments had significantly lower yields in Zone 1, which consisted of a higher sand content. These results support the hypothesis that management zones can be established with EC and verification strips can be used to indicate areas of a field that should or should not be treated with a nematicide (Overstreet et al. 2014). The lack of a treatment response by zone in 2016 were likely attributable to more frequent rainfall during the critical reproduction and grain-fill stages, reducing plant stress. The fumigant 1,3-D worked best in both zones in both years, while seed treatments provided acceptable levels of control in the zone with the lower sand content during the second year. Based on this research, a whole-field application of 1,3-D would be recommended as a two-year control application, due to the uniformity of CEC values across the field and the response to the fumigant across both zones in both years.

Site-specific placement of nematicides in soybean holds potential for managing *M. incognita* in an economically and environmentally sound way without whole-field applications.

The use of EC mapping technologies to predict soil texture variability within fields has been suggested to be an effective management tool for nematodes in cotton in the Mid-South. The use of EC values to establish management zones does not eliminate the need for understanding the spatial and temporal distribution of *M. incognita*. The use of verification strips should be an essential component in understanding the intensity of damage and should be extensively used by growers during each growing season to improve the efficiency of their pesticide program (Overstreet et al. 2014). Spatial data equipment, such as that of the Veris EC Mapping sensors, can be combined with aerial imagery, in relation to crop health, to allow growers to implement better management decisions.

The Food and Agriculture Organization predicts there will be 9.6 billion people in the world by the year 2050, which means food production needs to increase 70% despite the limited availability of arable land (Guerrini 2015). To resolve the issue of future food demands, current production systems need to dramatically increase yields per hectare. Computer software will soon be able to create and perform management decisions based on field performance with little to no human intervention. However, this technological based farming will generate a tremendous amount of data. Often data management is complex, and each aspect will create thousands of data points that could include many different properties for each one. This huge amount of data requires the use of complex software and great computational power to manipulate and analyze the data. Often the requirements to deal with the data and synthesize it are beyond the capabilities of growers, consultants, and retail agriculture professionals (even using proprietary software). Further, the outputs from specific software are likely not to be compatible with other software. The incompatibleness makes it impossible to exchange and share data, which makes the process even that much more complicated. Because of the complexity, the adoption of precision agriculture and

site-specific management will be reliant on technologically trained agronomists and more data collection to determine its true value.

Literature Cited

2016. *Arkansas Acreage Report.* National Agicultural Statistics Service. Little Rock, Arkansas: United States Department of Agriculture.

Allen, T. W., Bradley, C. A., Damicone, J. P., Dufault, N. S., Faske, T. R., Hollier, C. A., . . . Young, H. 2017. Southern United States Soybean Disease Loss Estimates for 2016. *Proceedings of the Southern Soybean Disease Workers, forty-fourth Annual Meeting.* Pensacola, FL: Southern Soybean Disease Workers.

Allen, T. W., Damicone, J. P., Dufault, N. S., Faske, T. R., Hershman, D. E., Hollier, C. A., . . . Young, H. 2015. Southern United States Soybean Disease Loss Estimates for 2014. *Proceedings of the Southern Soybean Disease Workers, forty-second Annual Meeting.* Pensacola Beach, FL: Southern Soybean Disease Workers.

Chitwood, D. J., & Perry, R. N. 2009. Reproduction, Physiology and Biochemistry. In R. N. Perry, M. Moens, & J. L. Starr, *Root-knot Nematodes* (pp. 182-200). Cambridge, MA: CABI.

Choi, I., Subramanian, P., Shim, D., Oh, B.-J., & Hahn, B.-S. 2017. RNA-Seq of Plant-Parasitic Nematode Meloidogyne incognita at Various Stages of Its Development. *Frontiers in Genetics*, https://doi.org/10.3389/fgene.2017.00190.

Coats, R., & Ashlock, L. 2000. The Arkansas Soybean Industry. *Arkansas Soybean Handbook*, 1-6.

Evans, A., & Perry, R. N. 2009. Survival Mechanisms. In R. Perry, M. Moens, & J. L. Starr, *Root-knot Nematodes* (pp. 201-222). Cambridge, MA: CABI.

Favery, B., Quentin, M., Jaubert-Possamai, S., & Abad, P. 2016. Gall-forming root-knot nematodes hijack key plant cellular functions to induce multinucleate and hypertrophied feeding cells. *Journal of Insect Physiology*, 60-69.

Guerrini, F. 2015. *The Future of Agiculture? Smart Famring.* Forbes. Retrieved from https://www.forbes.com/sites/federicoguerrini/2015/02/18/the-future-of-agriculture-smart-farming/#3ef960053c42

Hurd, K., & Faske, T. 2017. Reproduction of Meloidogyne incognita and M. graminis on Several Grain Sorghum Hybrids. *Journal of Nematology*, 156-161.

Hussey, R. S. 1989. Disease-inducing secretions of plant-parasitic nematodes. *Annual Review of Phytopathology*, 123-141.

Koenning, S. R. 2014. Southern United States Soybean Disease Loss Estimate For 2013. *Proceedings of the Southern Soybean Disease Workers, forty-first Annual Meeting.* Pensacola Beach, FL: Southern Soybean Disease Workers.

MacDonald, J. M., Korb, P., & Hoppe, R. A. 2013. *Farm size and the organization of U.S. crop farming.* Washington, D.C.: United States Department of Agriculture, Economic Research Service.

Matthews, S., & Yang, T.-C. 2012. Mapping the results of local statistics: Using geographically weighted regression. *Demographic Research*, 151-166.

Mitkowski, N. A., & Abawi, G. S. 2003. Root-knot nematodes. *The Plant Health Instructor*, doi: 10.1094/PHI-I-2003-0917-01.

Monfort, W. S., Kirkpatrick, T. L., Rothrock, C. S., & Mauromoustakos, A. 2007. Potential for site-specific management of Meloidogyne incognita in cotton using soil textural zones. *Journal of Nematology, 39*, 1-8.

Mueller, T. G., Hartsock, N. J., Stombaugh, T. S., Shearer, S. A., Cornelius, P. L., & Barnhisel, R. I. 2003. Soil electrical conductivity map variability in limestone soils overlain by loess. *Agronomy Journal*, 496-507.

Ortiz, B. V., Sullivan, D. G., Perry, C., & Vellidis, G. (2011). Delineation of Management Zones for Southern Root-Knot Nematode using Fuzzy Clustering of Terrain and Edaphic Field Characteristics. *Communications in Soil Science and Plant Analysis 42*, 1972–1994.

Overstreet, C., McGawley, E. C., Khalilian, A., Kirkpatrick, T. L., Monfort, W. S., Henderson, W., & Mueller, J. D. 2014. Site specific nematode managment-development and success in cotton production in the United States. *Journal of Nematology, 46*, 309-320.

Prot, J.-C., & Van Gundy, S. D. 1981. Effect of Soil Texture and the Clay Component on Migration of Meloidogyne incognita Second-stage Juveniles. *Jouranl of Nematology*, 213-217.

Seinhorst, J. W. 1965. The Relation Between Nematode Density and Damage To Plants. *Nematologica 11(1)*, 137–154.

Starr, J. L., Koenning, S. R., Kirkpatrick, T. L., Robinson, A. F., Roberts, P. A., & Nichols, R. L. 2007. The Future of Nematode Management in Cotton. *Journal of Nematology*, 283-294.

Wheeler, T. A., Baugh, B., Kaufman, H., Schuster, G., & Siders, K. 2000. Variability in Time and Space of Meloidogyne incognita Fall Population Density in Cotton Fields. *Journal of Nematology 32(3)*, 258–264.

Wrather, J. A., Stevens, W. E., Kirkpatrick, T. L., & Kitchen, N. R. 2002. Effects of Site-specific Application of Aldicarb on Cotton in a Meloidogyne incognita-infested Field. *Journal of Nematology 34(2)*, 115–119.

Tables

Table 1. Backgate, Arkansas 2016: *Meloidogyne incognita* population density at planting (Pi) was collected and sampled on 13 May 2016. *Meloidogyne incognita* populations at harvest (Pf), Root Galling (0-9), and Root Health (0-9) were collected and sampled on 15 September 2016. Treatment strips were harvested on 22 September 2016.

Treatments	Pi (nematodes/100cm^3)	Pf [Y] (nematodes/100cm^3)	Root Galling	Root Health [Z]	Yield (kg/ha)
1,3-D	0.0	7.6b	0.6b	2.3a	3,485.3a
Fluopyram	3.8	103.4a	5.3a	1.8ab	2,268.2b
Control	2.5	85.4ab	7.1a	1.3b	2,105.4b
Abamectin	1.3	38.1ab	6.2a	1.3b	2,067.2b
LSD	NS	54.32	2.18	0.75	377.72
CV	49.41	58.4	22.8	22.4	9.59

[Y] The same letters are not significantly different (P=0.10).
[z] Ratings were based on the percent of functional roots left on the plant

Table 2. Backgate, Arkansas 2017: *Meloidogyne incognita* population density at the beginning of plant reproduction (Pm) and after harvest (Pf) were collected and sampled on 30 May 2017 and 5 October 2017, respectively. Root Galling (0-9) and Root Health (0-9) were collected and sampled on 2 August 2017. Treatment strips were harvested on 19 September 2017.

Treatments	Pm (nematodes/100cm^3)	Pf[Y] (nematodes/100cm^3)	Root Galling	Root Health[Z]	Yield (kg/ha)
1,3-D		11.4b	0.7	5.5	6,442.03a
Residual		26.7ab	1.9	5.1	5,854.62ab
Fluopyram		25.4ab	1.7	5.3	4,358.51bc
Control		19.0ab	2.5	5.3	3,673.74c
Abamectin		33.0a	2.0	5.3	4,608.40bc
LSD		21.46	NS	NS	760.20
CV		14.13	67.1	0.31	10.04

[Y] The same letters are not significantly different (P=0.10).
[z] Ratings were based on the percent of functional roots left on the plant

Table 3. Meroney, Arkansas 2017: *Meloidogyne incognita* population density at the beginning of plant reproduction (Pm) and after harvest (Pf) were collected and sampled on 30 May 2017 and 5 October 2017, respectively. Root Galling (0-9) and Root Health (0-9) were collected and sampled on 10 August 2017. Treatment strips were harvested on 14 September 2017.

Treatments	Pm (nematodes/100cm^3)	Pf (nematodes/100cm^3)	Root Galling	Root Health[Y]	Yield[Z] (kg/ha)
1,3-D	6.3	0	0.08	5.12	4,722.37a
Control	15.5	391.9	0.18	5.06	4,078.61b
Abamectin	26.6	188.3	0.3	5.15	4,362.17b
LSD	NS	NS	NS	NS	312.29
CV	84.26	145.51	111.36	2.92	4.06

[Y] Ratings were based on the percent of functional roots left on the plant
[Z] The same letters are not significantly different (P=0.10).

Figures

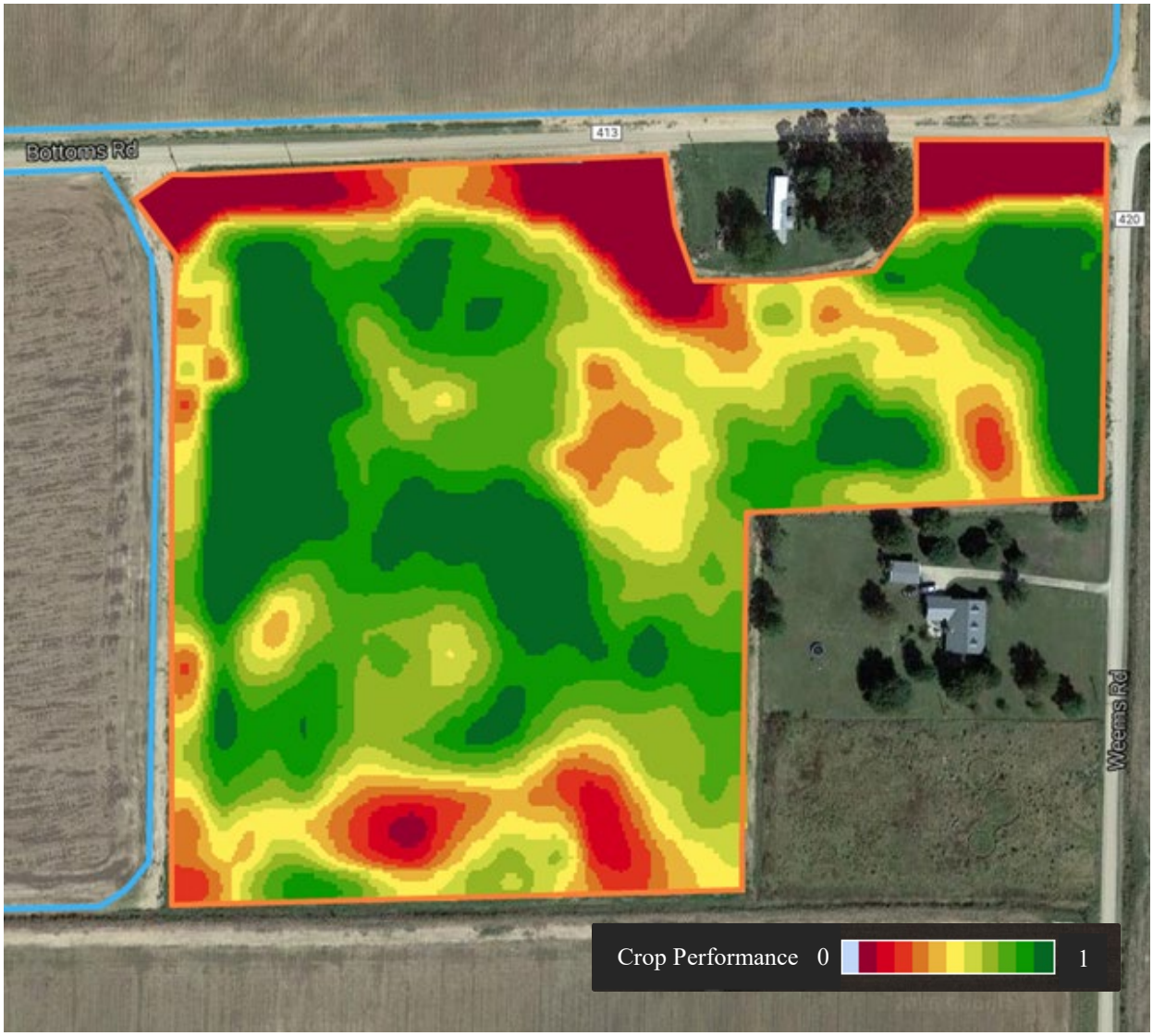

Figure 1. Normalized Difference Vegetation Index (NDVI) shows poor crop performance due to *Meloidogyne incognita* in a field near Backgate, Arkansas on 10 August 2015; the year prior to designing a test.

Figure 2. Soybeans in a field near Backgate, Arkansas showing symptoms caused by *Meloidogyne incognita*, including stunting and nutrient deficiency. Tissue samples collected on 6 June 2015 indicated that the plants were deficient in potassium and manganese.

Figure 3. Galling on soybean roots caused by *Meloidogyne incognita*.

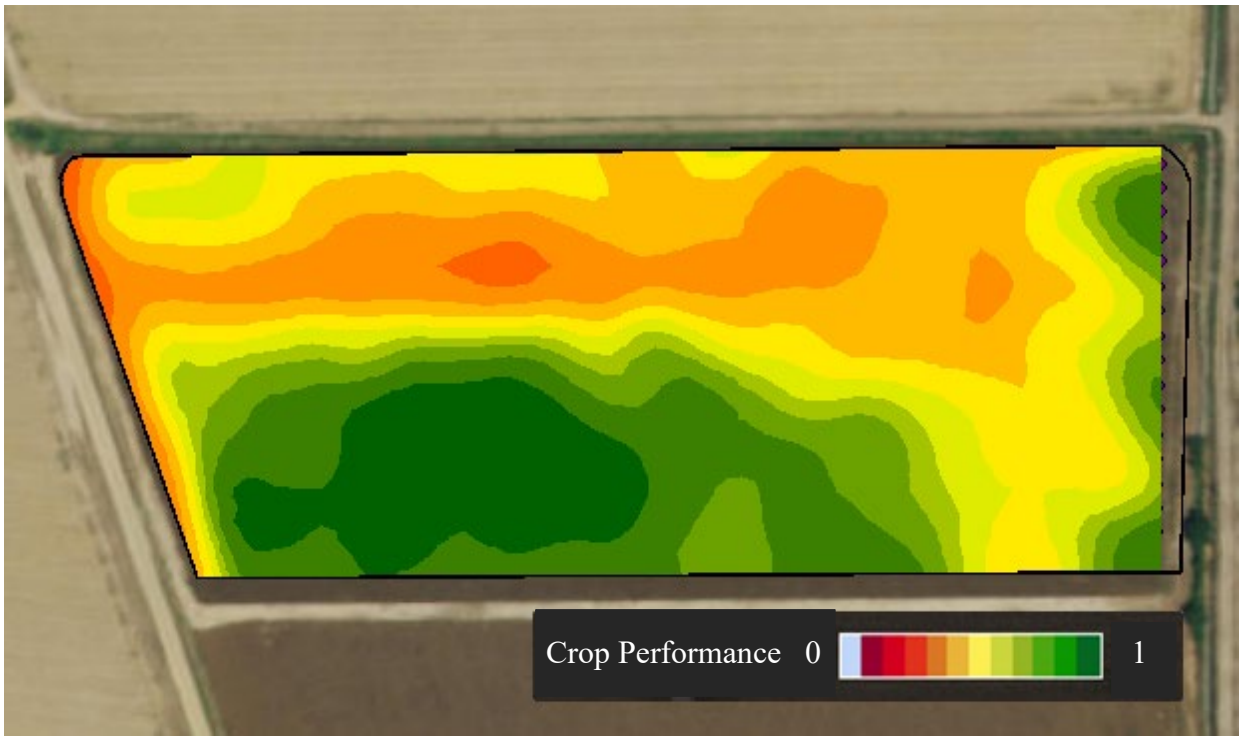

Figure 4. Normalized Difference Vegetation Index (NDVI) shows poor crop performance due to *Meloidogyne incognita* in a field near Meroney, Arkansas on 3 September 2016; the year prior to designing a test.

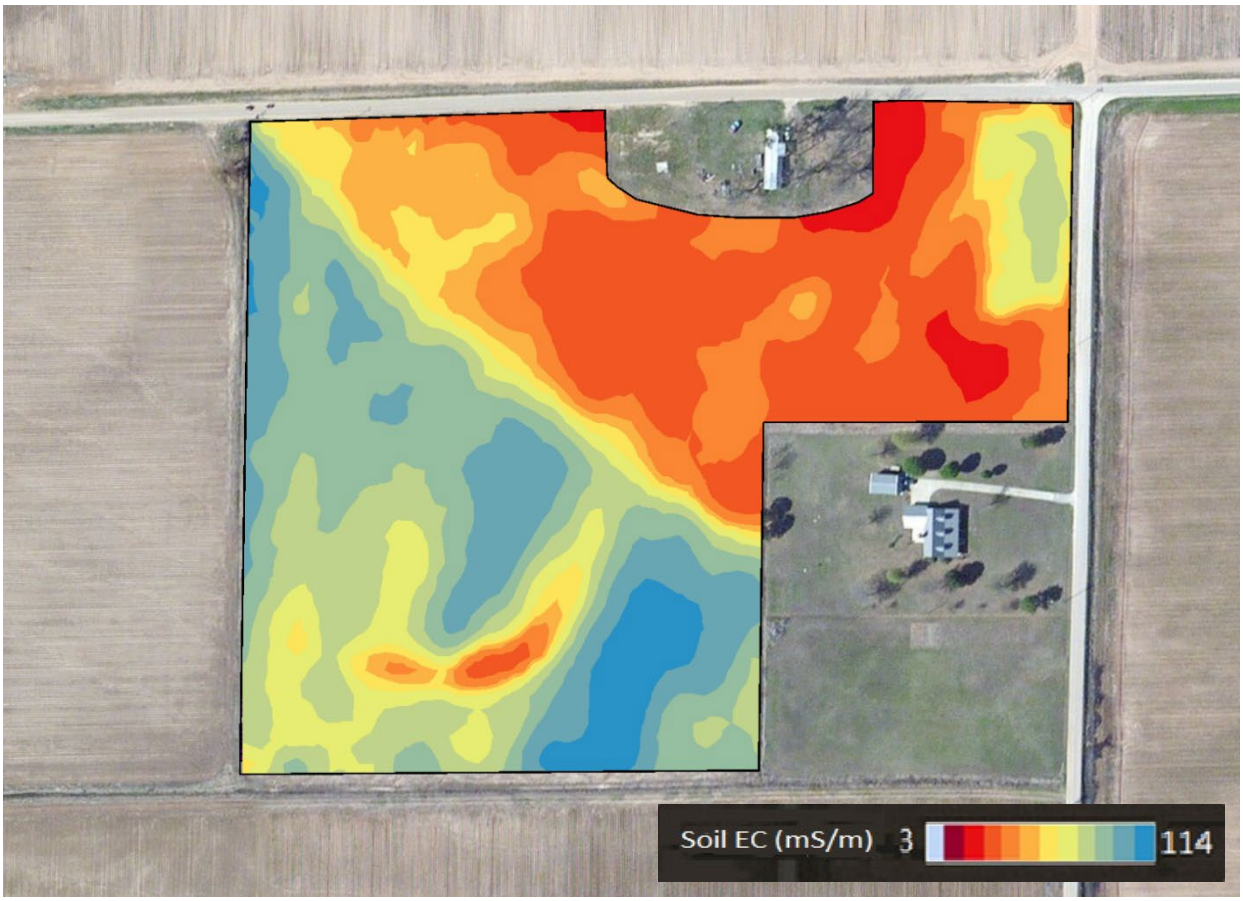

Figure 5. Soil EC Map from a field near Backgate, Arkansas. Red zones indicate soil texture with higher sand content, while dark blue zones indicate soil texture with higher silt content.

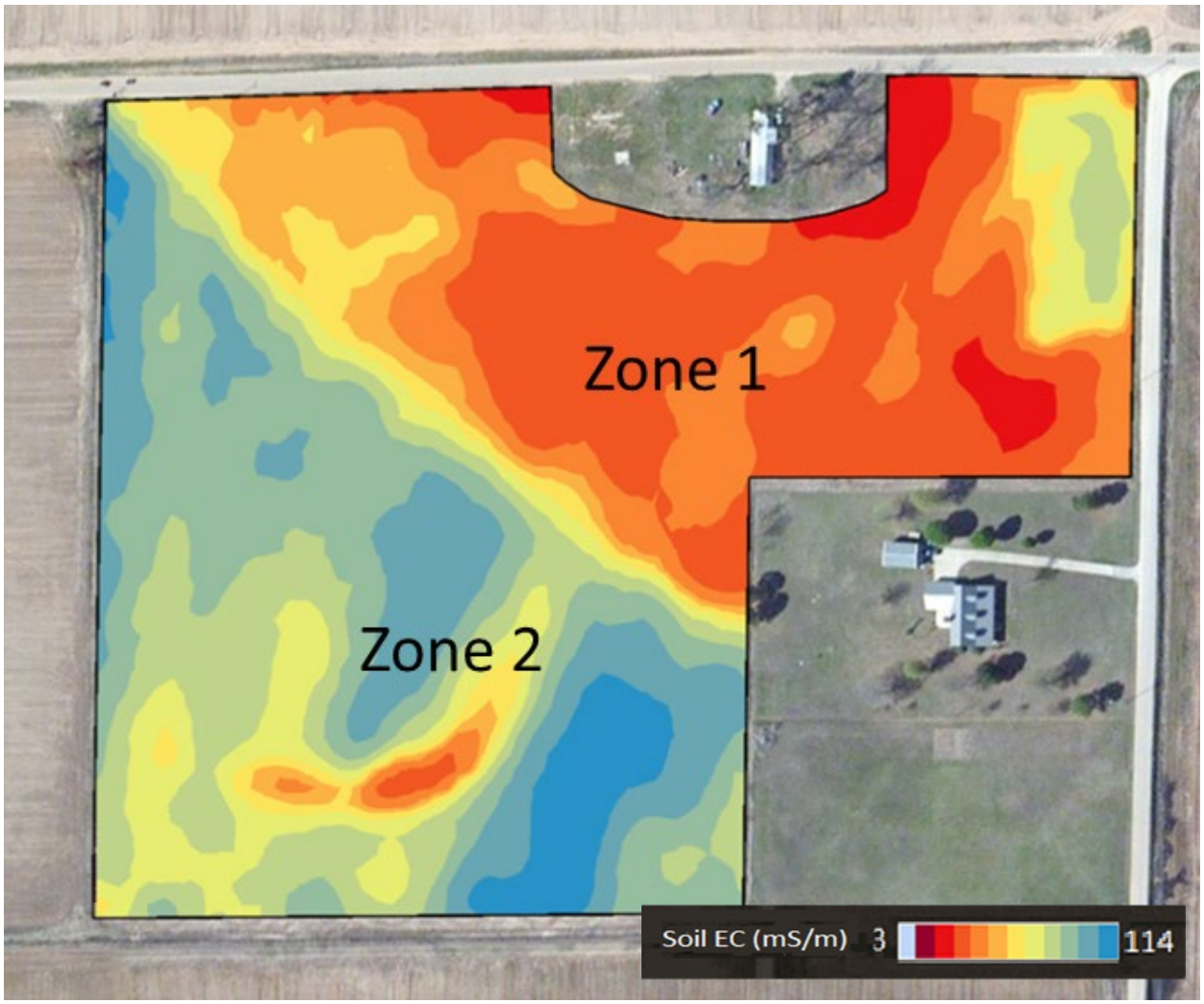

Figure 6. Soil EC Map from a field near Backgate, Arkansas indicating the two zones, represented by “Zone 1” and “Zone 2”, for data analysis.

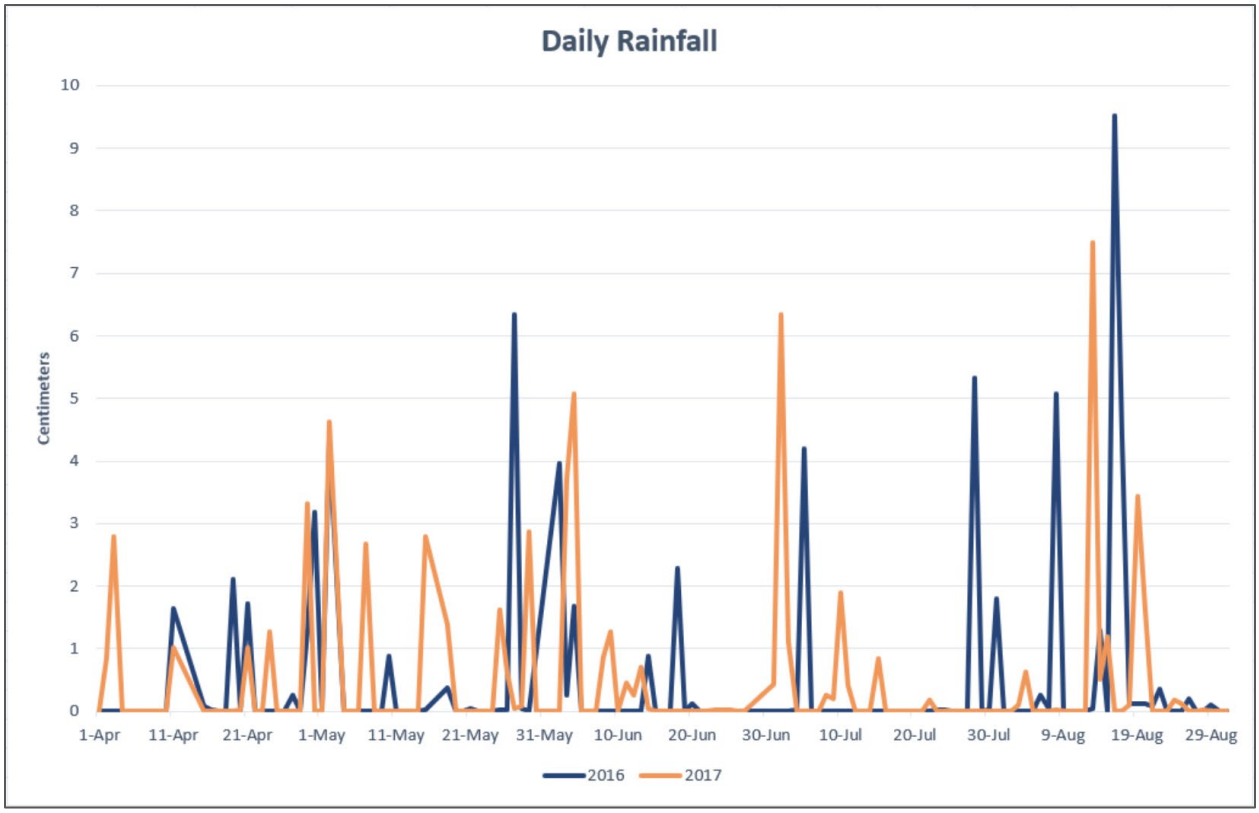

Figure 7. Daily rainfall amounts during the 2016 and 2017 growing seasons were collected from the Arkansas Post, Arkansas weather station with a coordinate location of 34.025° and -91.3444° (longitude and latitude, respectively), approximately nine kilometers from the Backgate, Arkansas location.

Figure 8. Difference in plant growth and appearance on 3 September 2016 due to *Meloidogyne incognita*; the untreated plots (left) matured earlier and were less dense than in the 1,3-D fumigated plots (right).

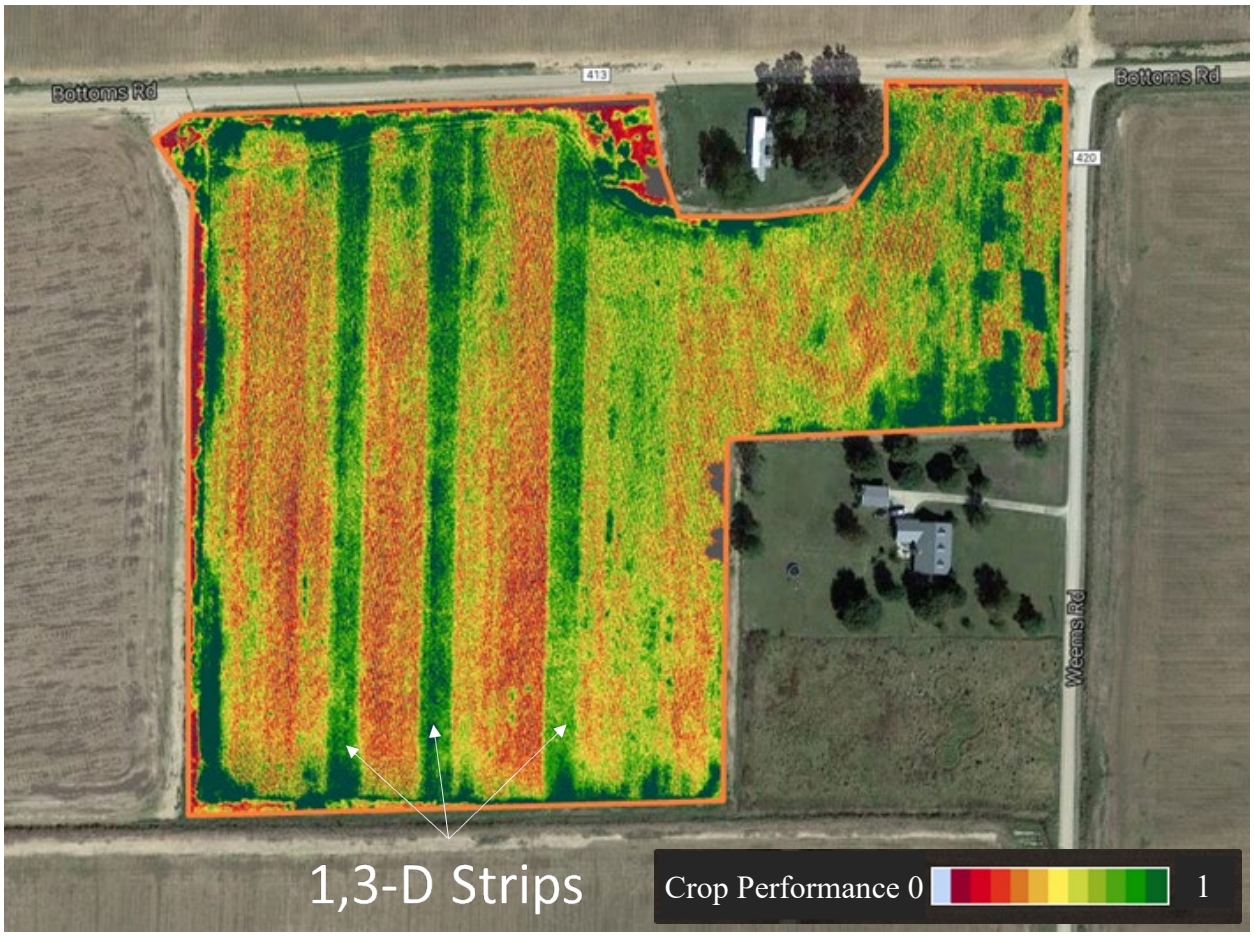

Figure 9. Normalized Difference Vegetation Index (NDVI) map at 20-centimeter resolution of a field near Backgate, Arkansas on 3 September 2016 was collected with a multispectral sensor attached to an airplane, showing an elevated level of crop performance in the three 1,3-D treated strips as opposed to the rest of the field.

Figure 10. Near infrared (NIR) map at 20-centimeter resolution of a field near Backgate, Arkansas on 3 September 2016 was collected with a multispectral sensor attached to an airplane, showing an elevated level of photosynthetic activity in the three 1,3-D treated strips as opposed to the rest of the field. Higher crop densities are characterized by bright red areas, while dark red to black areas indicate lower crop densities.

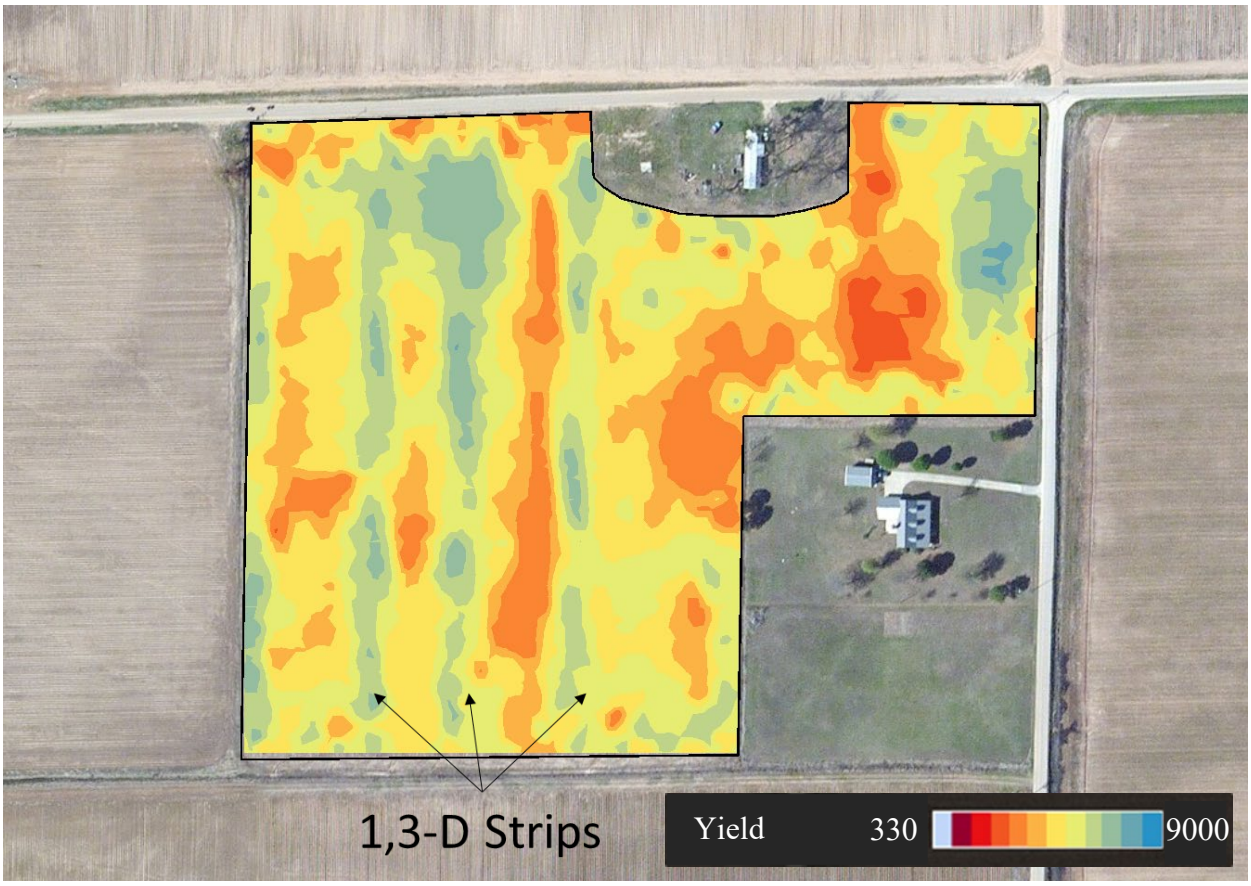

Figure 11. Interpolated yield map of a field near Backgate, Arkansas on 22 September 2016 indicate that 1,3-D treated strips had higher yields compared to the other treatments, as well as the entire field. Soybeans were harvested at an angle across the rows to generate an unbiased map.

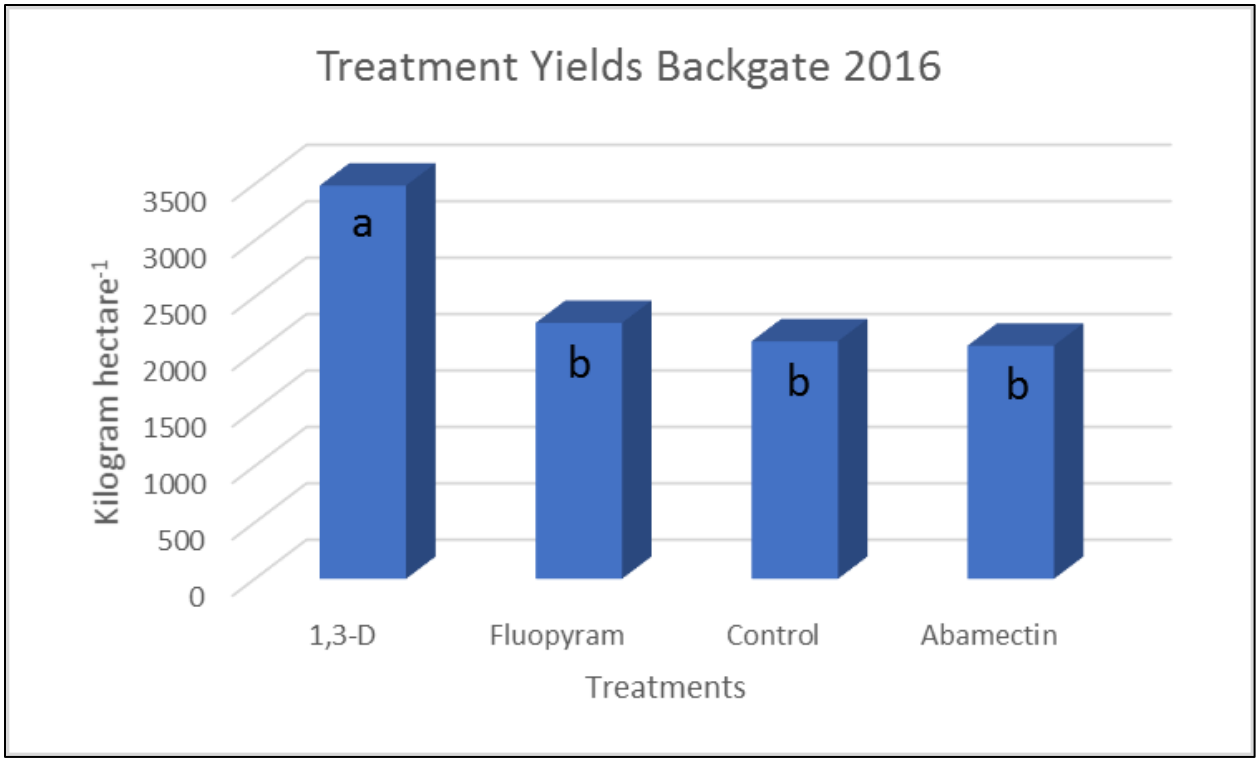

Figure 12. Soybean yield of treatment strips in a field near Backgate, Arkansas in 2016, showing that 1,3-D treated strips were significantly higher than the both nematicide seed treatments and the control treatment.

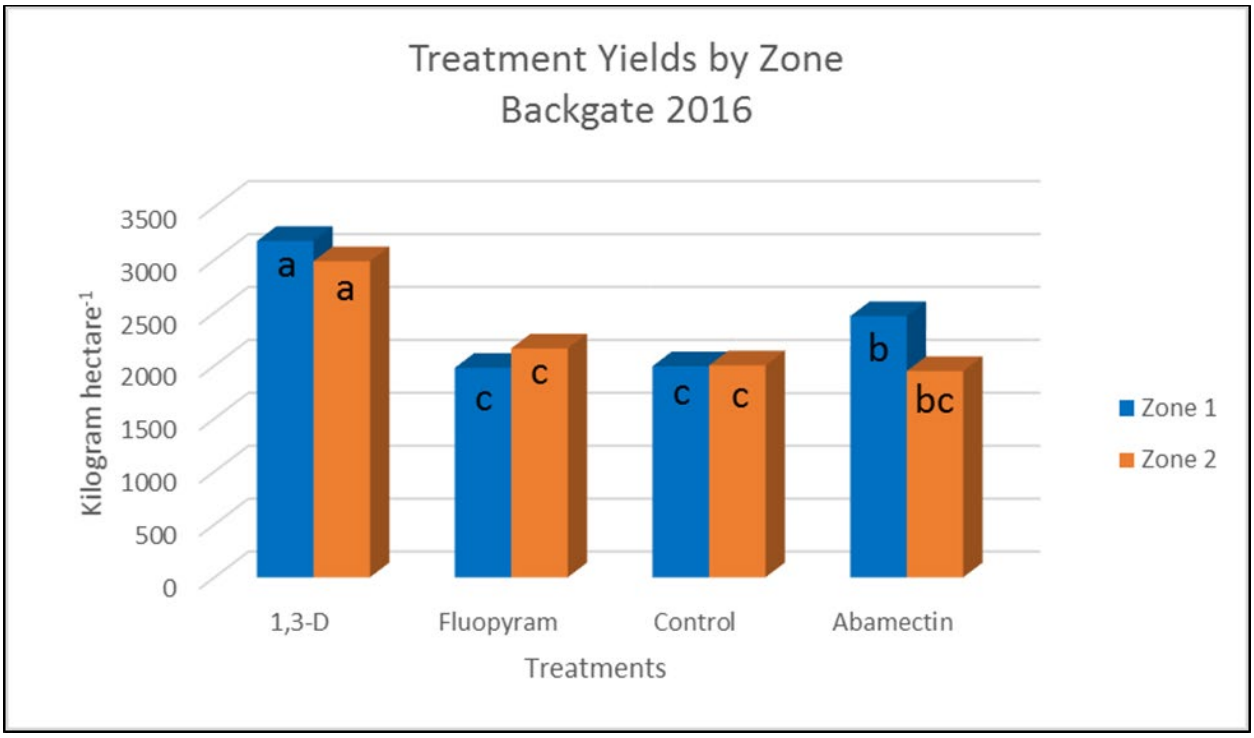

Figure 13. Soybean yield of treatment strips in a field near Backgate, Arkansas in 2016 was broken down into two soil textural zones, showing that treatment effects were not different between soil textural zones (P=0.01).

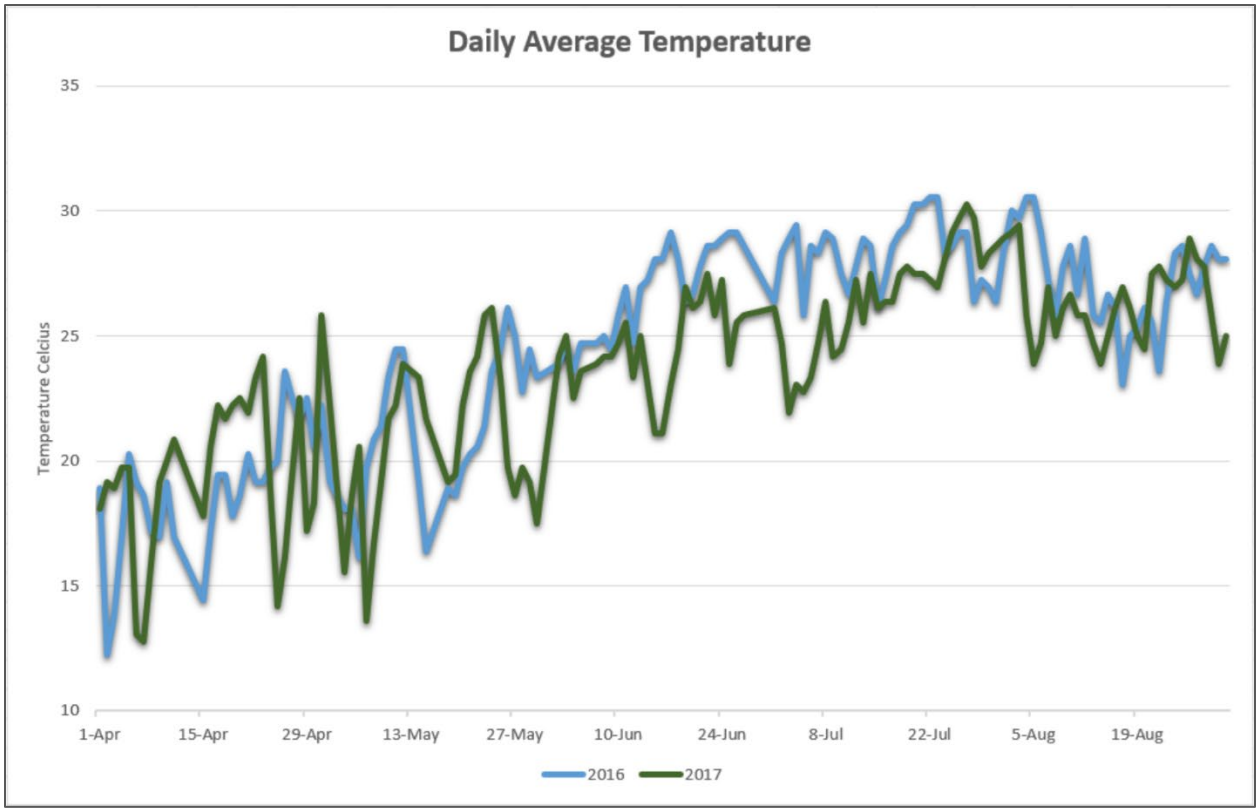

Figure 14. Daily average temperatures during the 2016 and 2017 growing seasons were collected from the Arkansas Post, Arkansas weather station with a coordinate location of 34.025° and -91.3444° (longitude and latitude, respectively), approximately nine kilometers from the Backgate, Arkansas location.

Figure 15. Visual differences between nematicide treated and untreated strips on 17 August 2017 in a field near Backgate, Arkansas. The control treatments (left) matured earlier due to poor plant health caused by *Meloidogyne incognita*, while 1,3-D fumigated strips (right) had an increase in crop density.

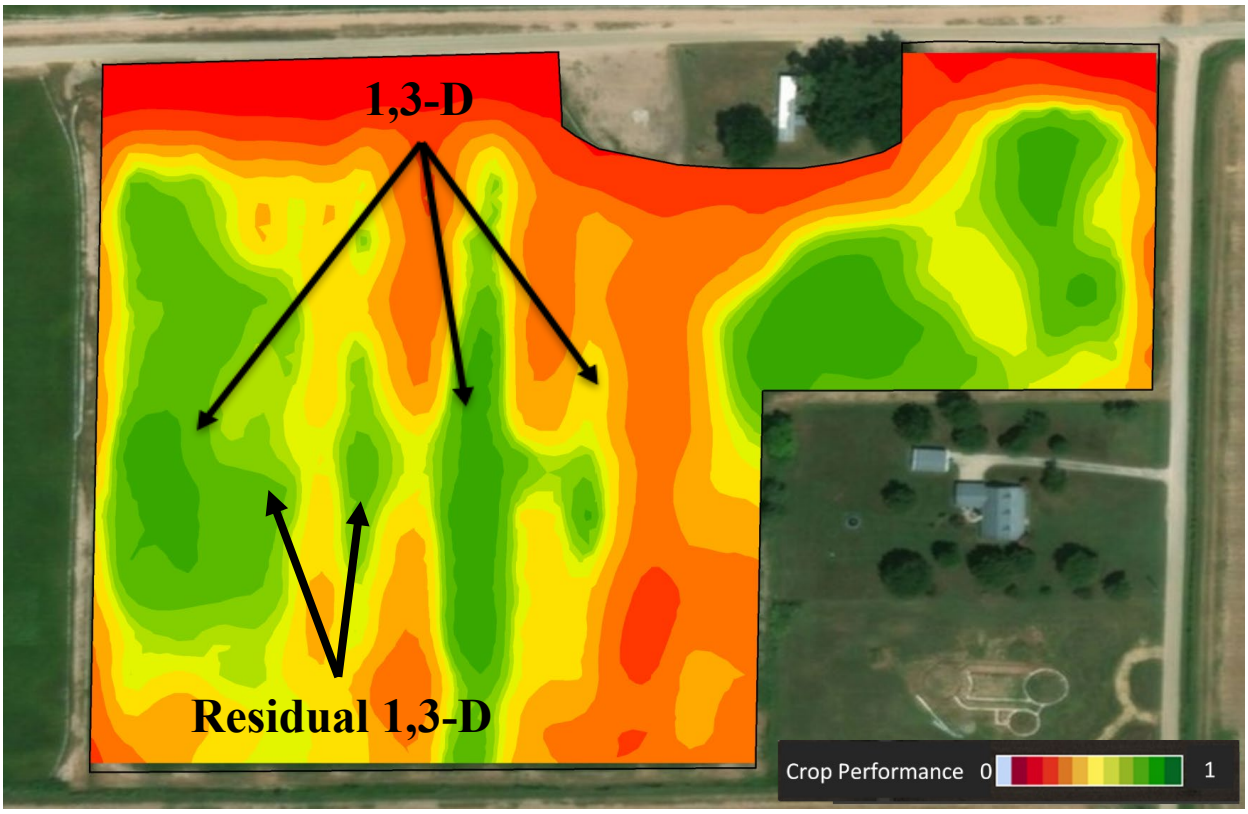

Figure 16. Normalized Difference Vegetation Index (NDVI) map at 10-meter resolution of a field near Backgate, Arkansas on 17 August 2017 was collected with the Sentinel-2 satellite showing an elevated level of crop performance in all three 1,3-D treated strips applied in 2017 and two of the three 1,3-D treated strips applied in 2016 (residual 1,3-D) as opposed to the entire field.

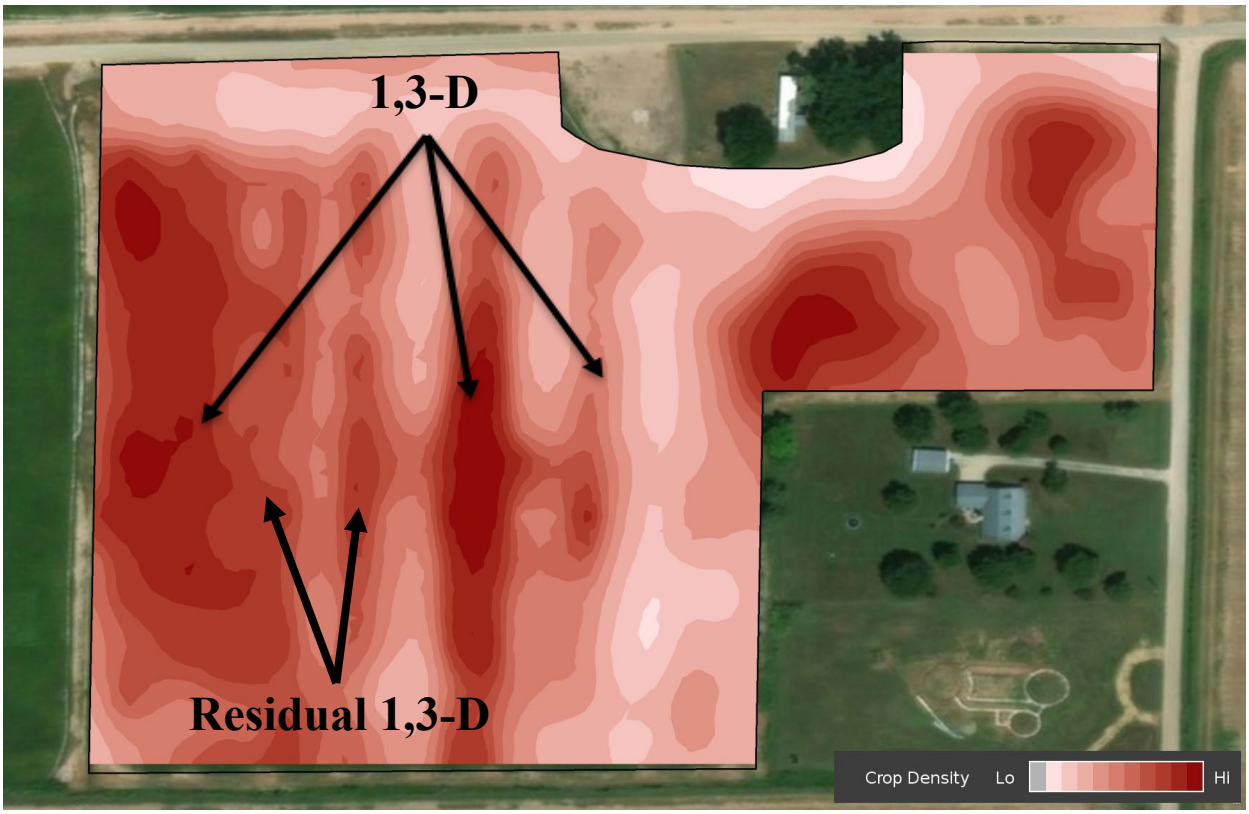

Figure 17. Near infrared (NIR) map at 10-meter resolution of a field near Backgate, Arkansas on 17 August 2017 was collected with the Sentinel-2 satellite, showing an elevated level of crop performance in all three 1,3-D treated strips applied in 2017 and two of the three 1,3-D treated strips applied in 2016 (residual 1,3-D) as opposed to the entire field.

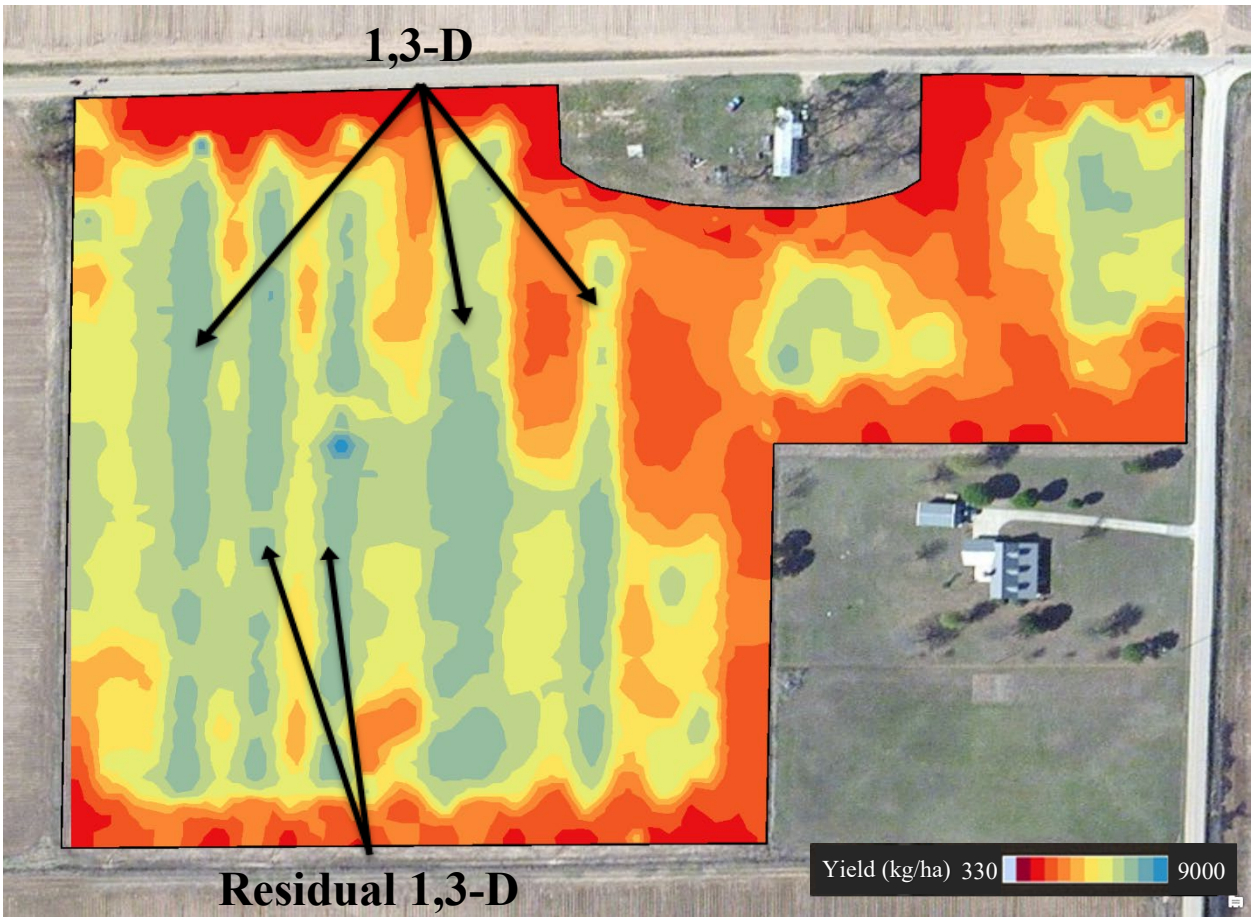

Figure 18. Interpolated soybean yield map of a field near Backgate, Arkansas on 19 September 2017, indicating that all three 1,3-D treated strips applied in 2017 and two of the three 1,3-D treated strips (residual 1,3-D) applied in 2016 had visibly higher yields when compared to the other treatments, as well as the entire field. Treatments were harvested one replication at a time.

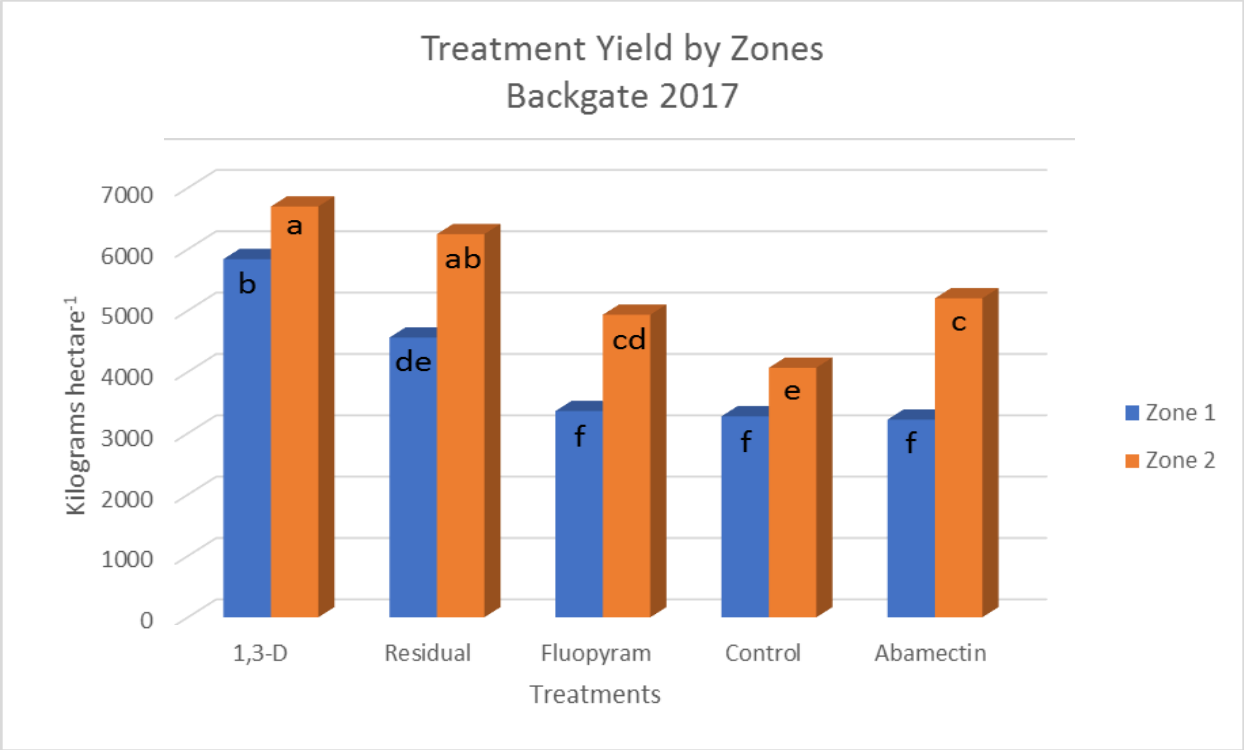

Figure 19. Soybean yield of a field near Backgate, Arkansas in 2017 was broken down into two soil textural zones, showing that 1,3-D treated strips applied in 2017 had an average yield of approximately 6699 kilogram hectare^{-1} in Zone 2, which was significantly greater than all other treatments in all other zones except the residual 1,3-D treated strips in Zone 2 that were applied in 2016 (residual 1,3-D). Fluopyram, abamectin, and the control treatments were not different in Zone 1, but all treatments were significantly different from each other by zones (P=0.01).

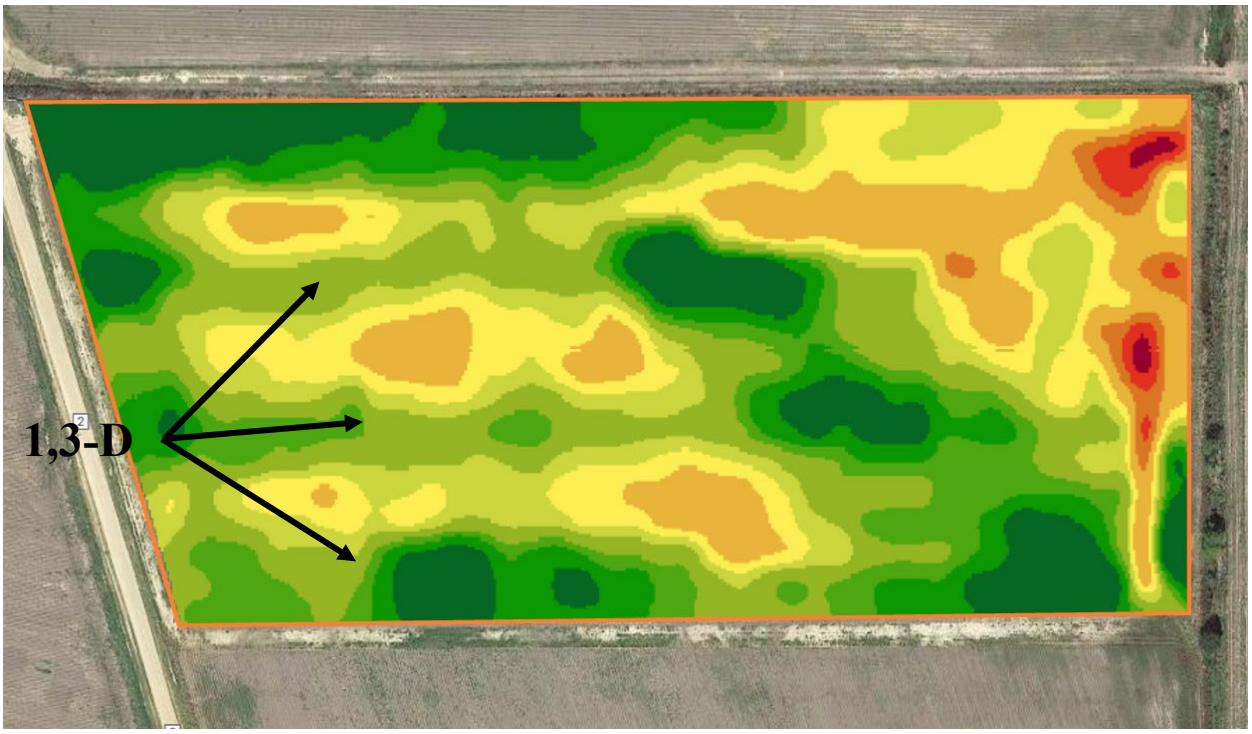

Figure 20. Normalized Difference Vegetation Index (NDVI) map at 10-meter resolution of a field near Meroney, Arkansas on 21 May 2017 was collected with the Sentinel-2 satellite, showing an elevated level of crop performance in all three 1,3-D treated strips as opposed to the entire field.

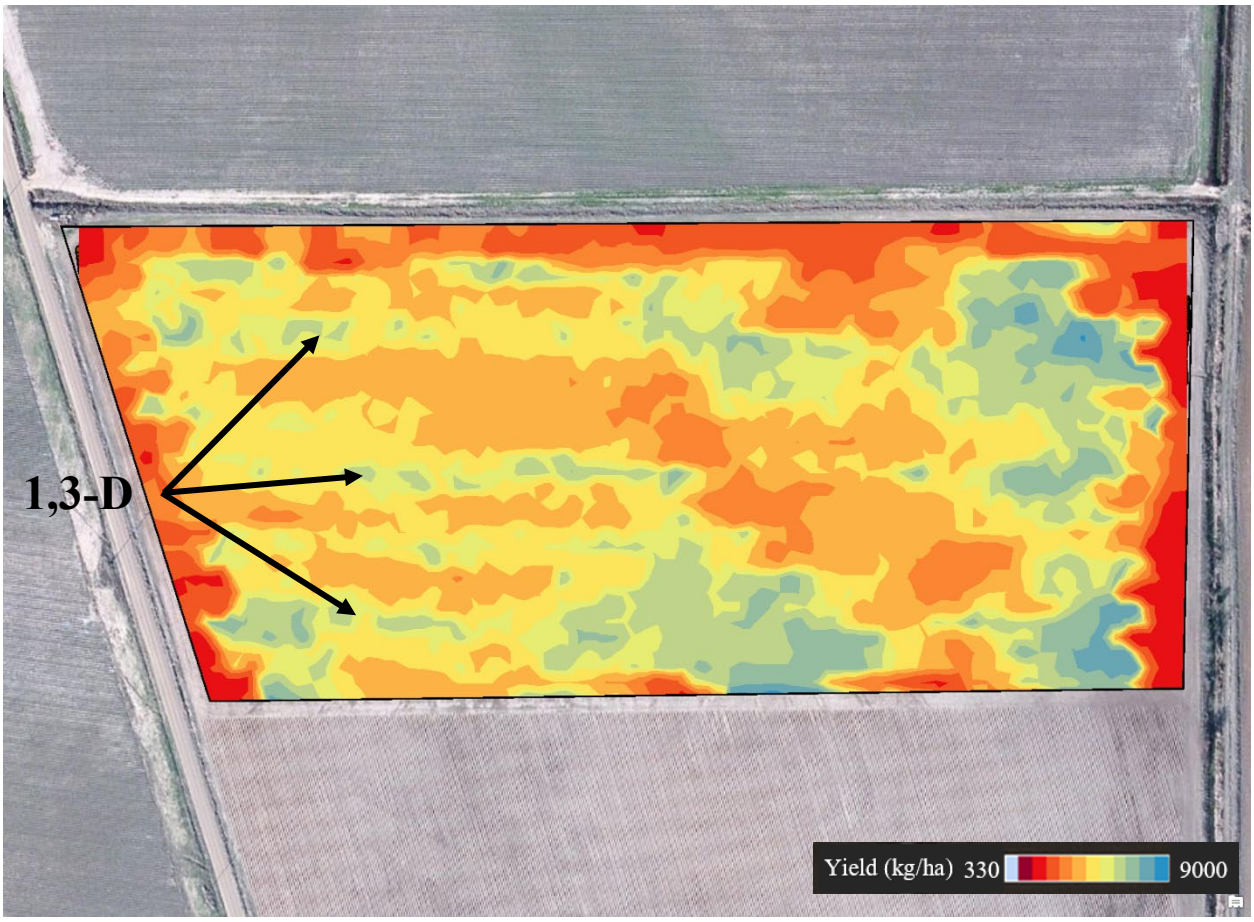

Figure 21. Interpolated soybean yield map of a field near Meroney, Arkansas on 14 September 2017, indicating that all three 1,3-D treated strips had higher yields when compared to the other treatments.

Chapter 3: Prediction of soybean yield using satellite imagery and spatial analysis

Introduction

Soybean were first introduced in Arkansas during the 1920's and gained popularity among growers around the mid-1900's. From 1960 to 1979, harvested hectares increased dramatically, and peaked in Arkansas in 1979 at 2.08 million hectares (Coats & Ashlock 2000). Although the amount is somewhat lower than in 1979, soybean are still grown on more hectares today than any other production crop in Arkansas, accounting for fifty-one percent of all principle crops planted in Arkansas; with 1.27 million hectares grown in 2016 (Arkansas Acreage Report 2016).

Evidence suggests, that a significant amount of soybean fields are affected by *Meloidogyne incognita* (southern root-knot nematode) in Arkansas (Allen et al. 2017). Recently, a cooperative effort between the Arkansas Soybean Promotion Board and the University of Arkansas System Division of Agriculture allowed subsidized nematode sampling for a period of three years. Approximately 16% and 28% of samples were positive for *M. incognita* in 2014 and 2015, respectively (Kikrpatrick et al. 2016).

Nematodes are microscopic roundworms many of which are soil-dwelling and plant-parasitic. Three *Meloidogyne* spp. (*M. incognita*, *M. javanica*, and *M. arenaria*) have been identified in the Mississippi Alluvial Plain and throughout the southern parts of Alabama, Georgia, South Carolina, and North Carolina, as well as in parts of California, Arizona, New Mexico, Texas, and Florida. In Arkansas *Meloidogyne incognita* is by far the predominant species, particularly in crop production (Kirkpatrick, personal communication). *Meloidogyne incognita* juveniles feed on plants by puncturing the root cells with a stylet. *Meloidogyne incognita* gets its common name, "root-knot", because infection results in the formation of galls or "knots" on infected soybean roots. Both feeding and the gall formation contribute to root dysfunction impacting the ability of

the plant to absorb water and translocate nutrients. Galls are visible on infected roots, and above ground symptoms may include stunted and yellowed plants. Also, nutrient deficiencies are commonly observed and associated with *M. incognita*-infected plants due to the reduced uptake of soil nutrients. Although nutrients in the soil may be optimum, root damage caused by nematodes may prevent essential nutrient uptake for plant growth and reduce yield. Management strategies are limited for nematodes in soybean.

Meloidogyne incognita overwinters in the soil as eggs in egg masses attached to the roots of the previous crop. Juveniles may also survive in the soil all winter, during favorable environments (Evans & Perry 2009). As the eggs develop, cells differentiate and the juvenile forms inside the egg protective coat, molting once inside the egg shell. At temperatures of 25° to 30°C, *M. incognita* eggs hatch and emerging second-stage juveniles (J2) move to soybean roots, targeting the root tip where cells are undifferentiated in the zone of root elongation. Upon root penetration, the nematode stylet secretes proteins and other compounds that allow the nematode to evade host defense response pathways and oxidative reactions. These secretions also help degrade the cell wall and allow for manipulation of cellular functions for nematode benefit (Hussey 1989). Cells are signaled to initiate cell division but do not complete the last stage, resulting in multi-nucleate cells called “giant-cells” (Favery et al. 2016). Once the giant-cell is formed, the nematode remains sedentary at the site and relies on the cell as the sole source of nutrients for the remainder of life (Choi et al. 2017). These structures along with the growing nematode result in the formation of visible galls or “knots” at the infection site on the roots (Mitkowski & Abawi 2003). The first juvenile stage (J1) forms completely within the egg shell, molts, then hatches into the J2 stage, completing the lifecycle (Chitwood & Perry 2009). The third and fourth molt occurs in the root,

becoming an adult, either male or female. Females begin to produce eggs in an exterior, gelatinous mass that can contain up to a thousand eggs.

In the field, distributions of *M. incognita* are associated with noticeable areas called "hot spots", which may suppress yield in sandy soils (Monfort et al. 2007). Because nematodes are clustered within a field, soil sampling using the grid sampling method may be effective in determining nematode populations but can be labor-intensive and cost-prohibitive (Wheeler et al. 2000; Wrather et al. 2002). Another sampling method is referred to as zone sampling. This method identifies areas (or zones) in a field with similar characteristics, such as crop yield, soil fertility or soil texture. Zone sampling could be an effective method to characterize the spatial distribution of nematode. Soils with ≥ 86% sand showed a significantly higher level of migration of *M. incognita* than soils between 75% and 86% (Prot & Van Gundy 1981). Also, Monfort et al. (2007) found that a smaller population of *M. incognita* are required to suppress yield in soil with a higher sand content. Therefore, soil texture is crucial in determining the infectivity of *M. incognita*, and percent sand is directly related to nematode migration and penetration of roots by the J2. Because classical soil texture analysis can be laborious, extensive research has been performed to identify other field characteristics that are less formidable to sample. Mueller et al. (2003) indicated that soil electric conductivity was correlated with soil texture, and based on research conducted in eleven cotton fields during 2005 and 2006, Ortiz et al. (2011) reported areas within a field that are likely to have high levels of *M. incognita* could be predicted using relative field changes in apparent EC.

The use of remote sensing to evaluate crop growth, development, and performance is a promising new area of agricultural research. Unmanned Aircraft Systems (UAS) and satellites have proven useful for evaluating crop health and managing pests site-specifically (Hunt et al. 2005; Sugiura et al. 2007; Torres-Sanchez et al. 2013). Nutrient requirements can be estimated

from chlorophyll concentration and biomass, which can be estimated from Leaf Area Index (Daughtry et al. 2000; Scharf & Lory 2002). Thermal sensors have been used to measure crop canopy temperature and to detect water stress of crops in agricultural fields (Wanjura et al. 2004). Evaporation can cool plant leaves close to air temperature, and sometimes below air temperature, as the crop transpires through stomata, resulting in plant canopy temperatures correlating with water stress of the crop (Luquet et al. 2003). However, the adoption of remote sensing by growers is limited by the lack of data collection and the understanding of data management. Furthermore, satellites are often linked with high costs and medocare resolution not sufficient for site-specific management, and UAS platforms are restricted by battery endurance and knowledge of data collection.

Increasing crop yields are crucial for creating a sustainable, economical, and environmental industry that will adequately solve the food demand of the world's popultaion now and in the future. Realtime and accurate prediction of crop yield can assist producers in making informed decisions regarding crop and nutrient management, yield estimation, marketing, storage, and transportation (Hammer et al. 2001; Kantanantha et al. 2010). Tucker et al. (1980) found that grain yields were highly correlated with normalized difference vegetation index (NDVI), and Das et al. (1993) used greenness and transformed vegetation indices to predict wheat yields at 85–110 days before harvest. These early studies led to crop yield estimation in several countries using satellite imagery. Ideally, satellite imagery could be used to predict accurate yield estimatations for any given field each year, regardless of the crop being grown. Providing yield prediction at a field level remains a challenge, because of limitations caused by the complicated relationships between remotely measurable parameters, crop productivity, and by the lack of data collected there of. Several models have been used to create yield predictions, but many current applications of these

models are only for large-scale production systems (Varela et al. 2017). Because commidties have leveled off at less profitable prices, farm management practices have shifted to more site-specific methods by evaluating in field varabilities, meaning more accurate yield predictions should be pursured.

Spatial regression examines, explores, and models geographical data, and it explains the factors that contribute to clustered distributions. Predictive modeling can also be derived from spatial regressions. Ordinary least squares (OLS) linear regression can be used to estimate the relationship between a dependent variable (y) and one or more independent variables (x) (Brusilovskiy 2010). Ordinary least squares regression generates predictions or models a dependent variable in terms of its relationships to a set of explanatory variables. The closer the data points are to the line, the more the variables are correlated with each other. Correlation is a statistical technique that can show if and how strongly variables are related. Probability-values (p-values) and coefficients in a regression analysis demonstrate which relationships in the model are statistically significant and the nature of those relationships. The coefficients describe the mathematical relationship between each independent variable and the dependent variable. The p-values for the coefficients indicate whether these relationships are statistically significant (Frost 2014). Recently these techniques have been used for more practical applications in pest management, specifically with *M. incognita*, and understanding losses (Liu et al. 2014). Geographically weighted regression (GWR) can be used when modeling spatial heterogeneity or uneven distributions across a study area. Unlike other regression models, GWR produces a separate equation for every feature and generates a set of location-specific parameters that can be mapped and analyzed (Matthews & Yang 2012). This technique can be used to predict spatial variability of a given variable. The Modifiable Areal Unit Problem (MAUP) impacts the results of

univariate and multivariate regressions and arises from errors that are created when data are grouped together for analysis (Openshaw 1984). The Modifiable Areal Unit Problem is associated with the use of scaling or zoning data related to geographical areas (Ervin 2012). The scale effect refers to how changing the number of areal units on a map can influence the interpretation, and the zoning effect refers to how changing the space within a map, while maintaining the same number of areal units, can also influence the interpretation (Jones 2011).

The objective of this work was to determine if a spatial predictive approach using GWR can be used to identify the value associated with nematode damage and field variability on a soybean farm. If successful, the technique could be used to determine the value of satellite imagery to help manage farms site-specifically and provide more accurate yield predictions.

Materials and Methods

Soybean fields were then planted with Armor 46-D08, which is tolerant to dicamba and glyphosate herbicides and susceptible to *M. incognita*, according to company data. The trials were harvested from 16 September 2017 to 19 September 2017 by a John Deere 9770 combine (Deere & Company, Moline, IL), using a John Deere 635F draper header (Deere & Company, Moline, IL), with John Deere GreenStar™ 3 2630 Display (Deere & Company, Moline, IL). Aerial imagery was captured by the Sentinel-2 satellite at 10-meter resolution and from an airplane mounted with a visual and near infrared (NIR) sensor at 20-centimeter resolution throughout the growing season (24 April 2017 until harvest) for observation of differences and treatment effects. Historical aerial imagery was also recovered with the Sentinel-2 satellite of prior years for comparison of normalized difference vegetation index (NDVI) and color infrared (CIR) variability throughout the field. Yield data was scaled and averaged, at 8-meter radii, to each centroid of the satellite image using the spatial join tool in ArcMap 10.4 (Esri, Carlsbad, CA). All data was projected to

WGS 1984 Web Mercator Auxiliary Sphere in order to align and merge data from different sources.

Verification Strips

In 2017, three fields with areas of sandy soil and known populations of *M. incognita* were chosen in Desha County, Arkansas, all bordering the Oakwood Bayou. The fields are informally named King Lee (33°55'40.26"N, 91°26'41.34"W), Lee East and West (33°55'13.66"N, 91°27'10.38"W), and Front (33°54'47.89"N, 91°26'53.48"W) (Figure 1). In each field, three verification strips of 1,3-dichloropropene (1,3-D) at a rate of 27.98 L/ha and a depth of approximately 10.16 cm were applied with a modified liquid manure applicator three weeks prior to planting, 12 rows wide measuring 96.52 cm per row, that extended the length of the field. Each coulter furrow was immediately sealed using press wheels mounted on the application rig and was left undisturbed until planting. Additionally, seven untreated strips were added to each field for adequate representation, and the strips were spaced in such a way to exhaust logical space and satisfy the MAUP. Point arrangement was based on the aggregation of observed nematode damage from previous seasons, existing within, across, and outside of damaged aggregated areas.

In each of the ten strips, ten georeferenced points were marked with a Yuma 2 (Trimble Inc., Sunnyvale, CA). Data were collected from each point in each field. Initially, a composite nematode sample was collected from the 1,3-D treated strips, as well as the untreated strips, and sent to the Plant Nematode Diagnostic Laboratory in Hope, Arkansas for analysis. During the growing season, at approximately the fifth reproductive growth stage, ten plants per point were collected, within a 3-meter radius, and rated for root galling and root health on a 0-9 percentage scale (Figure 2). At harvest, soil samples were collected and split with an appropriate amount of soil sent to the University of Arkansas Soil Testing Laboratory in Marianna, Arkansas for soil

chemical and fertility testing, and the other portion of the sample sent to the Plant Nematode Diagnostic Laboratory in Hope, Arkansas. This experimental design is consistent with the "strips and anchors" method developed by Dr. Terry Spurlock (Spurlock & Kirkpatrick 2017). The strips were used to determine treatment differences at specific areas of interest within a field as well as analyze data layers collected at different resolutions. Data were subjected to analysis of variance (ANOVA) and means of treatment effects and were separated using Fischer's least significant difference test in ARM 2016 (Gylling Data Management, INC., Brookings, SD). Treatment differences of 1,3-D versus the untreated adjacent points was determined using a two-sample t-test comparing data points within zones of the interpolated variables.

Remote Cluster

Also, in 2017, six fields near Backgate, Arkansas were chosen for yield prediction, which was determined by in-season crop health (captured by Sentinel-2) and actual yield recorded with a yield monitor. The fields are informally named Backgate (33°56'48.05"N, 91°23'57.34"W), Crossplace (33°57'3.01"N, 91°24'4.66"W), Robert 1 (33°57'11.52"N, 91°24'28.62"W), Robert 2 (33°57'3.24"N, 91°24'28.91"W), Robert 3 (33°56'56.19"N, 91°24'29.28"W), Glendon 2 (33°56'43.48"N, 91°24'52.83"W), Glendon 4 (33°56'31.06"N, 91°25'14.28"W), and Glendon 5 (33°56'30.31"N, 91°25'0.88"W) (Figures 3).

Satellite Imagery

Sentinel-2 is part of a fleet of satellites owned by the European Space Agency (ESA Headquarters, Paris, France) that was designed specifically for monitoring environmental aspects. The mission of Sentinel-2 is to provide information for agricultural practices by using the images to determine various plant indices, such as leaf area chlorophyll and water content indexes (Introducing Sentinel-2 2015). Sentinel-2 carries a high-resolution multispectral sensor with a span

of 13 spectral bands, from the visible and the near infrared to the shortwave infrared at different spatial resolutions, ranging from 10 to 60 meters (Table 1). The infrared spectrum is just outside of visible light, and multispectral sensors can capture what the human eye cannot see. These cameras capture near infrared (NIR) frequencies to help determine crop health and densities. Normalized difference vegetation index (NDVI) quantifies crop health by measuring the difference between NIR (B8) and visible red light (B4). To create NDVI maps, the normalized difference was taken from B8 and B4, and longitude and latitude were also added using a centroid placement to each pixel. Processing NIR maps included selecting B8 from each Sentinel-2 snapshot, and longitude and latitude were added using a centroid placement to each pixel. The values in each map were extracted as a Comma Separated Value (CSV) file and modified in Microsoft Excel (Microsoft Corporation, Redmond, WA) to separate the values by column.

Data Analysis

Aggregation of each variable was determined by univariate Moran's I in GeoDa 1.12 (GeoDa Center, University of Illinois-Chicago). Variables of interest were interpolated in ArcMap using ordinary kriging of spatially modeled semi-variograms. All variables were regressed with yield in GeoDa with univariate and multivariate models to determine biological phenomena driving yield differences using ordinary least squares (OLS) regression. Two models were determined and used for a few observations to adjust for spatial autocorrelation by using four Lagrange Multiplier (LM) tests, which are reported in the regression diagnostic output. The first two tests (LM-Lag and Robust LM-Lag) relate to the spatial lag model as the alternative. The next two tests (LM-Error and Robust LM-Error) refer to the spatial error model as the alternative. To determine a spatial regression specification, the results can be interpreted by using a flow chart (Figure 4). Quantifying spatial spillovers is a major advantage of spatial regression models. The

spatial error process can be characterized by the autoregressive or the moving average error process resulting in global and local spillovers, while spatial lag results in global spillovers (Liu et al. 2015).

Prediction

Predicted yield values were determined by using the Geographically Weighted Regression (GWR) tool in ArcMap. For each cluster, the observations with the highest R^2 and lowest P-values were used as the dependent and explanatory variables, as well as for the prediction location and prediction explanatory variables. Furthermore, a separate GWR model for every field in the cluster was determined by using the specific field as the dependent and explanatory variables and the prediction location and prediction explanatory variables were represented by the entire cluster (including the specific field). The predicted yield values were compared to actual yield values by using a joint hypothesis test in R.

Results

Verification Strips

The results of the two-sample t-test indicated that there were no differences in treatments in any fields, but NDVI imagery showed minor differences on 10 June 2017 (Figure 5). Furthermore, one field was thrown out, because yield data was not collected by a yield monitor. Since verification strips were not different, whole field satellite imagery was compared to yield. Spatial autocorrelation was observed by positive values of Moran's I, meaning that all observations were clustered. Of 15 NDVI and 15 NIR observations, 13 NDVI and 14 NIR images correlated with actual yield; the highest R^2 values being in the month July (P<0.001) (Tables 2 and 3; Figures 6 and 7, respectively). Furthermore, six and nine spatial models were used to adjust for spatial dependence in the NDVI and NIR images, relatively speaking, and all parameters but one tested

were highly significant (P<0.01) (Tables 4 and 5). Yield prediction using 25 July 2017 (NDVI0725; NIR0725) images of NDVI and NIR showed a significant correlation between the actual and predicted yeild (Tables 6 and 7; Figures 8 and 9).

Remote Cluster

Spatial autocorrelation was also observed by positive Moran's I values. Furthermore, 86.27% of 51 NDVI images and 84.31% of 51 NIR images correlated with actual yield (P<0.05) (Tables 8–15). Both NDVI and NIR images for the months of June and July significantly correlated with actual yield and average R^2 values for all fields were between 0.33 to 0.45 (P<0.0001) (Figures 10 and 11). Furthermore, six and nine spatial models were used to adjust for spatial dependence in the NDVI and NIR images, relatively speaking, and all parameters but one tested were highly significant (P<0.01) (Tables 16–23). Yield prediction using 10 June 2017 (NDVI0610; NIR0610) and 20 July 2017 (NDVI0720; NIR0720) images of NDVI and NIR shows a significant correlation between the actual and predicted yield (Tables 24–31; Figures 12–25).

Discussion

Yield prediction from early or even mid-season parameters can help assist growers in making informed decisions regarding marketing, storage and transportation. Furthermore, creating a yield prediction model based on historical data would help growers make future production decisions based on commodity prices and profitability. With the growing need of site-specific farm management, adequate understanding and interpretation of spatial analysis reports and production recommendations are crucial. Agronomists must be able to combine data from different sources, using different sample designs.

Spatial statistical techniques offer an opportunity to develop more precise yield estimates by exploiting spatial structures of explanatory variables (Liu et al. 2014). Aspatial standard, spatial

autoregressive error, and spatial autoregressive lag models were used to predict crop yield by using in-season crop health imagery. Of ten fields and 66 observations, 84.85% of NDVI and 86.36% of NIR images highly correlated with yield, suggesting that crop health can be used to determine yield variability within fields. Furthermore, 45 observations were spatially autocorrelated with yield. Both NDVI and NIR images resulted in higher R^2 values during the summer months of June and July, being the critical growth stages of reproduction and grain-fill for these fields. Using only the observations from June and July, yield was predicted with 17 NDVI and 17 NIR images and compared to actual yield. All the predicted values significantly correlated with yield ($P<0.0001$), but only 13 observations were spatial dependent. With this being said, crop health should be the main component of every yield prediction model, because it directly reflects yield in all ten fields.

Precision agriculture can generate a tremendous amount of data, and each practice can have thousands of associated data points with many different properties for each one. Manipulating and analysis of this huge quantity of data requires the use of complex software and high computation power. Most often synthesis and analysis of this data are beyond the capabilities of farmers, consultants, and retail agriculture professionals. In addition, outputs from many applications may not be universally compatible due to software proprietary concerns, making it impossible to exchange data. Because the concepts and technology that are associated with precision agriculture are relatively recent developments, not enough data has been collected to determine exactly what the results mean in certain scenarios. The adoption of precision agriculture and site-specific management will be reliant on trained agronomists and will require more data to determine its true value.

Literature Cited

2016. *Arkansas Acreage Report.* National Agricultural Statistics Service. Little Rock, Arkansas: United States Department of Agriculture.

Introducing Sentinel-2. 2015, April 23. Retrieved from European Space Agency: https://www.esa.int/Our_Activities/Observing_the_Earth/Copernicus/Sentinel-2/Introducing_Sentinel-2

Sentinel-2 User Handbook. 2015, 07 24. Retrieved from European Space Agency: https://earth.esa.int/documents/247904/685211/Sentinel-2_User_Handbook

Allen, T. W., Bradley, C. A., Damicone, J. P., Dufault, N. S., Faske, T. R., Hollier, C. A., . . . Young, H. 2017. Southern United States Soybean Disease Loss Estimates for 2016. *Proceedings of the Southern Soybean Disease Workers, forty-fourth Annual Meeting.* Pensacola, FL: Southern Soybean Disease Workers.

Anselin, L. 2005. *Exploring spatial data with GeoDa: A workbook.* Retrieved from Spatial Analysis Laboratory, Department of Geography, University of Illinois: http://www.unc.edu/~emch/gisph/geodaworkbook.pdf

Brusilovskiy, E. 2010. *Spatial Regression: A Brief Introduciton.* Philadelphia, PA: Business Intelligence Solutions. Retrieved from http://www.bisolutions.us/A-Brief-Introduction-to-Spatial-Regression.php

Chitwood, D. J., & Perry, R. N. 2009. Reproduction, Physiology and Biochemistry. In R. N. Perry, M. Moens, & J. L. Starr, *Root-knot Nematodes* (pp. 182-200). Cambridge, MA: CABI.

Choi, I., Subramanian, P., Shim, D., Oh, B.-J., & Hahn, B.-S. 2017. RNA-Seq of Plant-Parasitic Nematode Meloidogyne incognita at Various Stages of Its Development. *Frontiers in Genetics*, https://doi.org/10.3389/fgene.2017.00190.

Coats, R., & Ashlock, L. 2000. The Arkansas Soybean Industry. *Arkansas Soybean Handbook*, 1-6.

Das, D., Mishra, K., & Kalra, N. 1993. Assessing growth and yield of wheat using remotely-sensed canopy temperature and spectral indices. *International Journal of Remote Sensing*, 3081-3092.

Daughtry, C., Walthall, C. L., Kim, M. S., de Brown Colstoun, E., & McMurtrey, J. E. 2000. Estimating corn leaf chlorophyll concentration from leaf and canopy reflectance. *Remote Sensing of Environment*, 229–239.

Ervin, D. 2012. *MAUP.* Santa Barbara, CA: Advanced Spatial Analysis in the Population Sciences and Spatial Demography. Retrieved from http://gispopsci.org/maup/

Evans, A., & Perry, R. N. 2009. Survival Mechanisms. In R. Perry, M. Moens, & J. L. Starr, *Root-knot Nematodes* (pp. 201-222). Cambridge, MA: CABI.

Favery, B., Quentin, M., Jaubert-Possamai, S., & Abad, P. 2016. Gall-forming root-knot nematodes hijack key plant cellular functions to induce multinucleate and hypertrophied feeding cells. *Journal of Insect Physiology*, 60-69.

Frost, J. 2014. *How to Correctly Interpret P Values.* The Minitab Blog. Retrieved from http://blog.minitab.com/blog/adventures-in-statistics-2/how-to-correctly-interpret-p-values

Hammer, G. L., Hansen, J. W., Phillips, J. G., Mjelde, J. W., Hill, H., Love, A., & Potgieter, A. 2001. Advances in application of climate prediction in agriculture. *Agricultural Systems*, 515-553.

Hunt Jr, E. R., Cavigelli, M., Daughtry, C., McMurtrey III, J., & Walthall, C. L. 2005. Evaluation of Digital Photography from Model Aircraft for Remote Sensing of Crop Biomass and Nitrogen Status. *Precision Agriculture*, 359–378.

Hussey, R. S. 1989. Disease-inducing secretions of plant-parasitic nematodes. *Annual Review of Phytopathology*, 123-141.

Jones, R. 2011. *The Modifiable Areal Unit Problem in GIS.* Cartographica. Retrieved from https://blog.cartographica.com/blog/2011/5/19/the-modifiable-areal-unit-problem-in-gis.html

Kantanantha, N., Serban, N., & Griffin, P. 2010. Yield and price forecasting for stochastic crop decision planning. *Journal of Agricultural, Biological, and Environmental Statistics*, 362-380.

Kikrpatrick, T. L., Robinson, J., & Sullivan, K. 2016. A Survey of Arkansas Soybean Nematodes. *Proceedings of the 43rd Meeting of the Southern Soybean Disease Workers*, 35.

Liu, Z., Griffin, T., & Kirkpatrick, T. L. 2014. Statistical and Economic Techniques for Site-specific Nematode Managment. *Journal of Nematology, 46*, 12-17.

Liu, Z., Griffin, T., Kirkpatrick, T. L., & Monfort, W. S. 2015. Spatial econometric approaches to developing site-specific nematode management strategies in cotton production. *Precision Agriculture*, 587-600

Luquet, D., Begue, A., Vidal, A., Clouvel, P., Dauzat, J., Olioso, A., . . . Tao, Y. 2003. Using multidirectional thermography to characterize water status of cotton. *Remote Sensing of Environment*, 411–421.

Matthews, S., & Yang, T.-C. 2012. Mapping the results of local statistics: Using geographically weighted regression. *Demographic Research*, 151-166.

Mitkowski, N. A., & Abawi, G. S. 2003. Root-knot nematodes. *The Plant Health Instructor*, doi: 10.1094/PHI-I-2003-0917-01.

Monfort, W. S., Kirkpatrick, T. L., Rothrock, C. S., & Mauromoustakos, A. 2007. Potential for site-specific management of Meloidogyne incognita in cotton using soil textural zones. *Journal of Nematology, 39*, 1-8.

Mueller, T. G., Hartsock, N. J., Stombaugh, T. S., Shearer, S. A., Cornelius, P. L., & Barnhisel, R. I. 2003. Soil electrical conductivity map variability in limestone soils overlain by loess. *Agronomy Journal*, 496-507.

Openshaw, S. 1984. The Modifiable Areal Unit Problem. *Geo Books*.

Ortiz, B. V., Sullivan, D. G., Perry, C., & Vellidis, G. 2011. Delineation of Management Zones for Southern Root-Knot Nematode using Fuzzy Clustering of Terrain and Edaphic Field Characteristics. *Communications in Soil Science and Plant Analysis 42*, 1972–1994.

Prot, J.-C., & Van Gundy, S. D. 1981. Effect of Soil Texture and the Clay Component on Migration of Meloidogyne incognita Second-stage Juveniles. *Jouranl of Nematology*, 213-217.

Scharf, P. C., & Lory, J. A. 2002. Calibrating corn color from aerial photographs to predict sidedress nitrogen need. *Agronomy Journal*, 397–404.

Spurlock, T., & Kirkpatrick, T. L. 2017. Proceedings of the Southern Soybean Disease Workers 44th Annual Meeting. *Southern Soybean Disease Workers.* Pensacola, FL: Southern Soybean Disease Workers.

Sugiura, R., Noguchi, N., & Ishii, K. 2007. Correction of low-altitude thermal images applied to estimating of soil water status. *Biosystems Engineering*, 301–313.

Torres-Sanchez, J., Lopez-Granados, F., Isabel De Castro, A., & Manuel Pena-Barragan, J. 2013. Configuration and Specifications of an Unmanned Aerial Vehicle (UAV) for Early Site Specific Weed Management. *PLoS One*, e58210.

Tucker, C. J., Holben, B. N., Elgin Jr, J. H., & McMurtrey III, J. E. 1980. Relationship of spectral data to grain yield variation. *Photogrammetric Engineering and Remote Sensing*, 657–666.

Varela, S., Assefa, Y., Vara Prasad, P. V., Peralta, N. R., Griffin, T. W., Sharda, A., . . . Ciampitti, I. A. 2017. Spatio-temporal evaluation of plant height in corn via unmanned aerial systems. *Journal of Applied Remote Sensing*, 036013.

Wanjura, D. F., Maas, S. J., Winslow, J. C., & Upchurch, D. R. 2004. Scanned and spot measured canopy temperatures of cotton and corn. *Computers and Electronics in Agriculture*, 33-48.

Wheeler, T. A., Baugh, B., Kaufman, H., Schuster, G., & Siders, K. 2000. Variability in Time and Space of Meloidogyne incognita Fall Population Density in Cotton Fields. *Journal of Nematology 32(3)*, 258–264.

Wrather, J. A., Stevens, W. E., Kirkpatrick, T. L., & Kitchen, N. R. 2002. Effects of Site-specific Application of Aldicarb on Cotton in a Meloidogyne incognita-infested Field. *Journal of Nematology 34(2)*, 115–119.

Tables

Table 1. The spatial resolution of Sentinel-2 is dependent on each spectral band (Sentinel-2 User Handbook, 2015).

Sentinel-2 Bands	Central Wavelength (nm)	Resolution (m)	Bandwidth (nm)
Band 1 - Coastal aerosol	443	60	20
Band 2 - Blue	490	10	65
Band 3 - Green	560	10	35
Band 4 - Red	665	10	30
Band 5 - Vegetation Red Edge	705	20	15
Band 6 - Vegetation Red Edge	740	20	15
Band 7 - Vegetation Red Edge	783	20	20
Band 8 - NIR	842	10	115
Band 8B - Narrow NIR	865	20	20
Band 9 - Water vapour	945	60	20
Band 10 - SWIR - Cirrus	1375	60	30
Band 11 - SWIR	1610	20	90
Band 12 - SWIR	2190	20	180

Table 2. Satellite imagery of in-season crop health were regressed with actual yield to determine correlation by using classical OLS for the King Lee field.

Covariate	R-squared	Adjusted R-squared	Coefficient	Std Error	t-Statistic	Probability
NDVI0424	0.0128	0.0120	49.6708	11.8871	4.1785	< 0.0001
NDVI0501	0.0152	0.0145	49.9521	10.9345	4.5683	< 0.0001
NDVI0514	0.0436	0.0429	62.8643	8.0106	7.8477	< 0.0001
NDVI0610	0.2578	0.2573	87.4690	4.0359	21.6727	< 0.0001
NDVI0720	0.5441	0.5438	248.8000	6.1932	40.1732	< 0.0001
NDVI0725	0.5506	0.5502	276.0770	6.7839	40.6960	< 0.0001
NDVI0822	0.1828	0.1822	126.4970	7.2741	17.3901	< 0.0001
NDVI0906	0.1418	0.1412	-71.7509	4.8004	-14.9468	< 0.0001
NIR0424	0.0999	0.0992	0.0156	0.0013	12.2488	< 0.0001
NIR0501	0.1433	0.1427	0.0280	0.0019	15.0389	< 0.0001
NIR0514	0.1485	0.1479	0.0171	0.0011	15.3577	< 0.0001
NIR0610	0.2540	0.2535	0.0146	0.0007	21.4558	< 0.0001
NIR0720	0.4876	0.4872	0.0259	0.0007	35.8661	< 0.0001
NIR0725	0.4888	0.4884	0.0300	0.0008	35.9554	< 0.0001
NIR0822	0.1195	0.1188	0.0348	0.0026	13.5447	< 0.0001
NIR0906	0.0765	0.0758	-0.0191	0.0018	-10.5825	< 0.0001

Table 3. Satellite imagery of in-season crop health were regressed with actual yield to determine correlation by using classical ordinary least squares for the Lee field.

Covariate	R-squared	Adjusted R-squared	Coefficient	Std Error	t-Statistic	Probability
NDVI0424	0.0064	0.0058	-45.1447	13.4855	-3.3477	0.0008
NDVI0501	0.0003	-0.0003	-8.1031	11.8014	-0.6866	0.4924
NDVI0514	0.0000	-0.0005	-2.0705	9.0146	-0.2297	0.8184
NDVI0610	0.2107	0.2103	106.9020	4.9473	21.6081	< 0.0001
NDVI0725	0.5007	0.5004	189.6450	4.5288	41.8755	< 0.0001
NDVI0903	0.0115	0.0110	22.1947	4.9159	4.5149	< 0.0001
NDVI0906	0.0073	0.0067	-17.8605	4.9777	-3.5881	0.0003
NIR0424	0.0329	0.0324	-0.0074	0.0010	-7.7165	< 0.0001
NIR0501	0.0294	0.0288	-0.0082	0.0011	-7.2764	< 0.0001
NIR0514	0.0151	0.0146	-0.0036	0.0007	-5.1848	< 0.0001
NIR0610	0.0005	-0.0001	-0.0004	0.0005	-0.8922	0.3724
NIR0725	0.3431	0.3427	0.0296	0.0010	30.2229	< 0.0001
NIR0903	0.0897	0.0892	-0.0218	0.0017	-13.1295	< 0.0001
NIR0906	0.1621	0.1616	-0.0254	0.0014	-18.3950	< 0.0001

Table 4. Spatial Lag and spatial error models were determined and used for a few observations to adjust for spatial autocorrelation for the King Lee field.

Covariate[Y]	R-Square	Coefficient	Std Error	Z-Value	Probability	Spatial Model[Z]
NDVI0424	0.7816	3.3711	5.5913	0.6029	0.5466	Lag
NDVI0501						
NDVI0514	0.7815	10.4519	3.8899	2.6869	0.0072	Lag
NDVI0610	0.7917	88.3343	7.4277	11.8926	< 0.0001	Error
NDVI0720						
NDVI0725						
NDVI0822	0.7816	87.8451	13.4091	6.5512	< 0.0001	Error
NDVI0906	0.7908	-86.7601	9.3043	-9.3248	< 0.0001	Error
NIR0424	0.7817	0.0030	0.0007	4.6057	< 0.0001	Lag
NIR0501	0.7809	0.0050	0.0010	5.0101	< 0.0001	Lag
NIR0514	0.7816	0.0035	0.0006	5.6604	< 0.0001	Lag
NIR0610						
NIR0720	0.7963	0.0253	0.0013	18.8415	< 0.0001	Error
NIR0725	0.7978	0.0295	0.0016	18.9996	< 0.0001	Error
NIR0822	0.7808	0.0057	0.0013	4.3331	< 0.0001	Lag
NIR0906	0.7852	-0.0184	0.0030	-6.1156	< 0.0001	Error

[Y] Indicates that blank rows were not spatially dependent and classical ordinary least squares regression was sufficient for these snapshots.

[Z] Two spatial models were determined and used for a few observations to adjust for spatial autocorrelation by using the Lagrange Multiplier (LM) tests, which are reported in the regression diagnostic output.

Table 5. Spatial Lag and spatial error models were determined and used for a few observations to adjust for spatial autocorrelation for the Lee field.

Covariate[Y]	R-Square	Coefficient	Std Error	Z-Value	Probability	Spatial Model[Z]
NDVI0501						
NDVI0514						
NDVI0610	0.8028	67.4038	6.7296	10.0160	< 0.0001	Error
NDVI0725						
NDVI0903						
NDVI0906						
NIR0424						
NIR0501						
NIR0514						
NIR0610						
NIR0725	0.8008	0.0073	0.0006	11.5984	< 0.0001	Lag
NIR0903	0.8006	-0.0143	0.0023	-6.1006	< 0.0001	Error
NIR0906						

[Y] Indicates that blank rows were not spatially dependent and classical ordinary least squares regression was sufficient for these snapshots.

[Z] Two spatial models were determined and used for a few observations to adjust for spatial autocorrelation by using the Lagrange Multiplier (LM) tests, which are reported in the regression diagnostic output.

Table 6. Satellite imagery of in-season crop health for the month of July were used to determine predicted yield and the predicted values were regressed with actual yield to determine correlation by using classical ordinary least squares for the King Lee field.

Observation	Variable	Residual Df	RSS	Sum of Sq	F	Pr(>F)	Probability
NDVI0725	Actual	3085	306131				
	Predicted	3083	304670	1461.3	7.394	6.26E-04	<0.0001
NIR0725	Actual	3084	550354				
	Predicted	3082	404563	145791	555.3	< 2.2E-16	<0.0001

Table 7. Satellite imagery of in-season crop health for the month of July were used to determine predicted yield and the predicted values were regressed with actual yield to determine correlation by using classical ordinary least squares for the Lee field.

Observation	Variable	Residual Df	RSS	Sum of Sq	F	Pr(>F)	Probability
NDVI0725	Actual	3088	580166				
	Predicted	3086	502772	77394	237.5	< 2.2E-16	<0.0001
NIR0725	Actual	3077	791081				
	Predicted	3075	454190	336891	1140	< 2E-16	<0.0001

Table 8. Satellite imagery of in-season crop health were regressed with actual yield to determine correlation by using classical ordinary least squares for the Backgate field.

Covariate	R-squared	Adjusted R-squared	Coefficient	Std Error	t-Statistic	Probability
NDVI0501	0.1050	0.1032	-185.5330	24.3705	-7.6130	< 0.0001
NDVI0514	0.0895	0.0877	-198.1080	28.4246	-6.9696	< 0.0001
NDVI0610	0.2888	0.2874	164.8000	11.6349	14.1643	< 0.0001
NDVI0720	0.1878	0.1862	88.8582	8.3128	10.6893	< 0.0001
NDVI0817	0.2652	0.2637	236.8050	17.7347	13.3526	< 0.0001
NDVI0822	0.0252	0.0232	36.4586	10.2025	3.5735	0.0004
NDVI0906	0.0623	0.0604	-51.8788	9.0525	-5.7309	< 0.0001
NIR0424	0.0166	0.0146	-0.0226	0.0078	-2.8884	0.0040
NIR0501	0.0320	0.0300	-0.0304	0.0075	-4.0394	< 0.0001
NIR0514	0.0489	0.0469	-0.0427	0.0085	-5.0375	< 0.0001
NIR0610	0.4146	0.4134	0.0489	0.0026	18.7028	< 0.0001
NIR0720	0.4578	0.4567	0.0454	0.0022	20.4248	< 0.0001
NIR0817	0.3265	0.3251	0.1144	0.0074	15.4745	< 0.0001
NIR0822	0.0014	-0.0006	0.0028	0.0033	0.8384	0.4022
NIR0906	0.1851	0.1835	-0.0296	0.0028	-10.5943	< 0.0001

Table 9. Satellite imagery of in-season crop health were regressed with actual yield to determine correlation by using classical ordinary least squares for the Crossplace field.

Covariate	R-squared	Adjusted R-squared	Coefficient	Std Error	t-Statistic	Probability
NDVI0501	0.1014	0.1011	643.0430	34.8055	18.4753	< 0.0001
NDVI0514	0.3378	0.3376	451.2260	11.4867	39.2826	< 0.0001
NDVI0610	0.4529	0.4527	165.6270	3.3099	50.0397	< 0.0001
NDVI0817	0.2321	0.2319	323.7290	10.7059	30.2383	< 0.0001
NDVI0906	0.1053	0.1050	92.7425	4.9162	18.8647	< 0.0001
NIR0424	0.1852	0.1850	-0.0634	0.0024	-26.2235	< 0.0001
NIR0501	0.0650	0.0647	-0.0762	0.0053	-14.4966	< 0.0001
NIR0514	0.0227	0.0223	0.0266	0.0032	8.3732	< 0.0001
NIR0610	0.4179	0.4177	0.0337	0.0007	46.5974	< 0.0001
NIR0817	0.2841	0.2839	0.0948	0.0027	34.6496	< 0.0001
NIR0906	0.0008	0.0004	0.0030	0.0020	1.5222	0.1281

Table 10. Satellite imagery of in-season crop health were regressed with actual yield to determine correlation by using classical ordinary least squares for the Glendon 2 field.

Covariate	R-squared	Adjusted R-squared	Coefficient	Std Error	t-Statistic	Probability
NDVI0501	0.0002	-0.0006	-11.1243	21.4610	-0.5184	0.6043
NDVI0514	0.0289	0.0282	67.4454	10.9008	6.1872	< 0.0001
NDVI0610	0.4160	0.4155	179.3130	5.9250	30.2639	< 0.0001
NDVI0720	0.3908	0.3903	148.9140	5.1846	28.7225	< 0.0001
NDVI0906	0.0873	0.0866	-94.8391	8.5496	-11.0928	< 0.0001
NIR0424	0.0502	0.0494	0.0156	0.0019	8.2413	< 0.0001
NIR0501	0.0474	0.0467	-0.0393	0.0049	-7.9997	< 0.0001
NIR0514	0.0000	-0.0007	0.0004	0.0022	0.1980	0.8431
NIR0610	0.3321	0.3315	0.0302	0.0012	25.2847	< 0.0001
NIR0720	0.4664	0.4660	0.0379	0.0011	33.5272	< 0.0001
NIR0906	0.2837	0.2832	-0.0410	0.0018	-22.5703	< 0.0001

Table 11. Satellite imagery of in-season crop health were regressed with actual yield to determine correlation by using classical ordinary least squares for the Glendon 4 field.

Covariate	R-squared	Adjusted R-squared	Coefficient	Std Error	t-Statistic	Probability
NDVI0501	0.1648	0.1636	-247.2240	21.1686	-11.6788	< 0.0001
NDVI0514	0.0010	-0.0005	19.9742	24.2811	0.8226	0.4110
NDVI0610	0.4624	0.4616	151.0190	6.1945	24.3794	< 0.0001
NDVI0720	0.4625	0.4618	201.2800	8.2541	24.3854	< 0.0001
NDVI0906	0.1410	0.1397	-101.1280	9.4972	-10.6483	< 0.0001
NIR0424	0.0285	0.0271	0.0126	0.0028	4.5046	< 0.0001
NIR0501	0.2675	0.2664	-0.0906	0.0057	-15.8844	< 0.0001
NIR0514	0.0027	0.0013	0.0042	0.0030	1.3693	0.1714
NIR0610	0.3990	0.3981	0.0234	0.0011	21.4166	< 0.0001
NIR0720	0.5104	0.5097	0.0401	0.0015	26.8381	< 0.0001
NIR0906	0.0392	0.0378	-0.0289	0.0054	-5.3092	< 0.0001

Table 12. Satellite imagery of in-season crop health were regressed with actual yield to determine correlation by using classical ordinary least squares for the Glendon 5 field.

Covariate	R-squared	Adjusted R-squared	Coefficient	Std Error	t-Statistic	Probability
NDVI0501	0.0008	-0.0008	-15.8914	22.4478	-0.7079	0.4792
NDVI0514	0.0001	-0.0014	-3.8093	14.9148	-0.2554	0.7985
NDVI0610	0.2920	0.2909	122.9850	7.4541	16.4990	< 0.0001
NDVI0720	0.2457	0.2446	145.5190	9.9240	14.6633	< 0.0001
NDVI0906	0.0128	0.0114	50.2416	17.1413	2.9310	0.0035
NIR0424	0.0828	0.0814	0.0146	0.0019	7.7169	< 0.0001
NIR0501	0.0346	0.0331	-0.0331	0.0068	-4.8612	< 0.0001
NIR0514	0.0679	0.0665	0.0146	0.0021	6.9340	< 0.0001
NIR0610	0.2743	0.2732	0.0190	0.0012	15.7949	< 0.0001
NIR0720	0.1806	0.1793	0.0156	0.0013	12.0590	< 0.0001
NIR0906	0.0000	-0.0015	0.0003	0.0059	0.0427	0.9661

Table 13. Satellite imagery of in-season crop health were regressed with actual yield to determine correlation by using classical ordinary least squares for the Robert 1 field.

Covariate	R-squared	Adjusted R-squared	Coefficient	Std Error	t-Statistic	Probability
NDVI0501	0.1019	0.1002	-194.3360	24.7638	-7.8476	< 0.0001
NDVI0514	0.0026	0.0008	-18.7485	15.6144	-1.2007	0.2304
NDVI0610	0.2407	0.2393	119.0160	9.0714	13.1199	< 0.0001
NDVI0822	0.1908	0.1893	142.4430	12.5875	11.3162	< 0.0001
NDVI0906	0.0008	-0.0011	9.7778	15.0459	0.6499	0.5161
NIR0424	0.0514	0.0497	-0.0160	0.0029	-5.4252	< 0.0001
NIR0501	0.1957	0.1942	-0.0724	0.0063	-11.4935	< 0.0001
NIR0514	0.2199	0.2185	-0.0382	0.0031	-12.3731	< 0.0001
NIR0610	0.1159	0.1142	0.0195	0.0023	8.4352	< 0.0001
NIR0822	0.0037	0.0019	-0.0067	0.0047	-1.4284	0.1537
NIR0906	0.0490	0.0472	-0.0211	0.0040	-5.2871	< 0.0001

Table 14. Satellite imagery of in-season crop health were regressed with actual yield to determine correlation by using classical ordinary least squares for the Robert 2 field.

Covariate	R-squared	Adjusted R-squared	Coefficient	Std Error	t-Statistic	Probability
NDVI0501	0.1738	0.1722	-383.3760	37.4525	-10.2363	< 0.0001
NDVI0514	0.0010	-0.0010	20.9899	30.0386	0.6988	0.4850
NDVI0610	0.4530	0.4519	317.6110	15.6396	20.3081	< 0.0001
NDVI0720	0.5125	0.5115	331.8820	14.5041	22.8820	< 0.0001
NDVI0822	0.0102	0.0082	44.2579	19.5265	2.2666	0.0239
NDVI0906	0.3991	0.3979	-165.6560	9.1079	-18.1882	< 0.0001
NIR0424	0.0252	0.0232	0.0140	0.0039	3.5875	0.0004
NIR0501	0.0241	0.0221	-0.0351	0.0100	-3.5062	0.0005
NIR0514	0.0015	-0.0005	0.0038	0.0044	0.8680	0.3858
NIR0610	0.4144	0.4132	0.0459	0.0024	18.7724	< 0.0001
NIR0720	0.5569	0.5560	0.0455	0.0018	25.0172	< 0.0001
NIR0822	0.0664	0.0645	-0.0345	0.0058	-5.9517	< 0.0001
NIR0906	0.4518	0.4507	-0.0444	0.0022	-20.2589	< 0.0001

Table 15. Satellite imagery of in-season crop health were regressed with actual yield to determine correlation by using classical ordinary least squares for the Robert 3 field.

Covariate	R-squared	Adjusted R-squared	Coefficient	Std Error	t-Statistic	Probability
NDVI0501	0.1213	0.1204	190.1130	16.6169	11.4409	< 0.0001
NDVI0514	0.2127	0.2119	128.1440	8.0074	16.0033	< 0.0001
NDVI0610	0.4564	0.4559	135.8490	4.8149	28.2145	< 0.0001
NDVI0720	0.4490	0.4484	154.4820	5.5579	27.7953	< 0.0001
NDVI0906	0.0319	0.0309	-36.2294	6.4784	-5.5924	< 0.0001
NIR0424	0.0006	-0.0005	0.0011	0.0016	0.7313	0.4648
NIR0501	0.1660	0.1652	-0.0461	0.0034	-13.7388	< 0.0001
NIR0514	0.0149	0.0138	-0.0062	0.0016	-3.7832	0.0002
NIR0610	0.2545	0.2537	0.0193	0.0011	17.9886	< 0.0001
NIR0720	0.5171	0.5166	0.0489	0.0015	31.8623	< 0.0001
NIR0906	0.0572	0.0562	-0.0109	0.0014	-7.5851	< 0.0001

Table 16. Spatial Lag and spatial error models were determined and used for a few observations to adjust for spatial autocorrelation for the Backgate field.

Covariate[Y]	R-Square	Coefficient	Std Error	Z-Value	Probability	Spatial Model[Z]
NDVI0501	0.8140	-37.8426	11.5251	-3.2835	0.0010	Lag
NDVI0514	0.8137	-38.8731	13.0776	-2.9725	0.0030	Lag
NDVI0610	0.8186	42.9342	6.7297	6.3798	< 0.0001	Lag
NDVI0720	0.8189	24.0857	4.2994	5.6021	< 0.0001	Lag
NDVI0817	0.8175	59.2811	10.2548	5.7808	< 0.0001	Lag
NDVI0822						
NDVI0906	0.8127	-6.1081	4.1015	-1.4892	0.1364	Lag
NIR0424	0.8153	-0.0193	0.0069	-2.7876	0.0053	Error
NIR0501	0.8156	-0.0206	0.0066	-3.1168	0.0018	Error
NIR0514	0.8143	-0.0176	0.0067	-2.6435	0.0082	Error
NIR0610						
NIR0720	0.8157	0.0120	0.0017	7.2430	< 0.0001	Lag
NIR0817	0.8166	0.0282	0.0046	6.0729	< 0.0001	Lag
NIR0822						
NIR0906						

[Y] Indicates that blank rows were not spatially dependent and classical ordinary least squares regression was sufficient for these snapshots.

[Z] Two spatial models were determined and used for a few observations to adjust for spatial autocorrelation by using the Lagrange Multiplier (LM) tests, which are reported in the regression diagnostic output.

Table 17. Spatial Lag and spatial error models were determined and used for a few observations to adjust for spatial autocorrelation for the Crossplace field.

Covariate[Y]	R-Square	Coefficient	Std Error	Z-Value	Probability	Spatial Model[Z]
NDVI0501	0.8649	83.4637	13.9727	5.9734	< 0.0001	Lag
NDVI0514						
NDVI0610						
NDVI0817						
NDVI0906	0.8649	11.9954	2.0046	5.9839	< 0.0001	Lag
NIR0424	0.8645	-0.0083	0.0011	-7.7627	< 0.0001	Lag
NIR0501	0.8649	-0.0085	0.0020	-4.2083	< 0.0001	Lag
NIR0514						
NIR0610	0.8720	0.0327	0.0016	20.2717	< 0.0001	Error
NIR0817						
NIR0906						

[Y] Indicates that blank rows were not spatially dependent and classical ordinary least squares regression was sufficient for these snapshots.

[Z] Two spatial models were determined and used for a few observations to adjust for spatial autocorrelation by using the Lagrange Multiplier (LM) tests, which are reported in the regression diagnostic output.

Table 18. Spatial Lag and spatial error models were determined and used for a few observations to adjust for spatial autocorrelation for the Glendon 2 field.

Covariate[Y]	R-Square	Coefficient	Std Error	Z-Value	Probability	Spatial Model[Z]
NDVI0501						
NDVI0514						
NDVI0610						
NDVI0720	0.5349	95.3453	5.5240	17.2603	< 0.0001	Lag
NDVI0906	0.4747	-46.2537	6.7736	-6.8286	< 0.0001	Lag
NIR0424						
NIR0501						
NIR0514						
NIR0610	0.5326	0.0308	0.0017	18.3785	< 0.0001	Error
NIR0720	0.5623	0.0383	0.0015	25.2920	< 0.0001	Error
NIR0906	0.5037	-0.0405	0.0026	-15.3240	< 0.0001	Error

[Y] Indicates that blank rows were not spatially dependent and classical ordinary least squares regression was sufficient for these snapshots.

[Z] Two spatial models were determined and used for a few observations to adjust for spatial autocorrelation by using the Lagrange Multiplier (LM) tests, which are reported in the regression diagnostic output.

Table 19. Spatial Lag and spatial error models were determined and used for a few observations to adjust for spatial autocorrelation for the Glendon 4 field.

Covariate[Y]	R-Square	Coefficient	Std Error	Z-Value	Probability	Spatial Model[Z]
NDVI0501						
NDVI0514						
NDVI0610						
NDVI0720	0.6965	98.3380	7.6741	12.8142	< 0.0001	Lag
NDVI0906	0.6568	-84.9822	17.8949	-4.7490	< 0.0001	Error
NIR0424						
NIR0501	0.6611	-0.0311	0.0044	-7.1083	< 0.0001	Lag
NIR0514						
NIR0610						
NIR0720						
NIR0906						

[Y] Indicates that blank rows were not spatially dependent and classical ordinary least squares regression was sufficient for these snapshots.

[Z] Two spatial models were determined and used for a few observations to adjust for spatial autocorrelation by using the Lagrange Multiplier (LM) tests, which are reported in the regression diagnostic output.

Table 20. Spatial Lag and spatial error models were determined and used for a few observations to adjust for spatial autocorrelation for the Glendon 5 field.

Covariate[Y]	R-Square	Coefficient	Std Error	Z-Value	Probability	Spatial Model[Z]
NDVI0501						
NDVI0514						
NDVI0610						
NDVI0720	0.3636	144.3750	11.8421	12.1917	< 0.0001	Error
NDVI0906						
NIR0424						
NIR0501						
NIR0514						
NIR0610						
NIR0720						
NIR0906						

[Y] Indicates that blank rows were not spatially dependent and classical ordinary least squares regression was sufficient for these snapshots.

[Z] Two spatial models were determined and used for a few observations to adjust for spatial autocorrelation by using the Lagrange Multiplier (LM) tests, which are reported in the regression diagnostic output.

Table 21. Spatial Lag and spatial error models were determined and used for a few observations to adjust for spatial autocorrelation for the Robert 1 field.

Covariate[Y]	R-Square	Coefficient	Std Error	Z-Value	Probability	Spatial Model[Z]
NDVI0501	0.8437	29.5848	11.0159	-2.6857	0.0072	Lag
NDVI0514						
NDVI0610	0.8551	82.4373	9.8671	8.3548	< 0.0001	Error
NDVI0822	0.8531	123.8050	16.7107	7.4087	< 0.0001	Error
NDVI0906						
NIR0424						
NIR0501						
NIR0514						
NIR0610						
NIR0822	0.8439	0.0013	0.0019	0.6938	0.4878	Lag
NIR0906						

[Y] Indicates that blank rows were not spatially dependent and classical ordinary least squares regression was sufficient for these snapshots.

[Z] Two spatial models were determined and used for a few observations to adjust for spatial autocorrelation by using the Lagrange Multiplier (LM) tests, which are reported in the regression diagnostic output.

Table 22. Spatial Lag and spatial error models were determined and used for a few observations to adjust for spatial autocorrelation for the Robert 2 field.

Covariate[Y]	R-Square	Coefficient	Std Error	Z-Value	Probability	Spatial Model[Z]
NDVI0501						
NDVI0514						
NDVI0610						
NDVI0720	0.7944	138.1970	12.8606	10.7458	< 0.0001	Lag
NDVI0822						
NDVI0906						
NIR0424						
NIR0501						
NIR0514						
NIR0610						
NIR0720	0.7871	0.0439	0.0031	14.0361	< 0.0001	Error
NIR0822	0.7680	-0.0309	0.0072	-4.3060	< 0.0001	Error
NIR0906						

[Y] Indicates that blank rows were not spatially dependent and classical ordinary least squares regression was sufficient for these snapshots.

[Z] Two spatial models were determined and used for a few observations to adjust for spatial autocorrelation by using the Lagrange Multiplier (LM) tests, which are reported in the regression diagnostic output.

Table 23. Spatial Lag and spatial error models were determined and used for a few observations to adjust for spatial autocorrelation for the Robert 3 field.

Covariate[Y]	R-Square	Coefficient	Std Error	Z-Value	Probability	Spatial Model[Z]
NDVI0501						
NDVI0514						
NDVI0610	0.7387	124.6160	7.8966	15.7810	< 0.0001	Error
NDVI0720	0.7364	62.5065	4.9291	12.6811	< 0.0001	Lag
NDVI0906						
NIR0424						
NIR0501	0.7272	-0.0387	0.0044	-8.8650	< 0.0001	Error
NIR0514						
NIR0610						
NIR0720						
NIR0906						

[Y] Indicates that blank rows were not spatially dependent and classical ordinary least squares regression was sufficient for these snapshots.

[Z] Two spatial models were determined and used for a few observations to adjust for spatial autocorrelation by using the Lagrange Multiplier (LM) tests, which are reported in the regression diagnostic output.

Table 24. Satellite imagery of in-season crop health for the months June and July were used to determine predicted yield and the predicted values were regressed with actual yield to determine correlation by using classical ordinary least squares for the Backgate field.

Observation	Variable	Residual Df	RSS	Sum of Sq	F	Pr(>F)	Probability
NDVI0610	Actual	8105	8225952				
	Predicted	8103	3668708	4557244	5032.7	< 2.20E-16	< 0.0001
NIR0610	Actual	6684	3521673				
	Predicted	6682	2913624	608048	697.24	< 2.20E-16	< 0.0001
NDVI0720	Actual	7981	23900771				
	Predicted	7979	5048031	18852739	14899	< 2.20E-16	< 0.0001
NIR0720	Actual	6659	5395172				
	Predicted	6657	3836071	1559101	1352.8	< 2.20E-16	< 0.0001

Table 25. Satellite imagery of in-season crop health for the months June and July were used to determine predicted yield and the predicted values were regressed with actual yield to determine correlation by using classical ordinary least squares for the Crossplace field.

Observation	Variable	Residual Df	RSS	Sum of Sq	F	Pr(>F)	Probability
NDVI0610	Actual	7953	8238599				
	Predicted	7951	3972986	4265613	4268.3	< 2.20E-16	< 0.0001
NIR0610	Actual	7912	17041908				
	Predicted	6682	2913624	11957548	9301.5	< 2.20E-16	< 0.0001

Table 26. Satellite imagery of in-season crop health for the months June and July were used to determine predicted yield and the predicted values were regressed with actual yield to determine correlation by using classical ordinary least squares for the Glendon 2 field.

Observation	Variable	Residual Df	RSS	Sum of Sq	F	Pr(>F)	Probability
NDVI0610	Actual	8105	4434075				
	Predicted	8103	3448384	985690	1158.1	< 2.20E-16	< 0.0001
NIR0610	Actual	6637	3872976				
	Predicted	6635	3077761	795215	857.16	< 2.20E-16	< 0.0001
NDVI0720	Actual	8105	9695954				
	Predicted	8103	5012221	4683733	3786	< 2.20E-16	< 0.0001
NIR0720	Actual	6684	4880095				
	Predicted	6682	3784462	1095633	967.25	< 2.20E-16	< 0.0001

Table 27. Satellite imagery of in-season crop health for the months June and July were used to determine predicted yield and the predicted values were regressed with actual yield to determine correlation by using classical ordinary least squares for the Glendon 4 field.

Observation	Variable	Residual Df	RSS	Sum of Sq	F	Pr(>F)	Probability
NDVI0610	Actual	8079	5058257				
	Predicted	8077	3395868	1662389	1977	< 2.20E-16	< 0.0001
NIR0610	Actual	6654	4242544				
	Predicted	6652	3219911	1022634	1056.3	< 2.20E-16	< 0.0001
NDVI0720	Actual	8105	11780350				
	Predicted	8103	4861569	6918781	5765.9	< 2.20E-16	< 0.0001
NIR0720	Actual	6654	5894736				
	Predicted	6652	3543688	2351048	2206.6	< 2.20E-16	< 0.0001

Table 28. Satellite imagery of in-season crop health for the months June and July were used to determine predicted yield and the predicted values were regressed with actual yield to determine correlation by using classical ordinary least squares for the Glendon 5 field.

Observation	Variable	Residual Df	RSS	Sum of Sq	F	Pr(>F)	Probability
NDVI0610	Actual	8104	5851024				
	Predicted	8102	3455614	2395410	2808.1	< 2.20E-16	< 0.0001
NIR0610	Actual	6521	3023713				
	Predicted	6519	2296499	727214	1032.2	< 2.20E-16	< 0.0001
NDVI0720	Actual	8105	11289669				
	Predicted	8103	4843257	6446412	5392.6	< 2.20E-16	< 0.0001
NIR0720	Actual	6684	5123278				
	Predicted	6682	3191104	1932174	2022.9	< 2.20E-16	< 0.0001

Table 29. Satellite imagery of in-season crop health for the months June and July were used to determine predicted yield and the predicted values were regressed with actual yield to determine correlation by using classical ordinary least squares for the Robert 1 field.

Observation	Variable	Residual Df	RSS	Sum of Sq	F	Pr(>F)	Probability
NDVI0610	Actual	7571	9042899				
	Predicted	7569	3371048	5671851	6367.5	< 2.20E-16	< 0.0001
NIR0610	Actual	8104	10603748				
	Predicted	8102	5104882	5498866	4363.6	< 2.20E-16	< 0.0001

Table 30. Satellite imagery of in-season crop health for the months June and July were used to determine predicted yield and the predicted values were regressed with actual yield to determine correlation by using classical ordinary least squares for the Robert 2 field.

Observation	Variable	Residual Df	RSS	Sum of Sq	F	Pr(>F)	Probability
NDVI0610	Actual	7272	10523209				
	Predicted	7270	2846070	7677140	9805.2	< 2.20E-16	< 0.0001
NIR0610	Actual	6644	3425835				
	Predicted	6642	2752018	673817	813.13	< 2.20E-16	< 0.0001
NDVI0720	Actual	7702	13378367				
	Predicted	7700	4920573	8457793	6617.6	< 2.20E-16	< 0.0001
NIR0720	Actual	6613	4675479				
	Predicted	6611	3090742	1584737	1694.9	< 2.20E-16	< 0.0001

Table 31. Satellite imagery of in-season crop health for the months June and July were used to determine predicted yield and the predicted values were regressed with actual yield to determine correlation by using classical ordinary least squares for the Robert 3 field.

Observation	Variable	Residual Df	RSS	Sum of Sq	F	Pr(>F)	Probability
NDVI0610	Actual	8104	3094978				
	Predicted	8102	3071528	23450	30.928	4.16E-14	< 0.0001
NIR0610	Actual	6684	4238493				
	Predicted	6682	4020300	218193	181.33	< 2.20E-16	< 0.0001
NDVI0720	Actual	8105	5236339				
	Predicted	8103	4900621	335718	277.55	< 2.20E-16	< 0.0001
NIR0720	Actual	6666	4420647				
	Predicted	6664	2969883	1450764	1627.7	< 2.20E-16	< 0.0001

Figures

Figure 1. The yellow pins designate the middle of the fields studied in the Verification Strip cluster near Dumas, Arkansas.

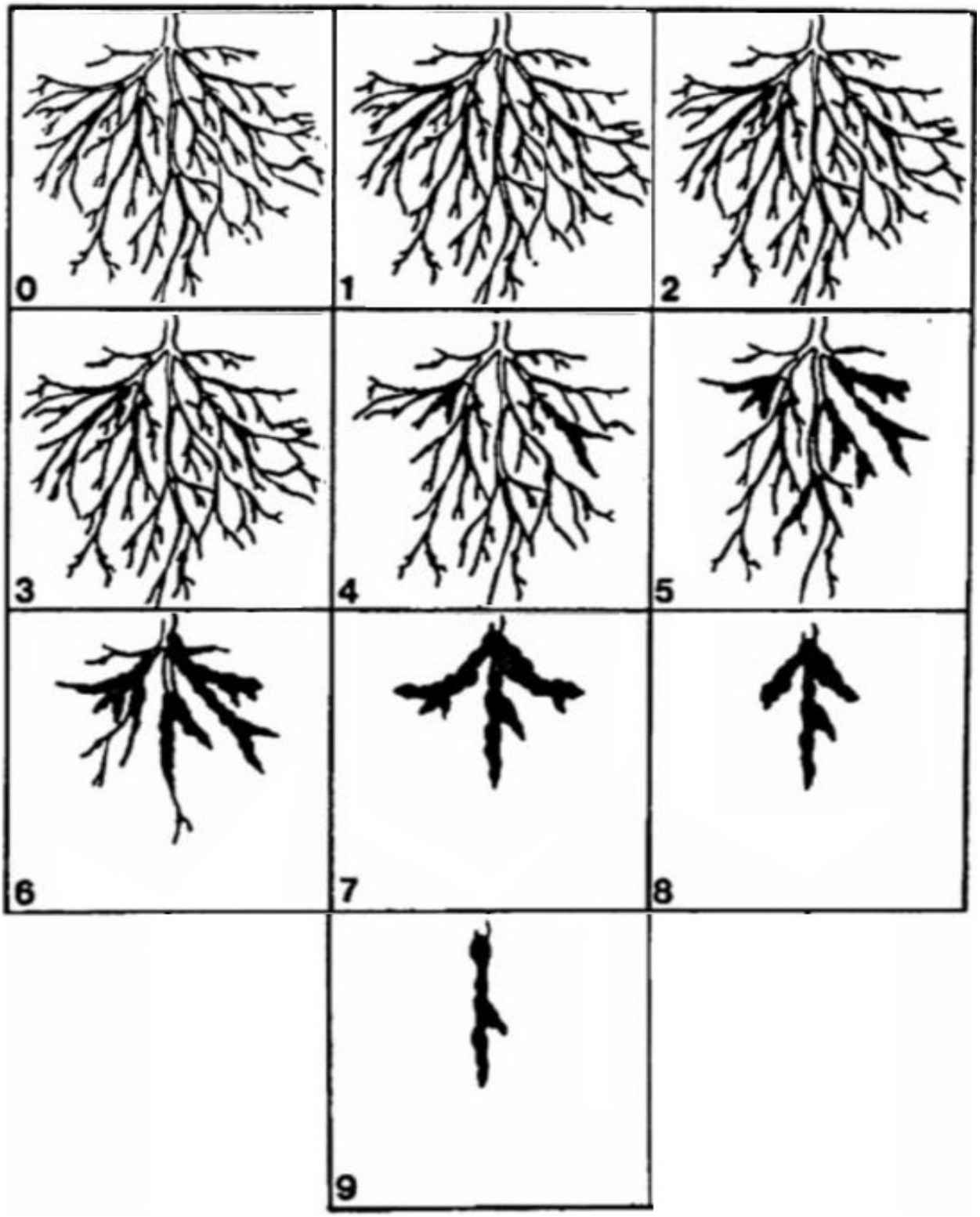

Figure 2. This representation indicates the 0-9 scale that the soybean roots were rated for *Meloidogyne incognita* galling and overall root health.

Figure 3. The yellow pins designate the middle of the fields studied in the Remote Cluster near Backgate, Arkansas.

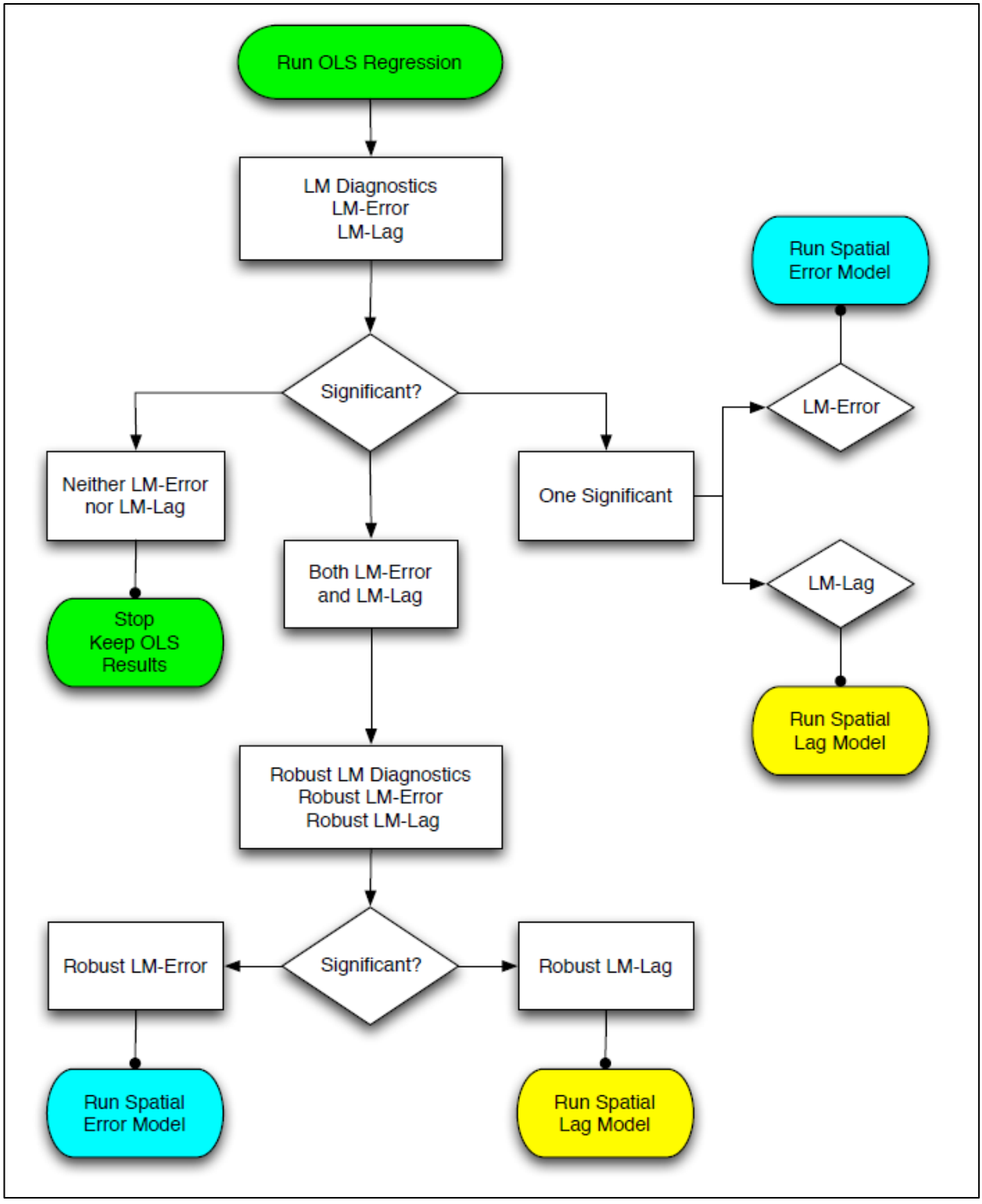

Figure 4. Determining whether to use a spatial regression model can be overwhelming, but a flow chart was created to help with the decision process (Anselin, 2005).

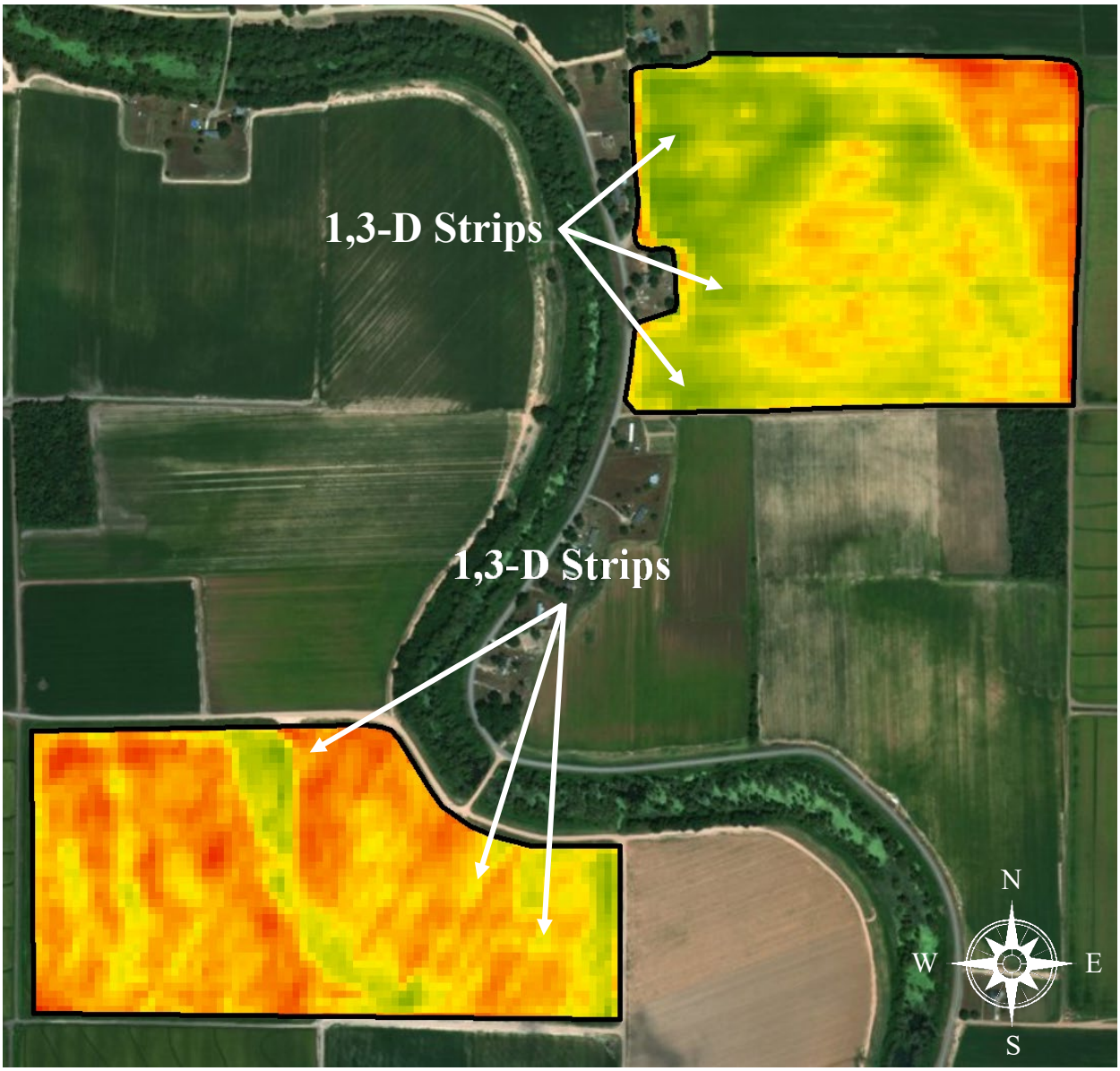

Figure 5. Normalized difference vegetation index (NDVI) on 10 June 2017 shows the three 1,3-D strips in both King Lee (top) and Lee E&W (bottom) fields. King Lee rows lay lengthwise east and west, while Lee rows lay northeast and southwest.

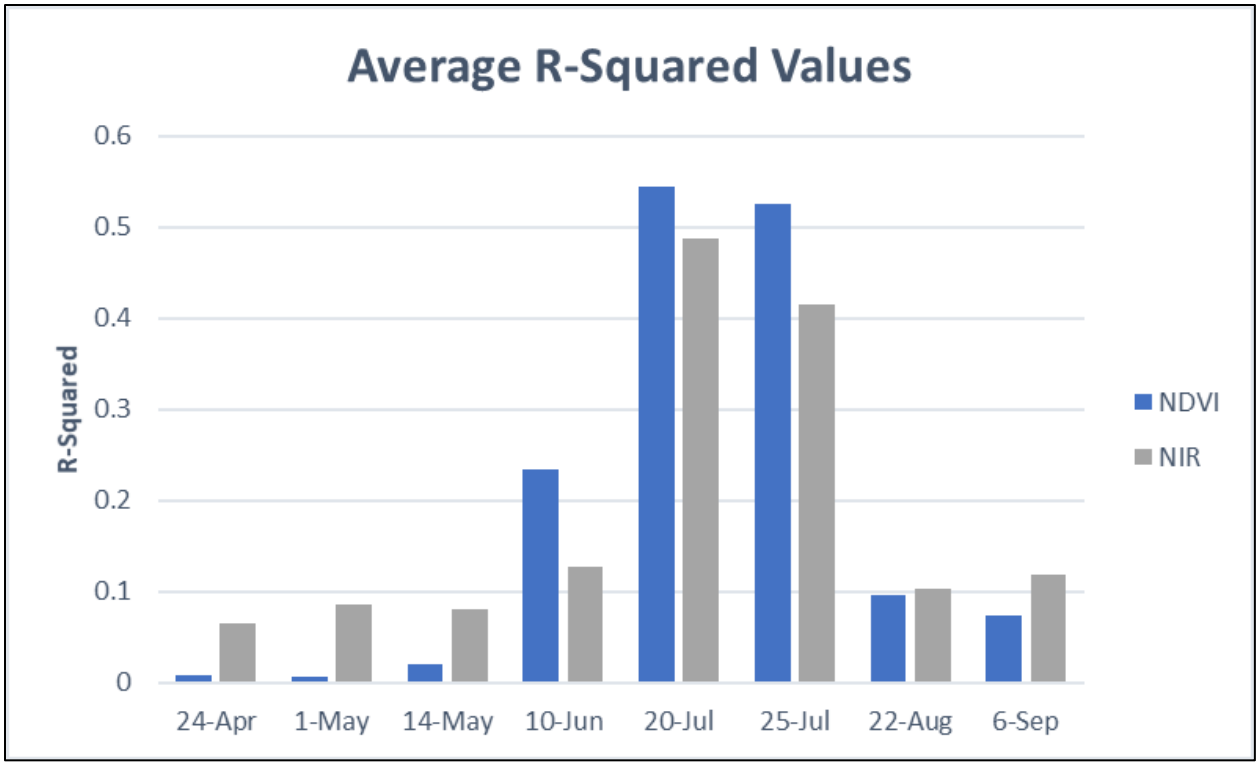

Figure 6. Ordinary least square regression resulted in the highest average R^2 values for all fields in the Verification Strip cluster being in the month of July (*n*=30).

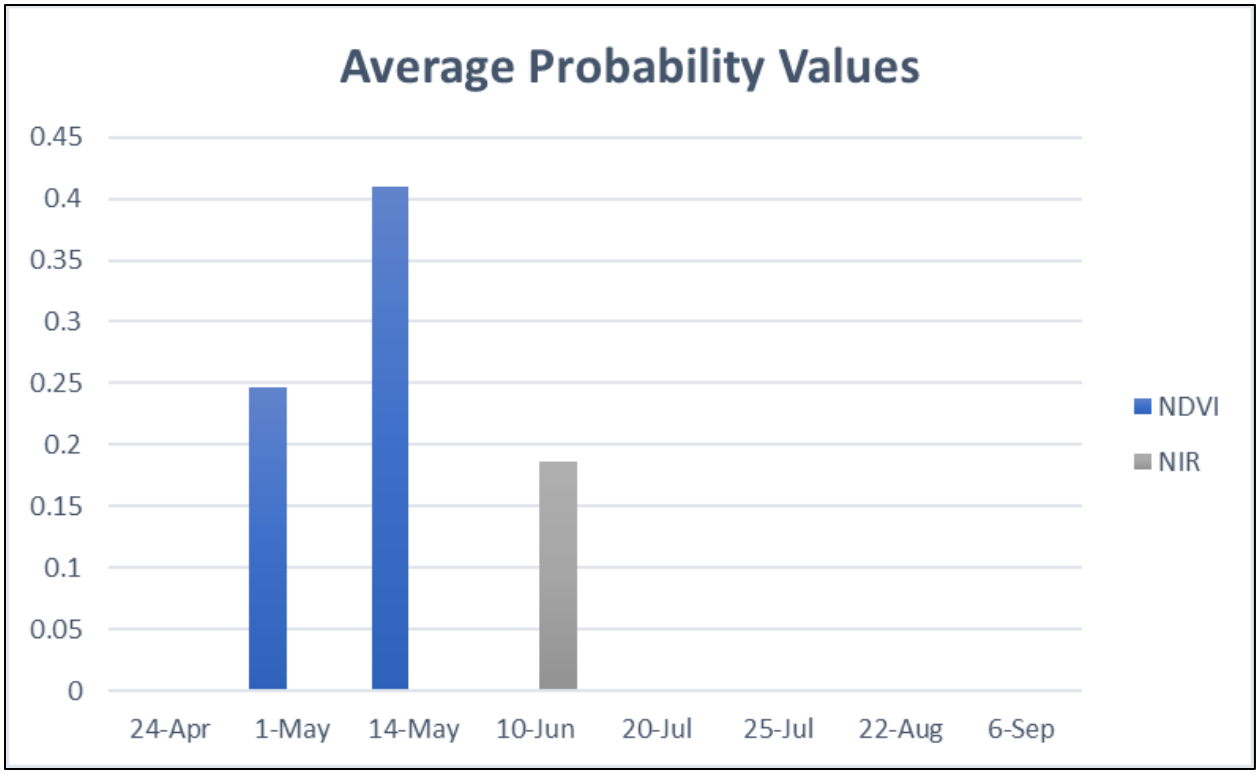

Figure 7. Ordinary least square regression resulted in NDVI and NIR images for all fields in the Verification Strip cluster being significantly correlated with yield in the month of July ($P<0.001$) ($n=30$).

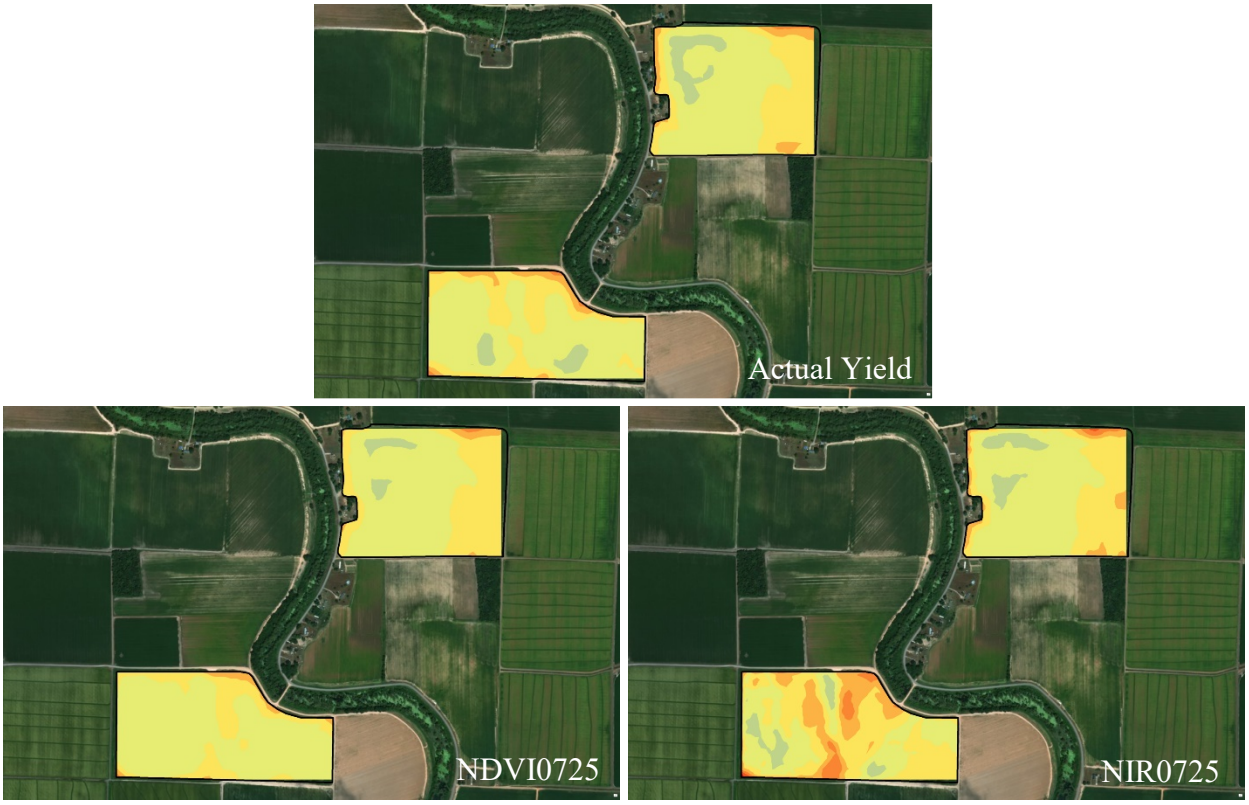

Figure 8. Interpolation of predicted yield prediction using satellite normalized difference vegetation index (NDVI0725) and near infrared (NIR0725) images on 25 July 2017 of King Lee showed a significant correlation between the actual and predicted yield.

Figure 9. Interpolation of predicted yield prediction using satellite normalized difference vegetation index (NDVI0725) and near infrared (NIR0725) images on 25 July 2017 of Lee showed a significant correlation between the actual and predicted yield.

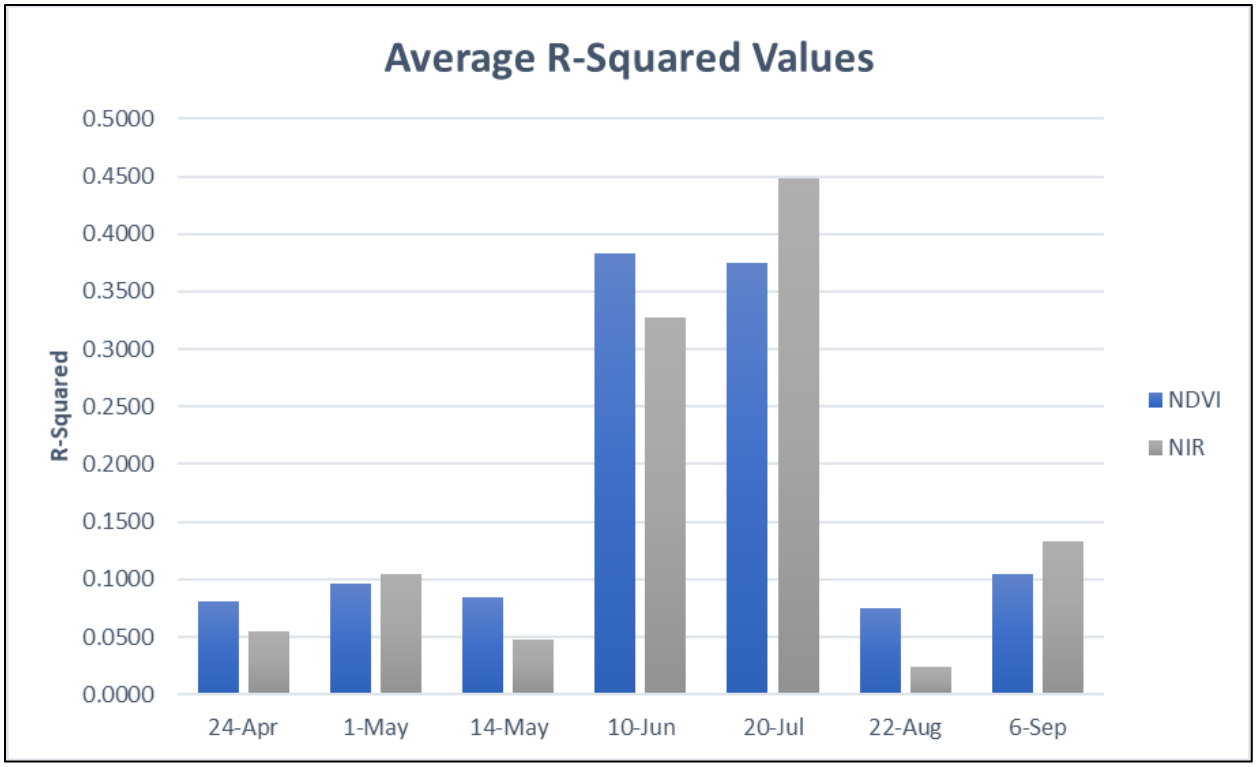

Figure 10. Ordinary least square regression resulted in the highest average R2 values for all fields in the Remote Cluster being in the June and July months (*n*=102).

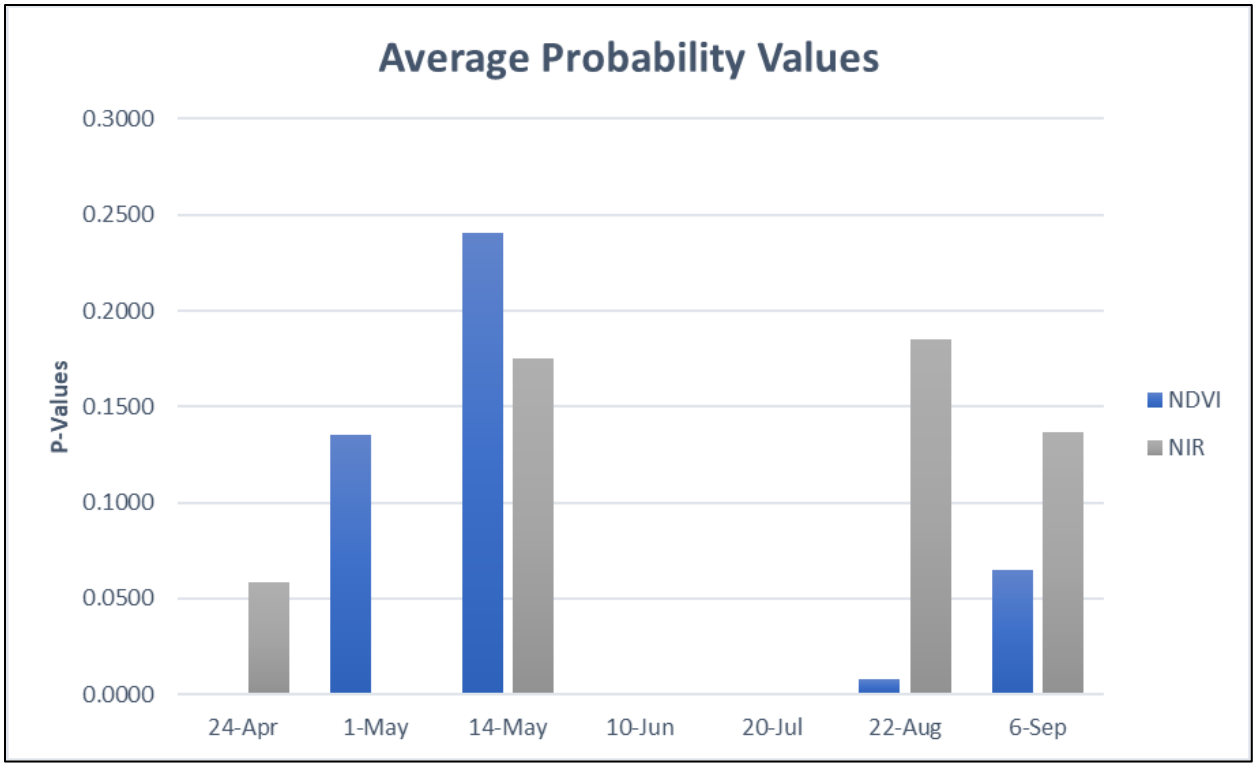

Figure 11. Ordinary least square regression resulted in NDVI and NIR images for all fields in the Remote Cluster being significantly correlated with yield in the months of June and July ($P<0.001$) ($n=102$).

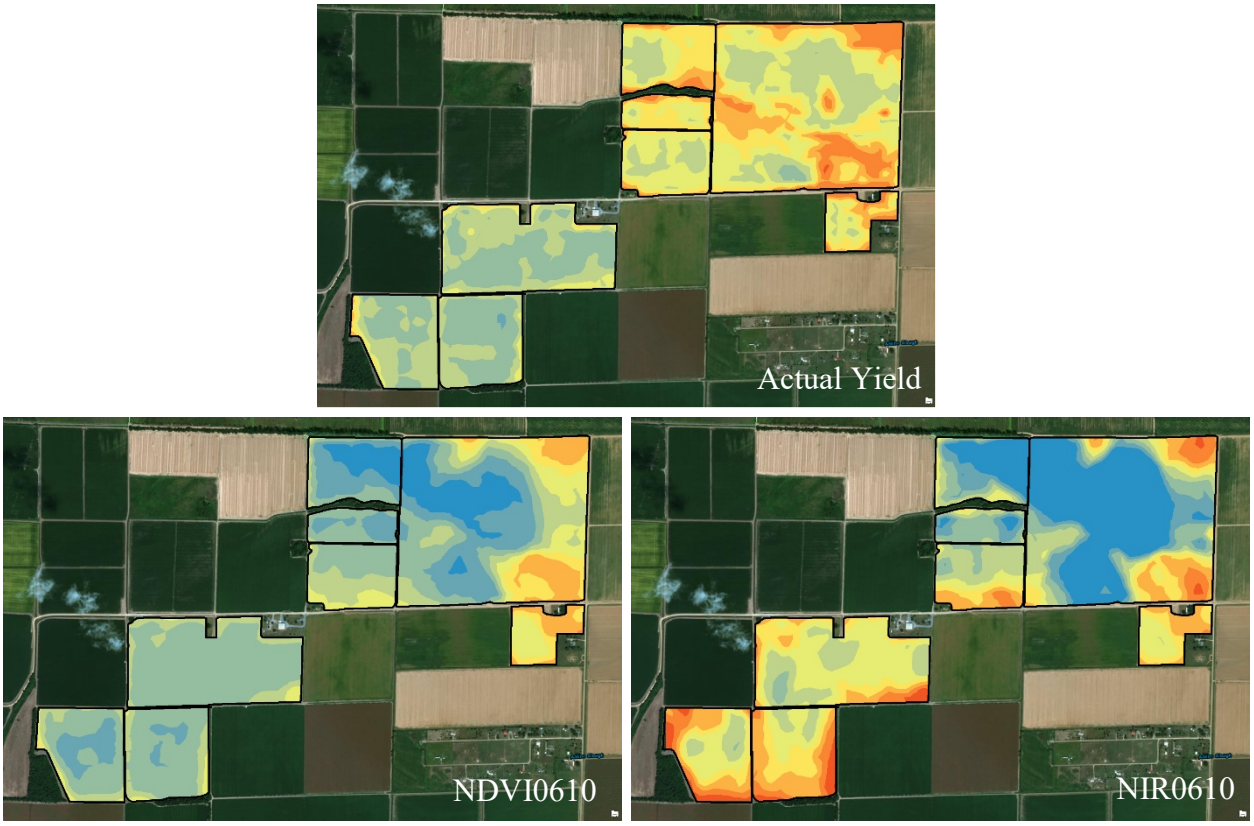

Figure 12. Interpolation of predicted yield using satellite normalized difference vegetation index (NDVI0610) and near infrared (NIR0610) images on 10 June 2017 of Backgate showed a significant correlation between the actual and predicted yield.

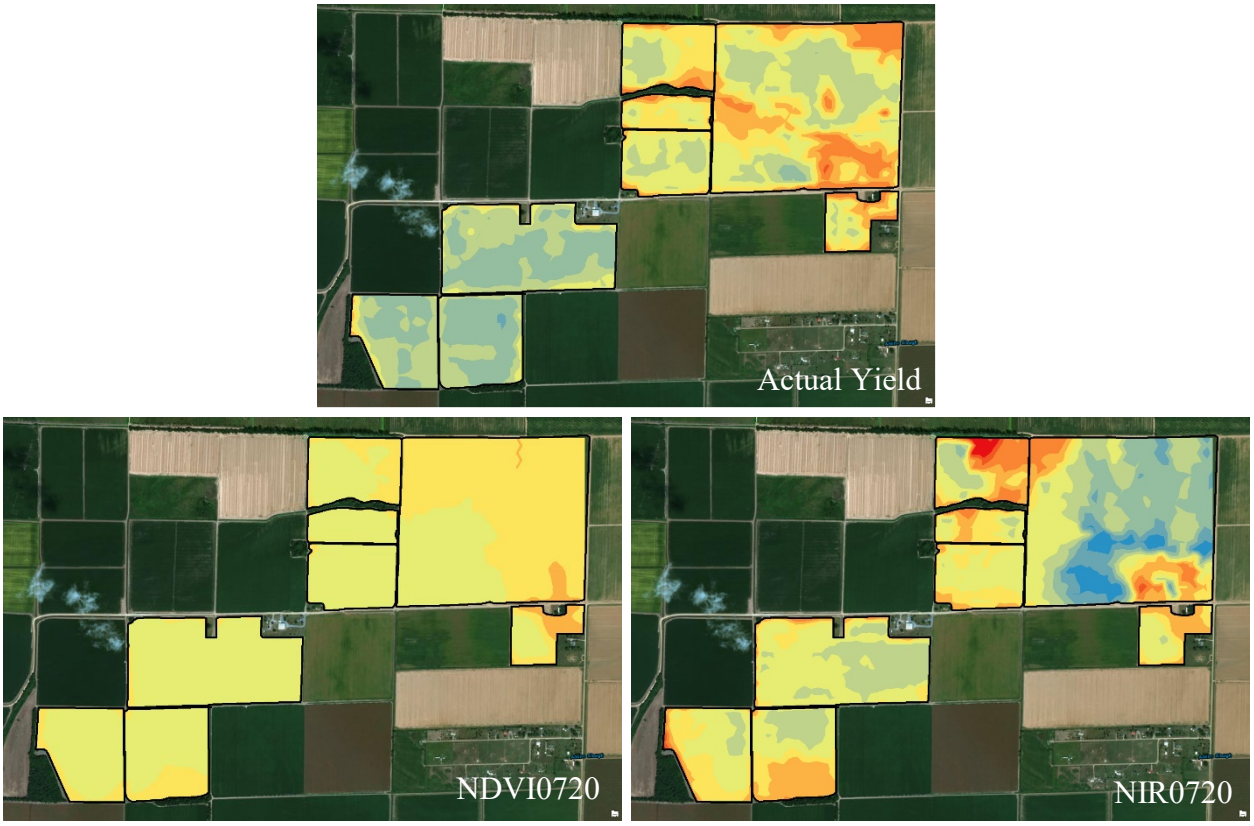

Figure 13. Interpolation of predicted yield using satellite normalized difference vegetation index (NDVI0720) and near infrared (NIR0720) images on 20 July 2017 of Backgate showed a significant correlation between the actual and predicted yield.

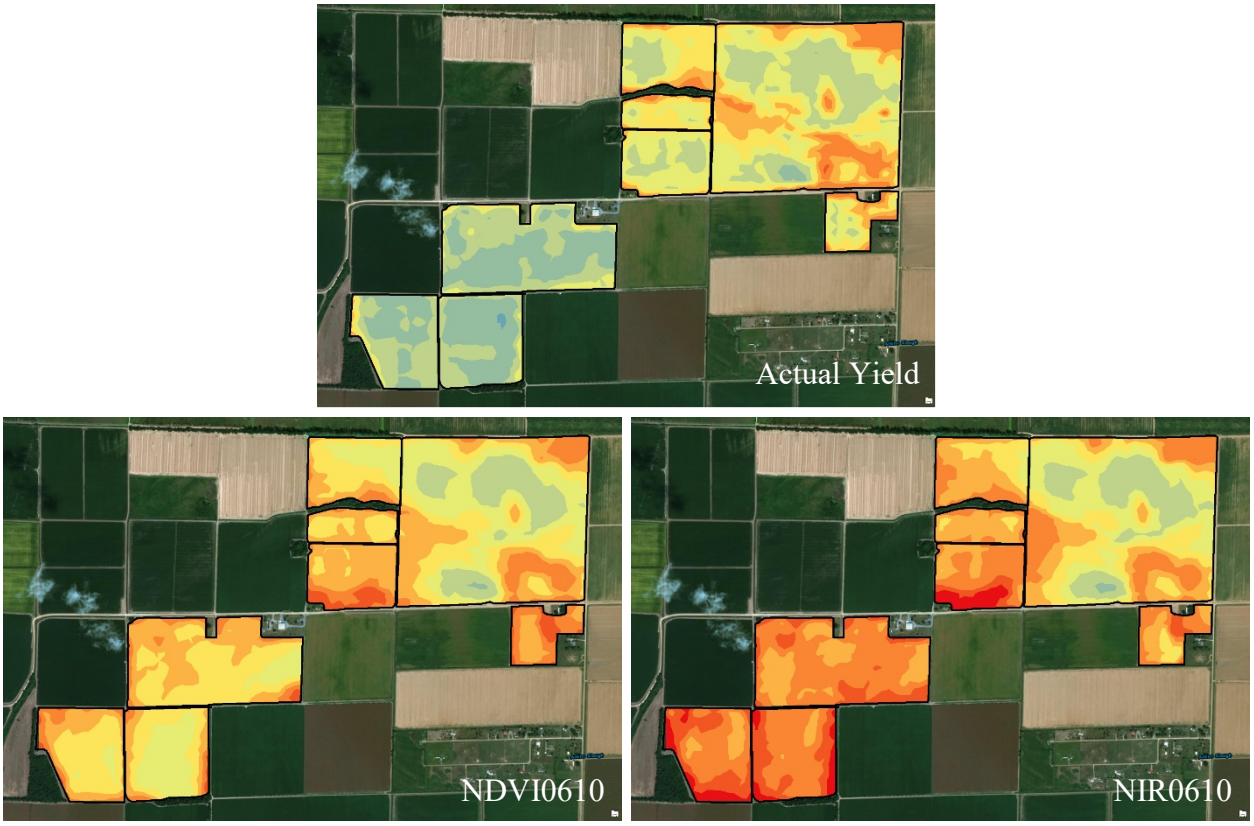

Figure 14. Interpolation of predicted yield using satellite normalized difference vegetation index (NDVI0610) and near infrared (NIR0610) images on 10 June 2017 of Crossplace showed a significant correlation between the actual and predicted yield.

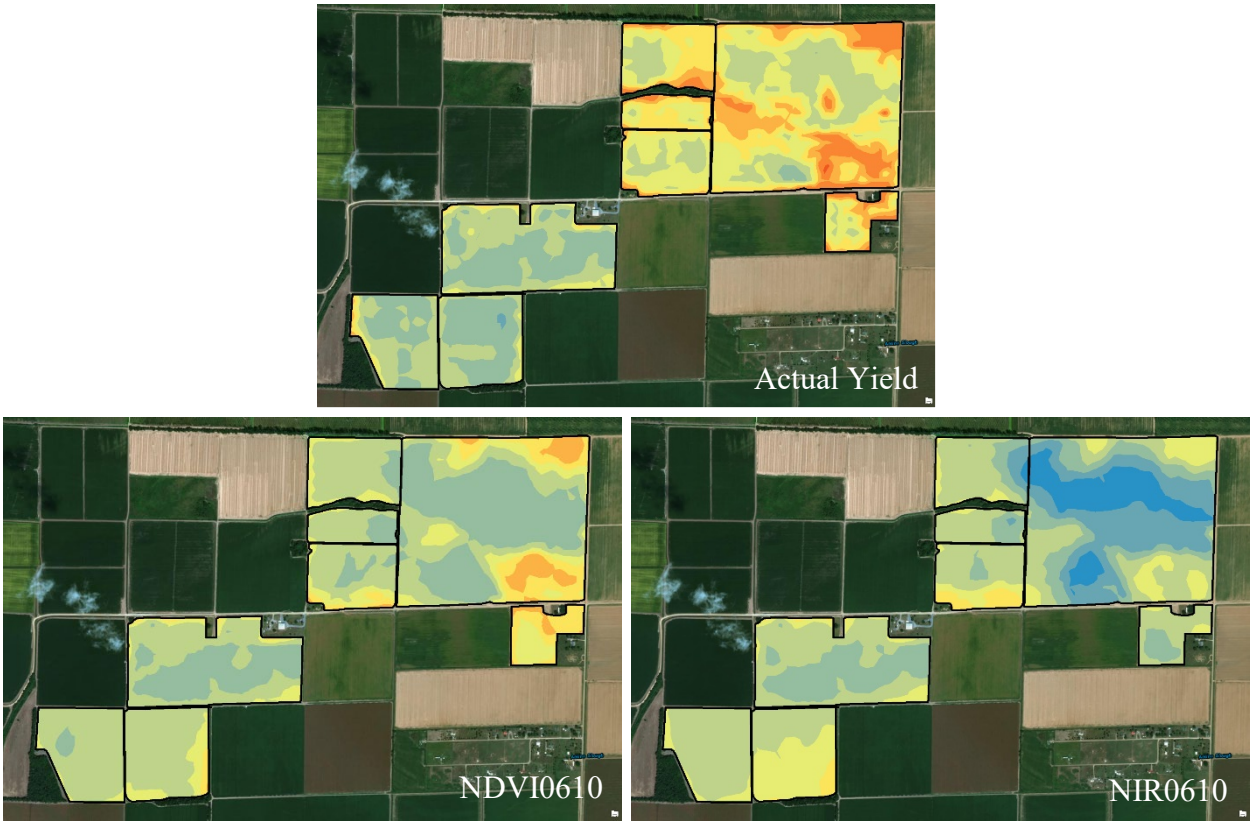

Figure 15. Interpolation of predicted yield using satellite normalized difference vegetation index (NDVI0610) and near infrared (NIR0610) images on 10 June 2017 of Glendon 2 showed a significant correlation between the actual and predicted yield.

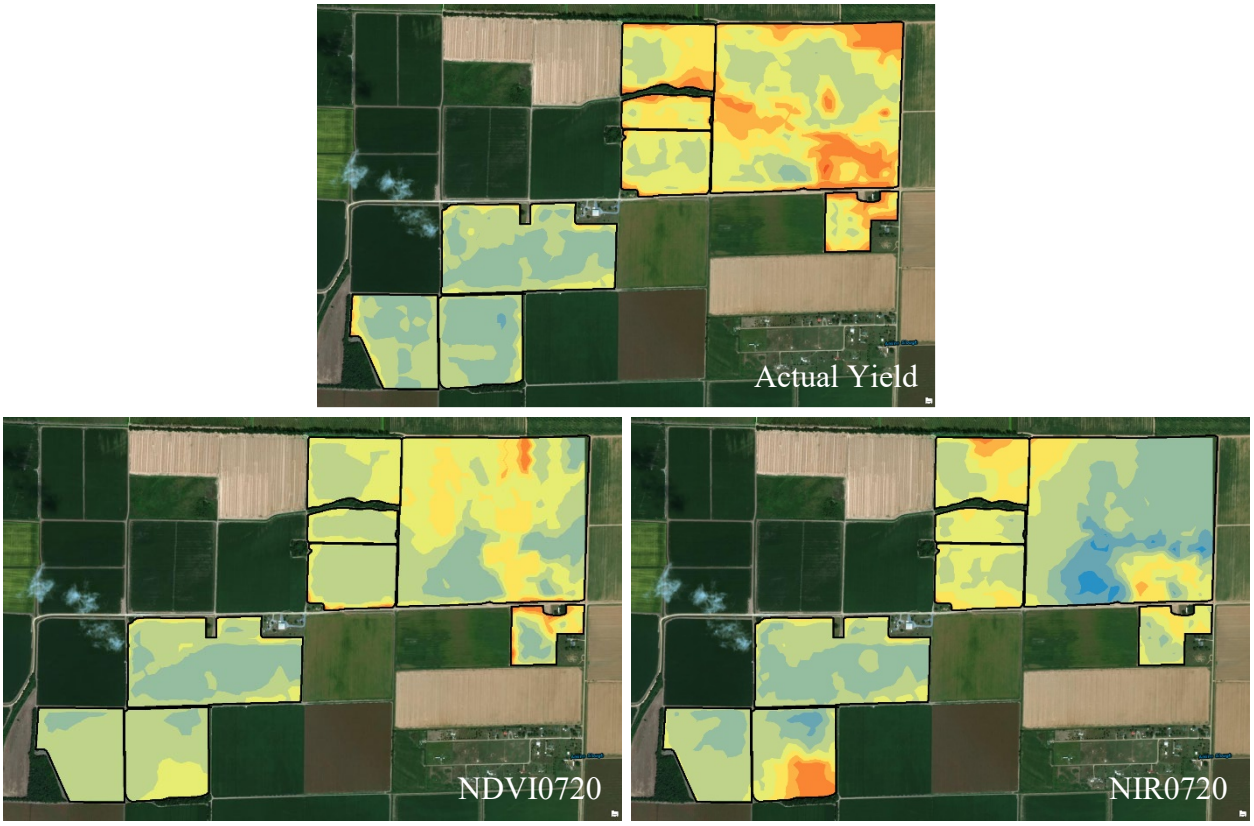

Figure 16. Interpolation of predicted yield using satellite normalized difference vegetation index (NDVI0720) and near infrared (NIR0720) images on 20 July 2017 of Glendon 2 showed a significant correlation between the actual and predicted yield.

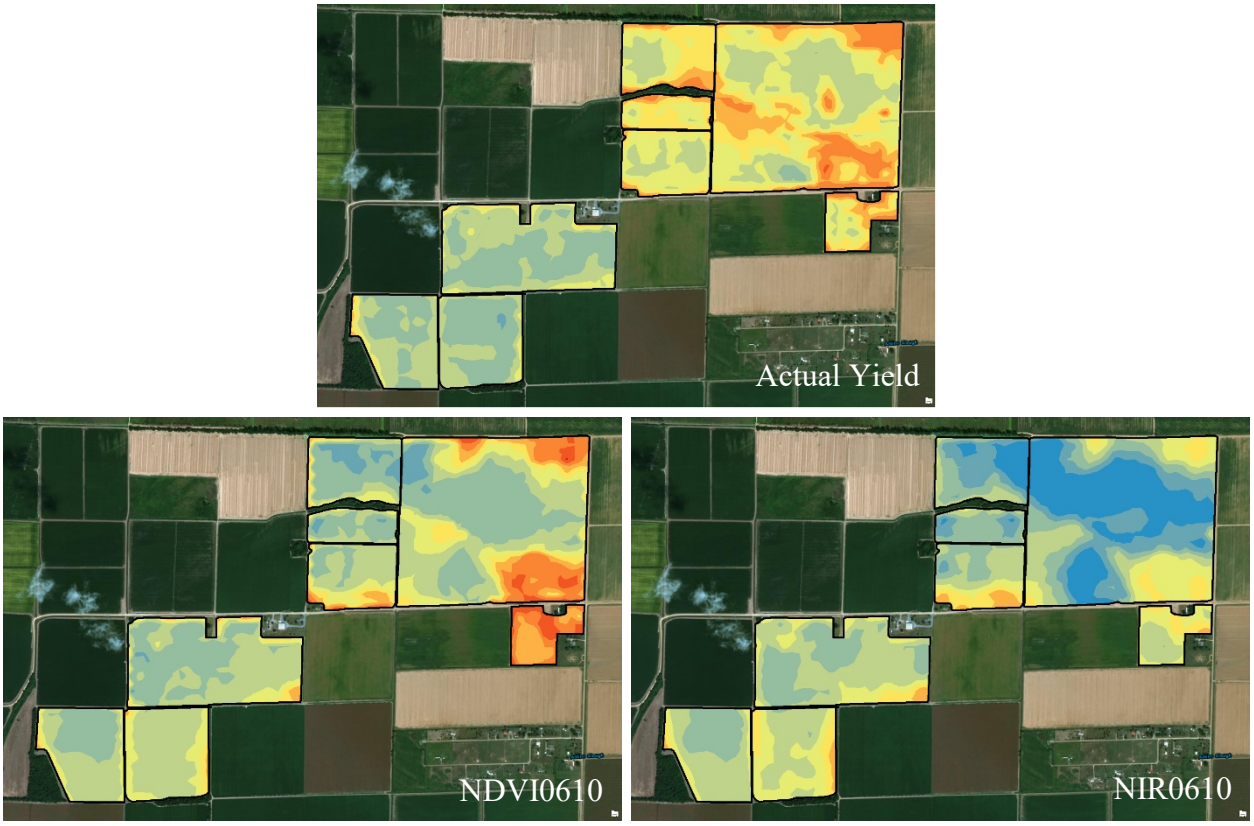

Figure 17. Interpolation of predicted yield using satellite normalized difference vegetation index (NDVI0610) and near infrared (NIR0610) images on 10 June 2017 of Glendon 4 showed a significant correlation between the actual and predicted yield.

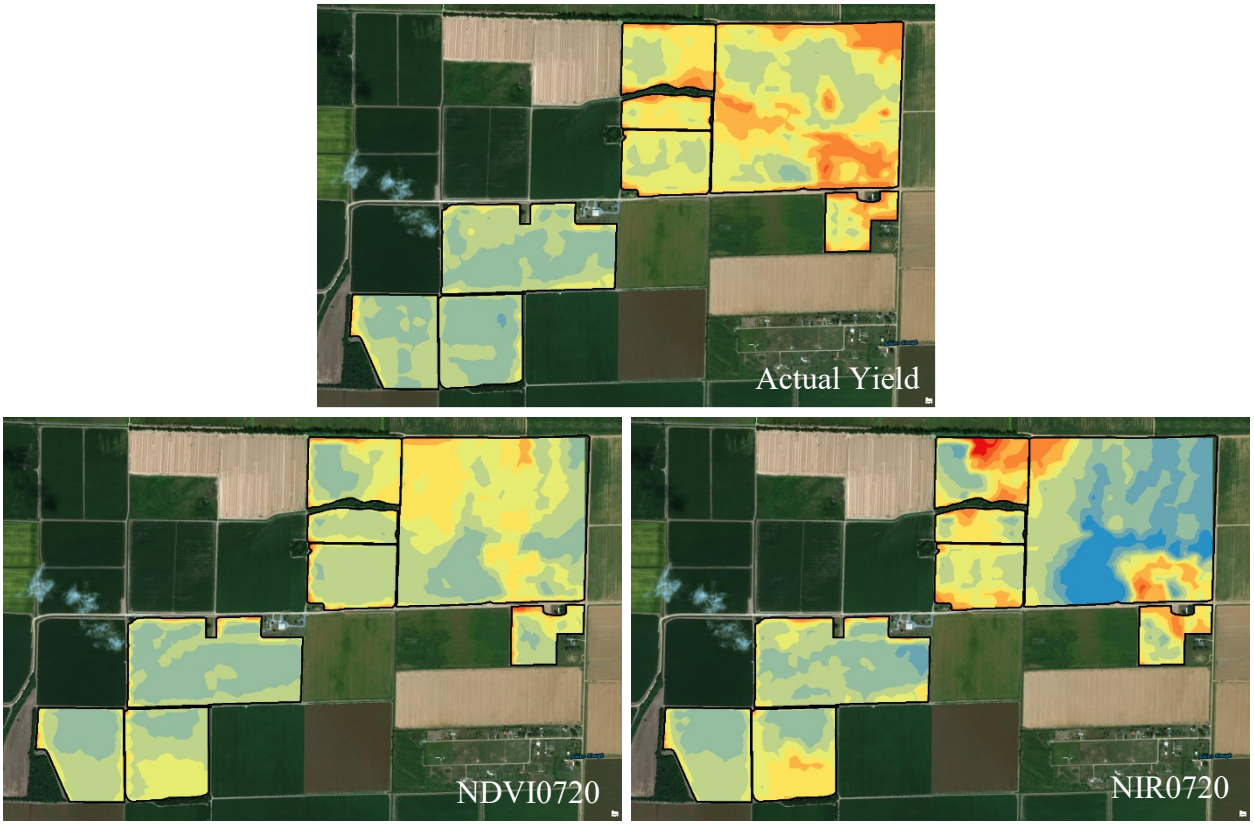

Figure 18. Interpolation of predicted yield using satellite normalized difference vegetation index (NDVI0720) and near infrared (NIR0720) images on 20 July 2017 of Glendon 4 showed a significant correlation between the actual and predicted yield.

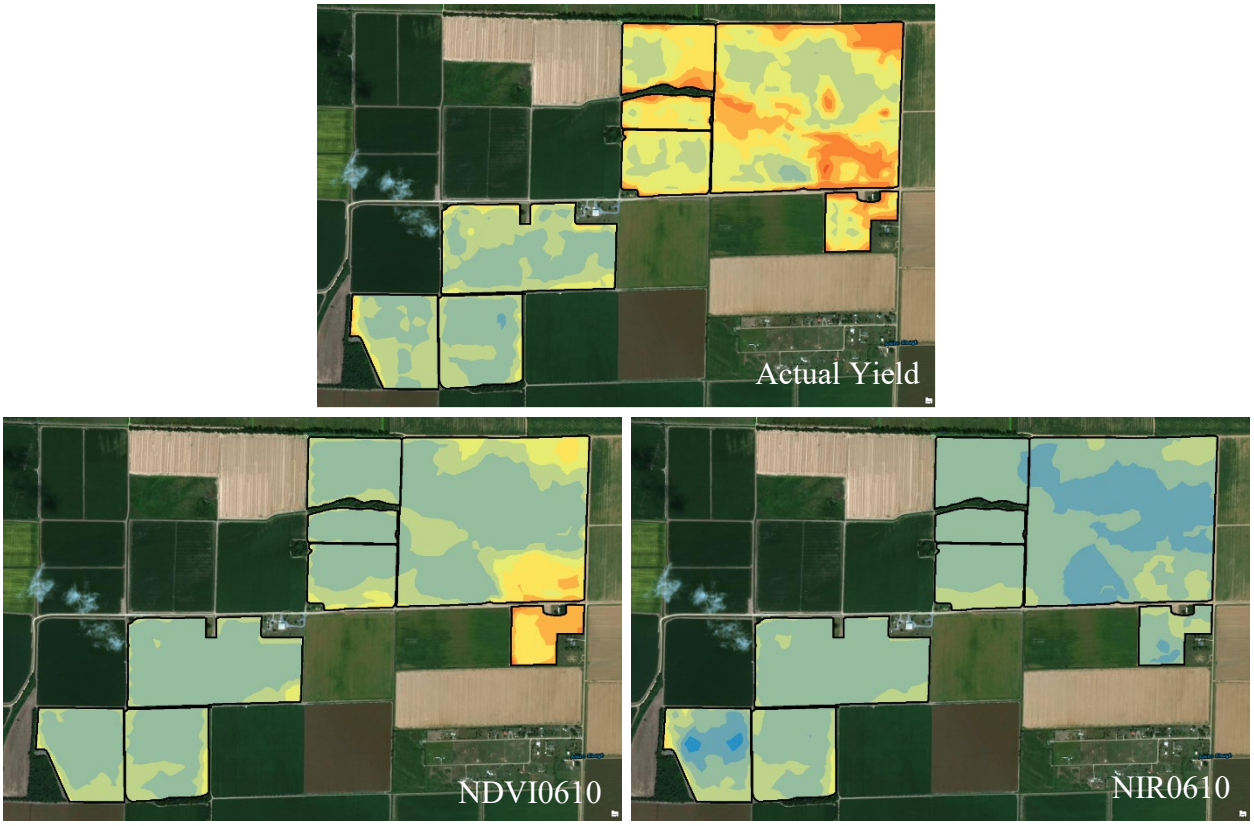

Figure 19. Interpolation of predicted yield using satellite normalized difference vegetation index (NDVI0610) and near infrared (NIR0610) images on 10 June 2017 of Glendon 5 showed a significant correlation between the actual and predicted yield Glendon.

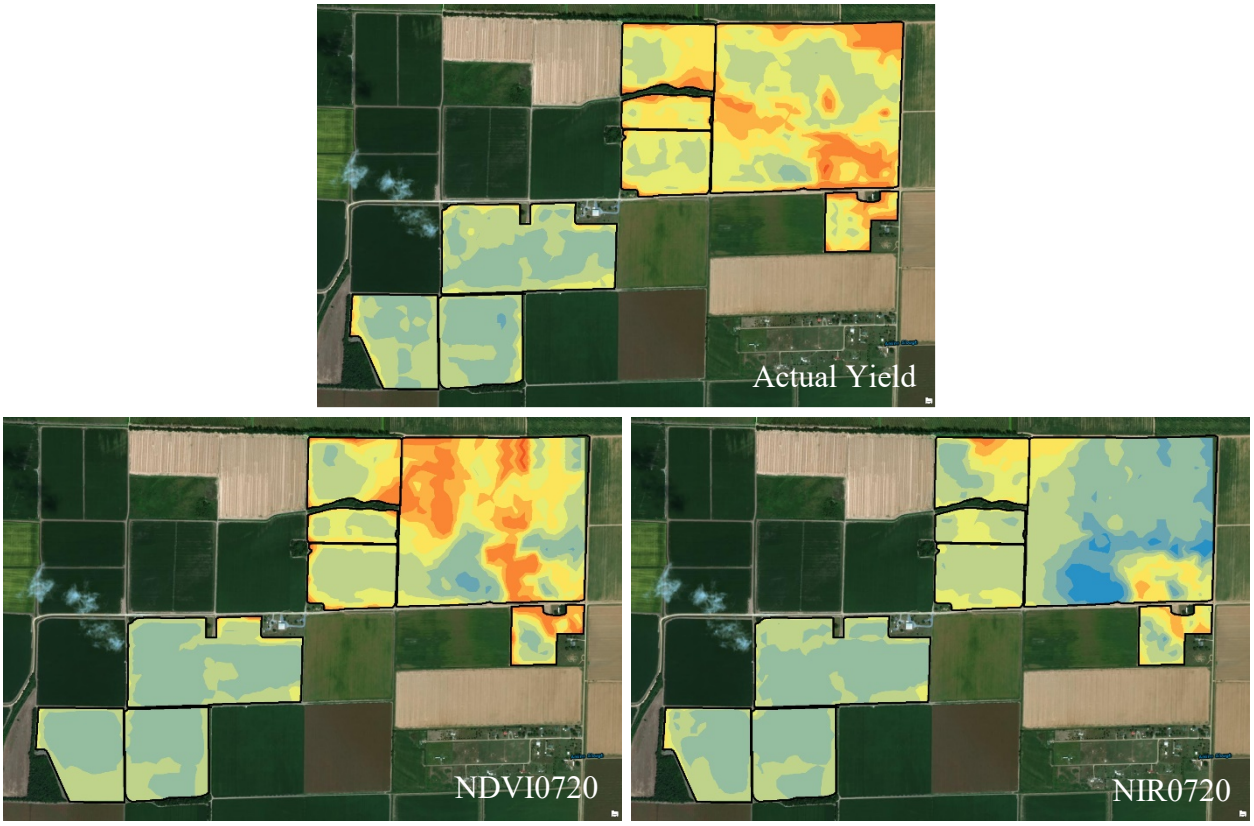

Figure 20. Interpolation of predicted yield using satellite normalized difference vegetation index (NDVI0720) and near infrared (NIR0720) images on 20 July 2017 of Glendon 5 showed a significant correlation between the actual and predicted yield.

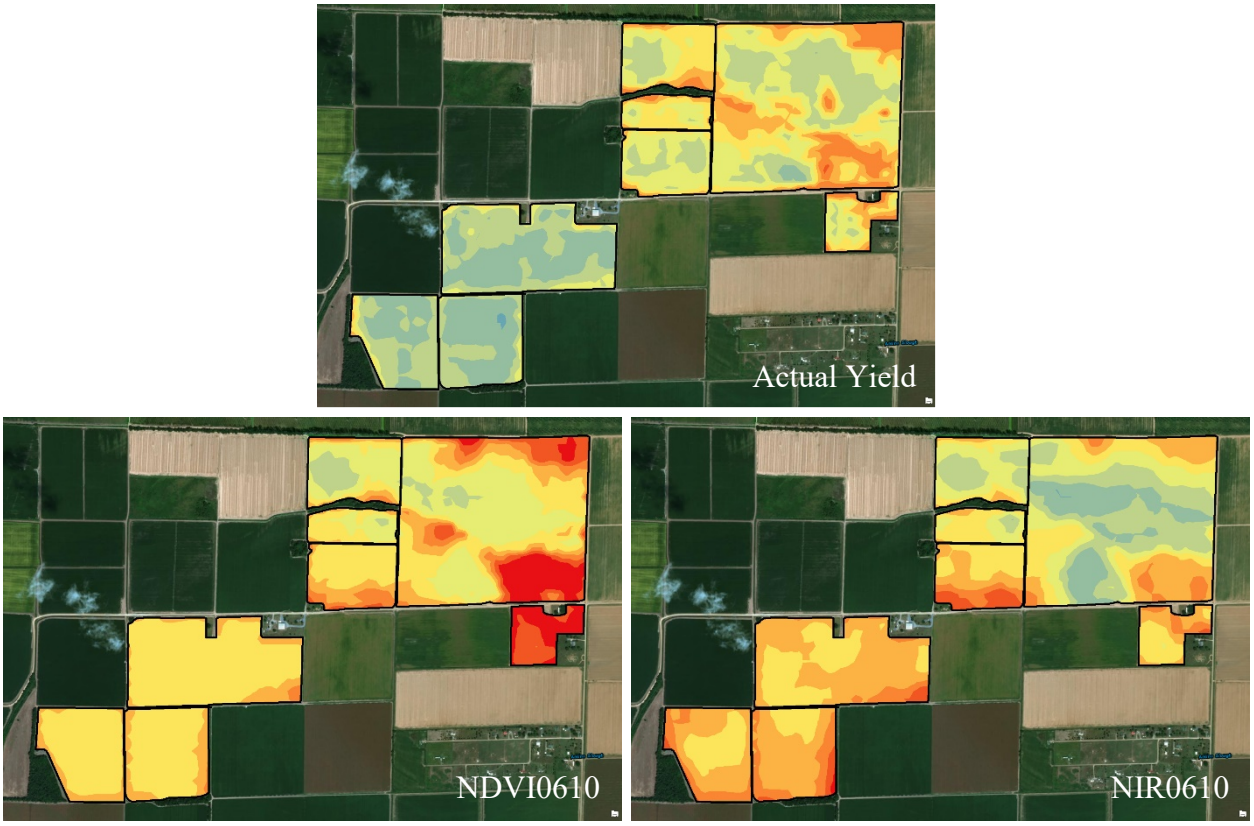

Figure 21. Interpolation of predicted yield using satellite normalized difference vegetation index (NDVI0610) and near infrared (NIR0610) images on 10 June 2017 of Robert 1 showed a significant correlation between the actual and predicted yield.

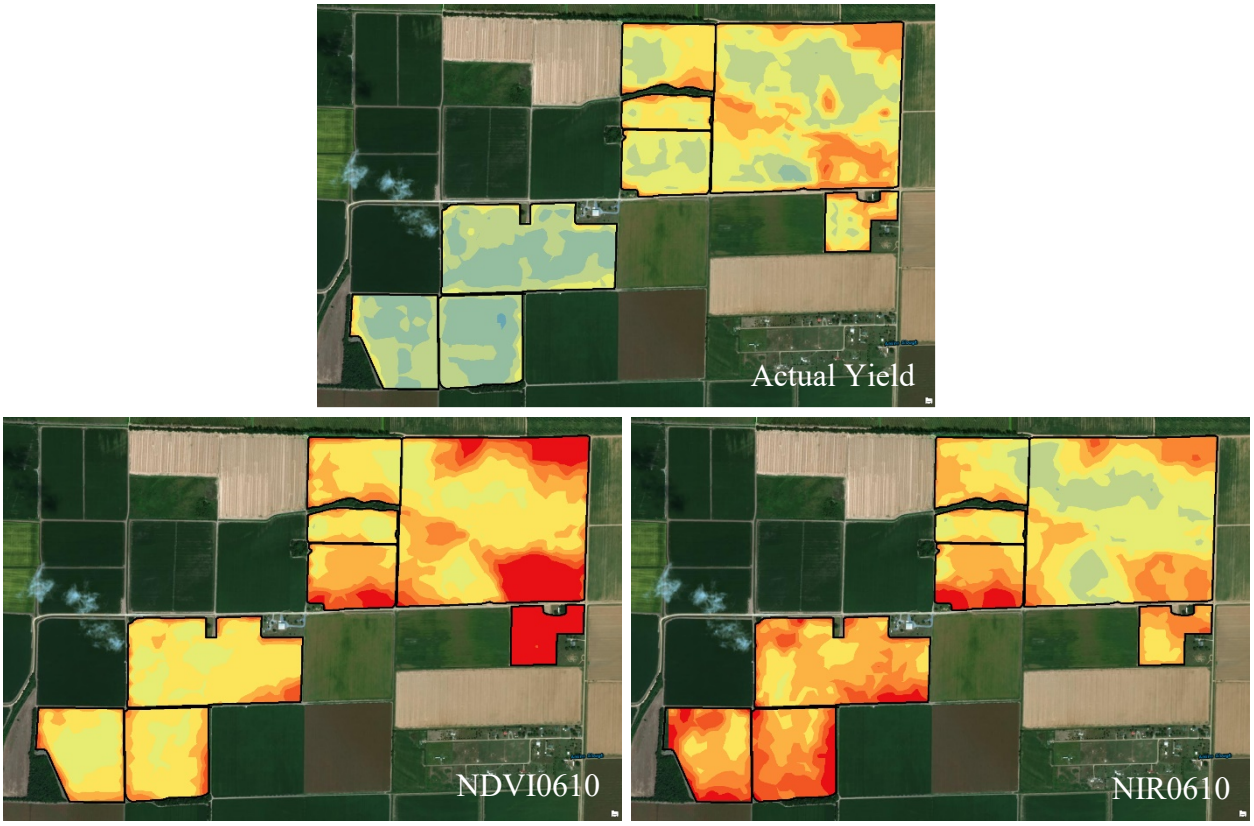

Figure 22. Interpolation of predicted yield using satellite normalized difference vegetation index (NDVI0610) and near infrared (NIR0610) images on 10 June 2017 of Robert 2 showed a significant correlation between the actual and predicted yield.

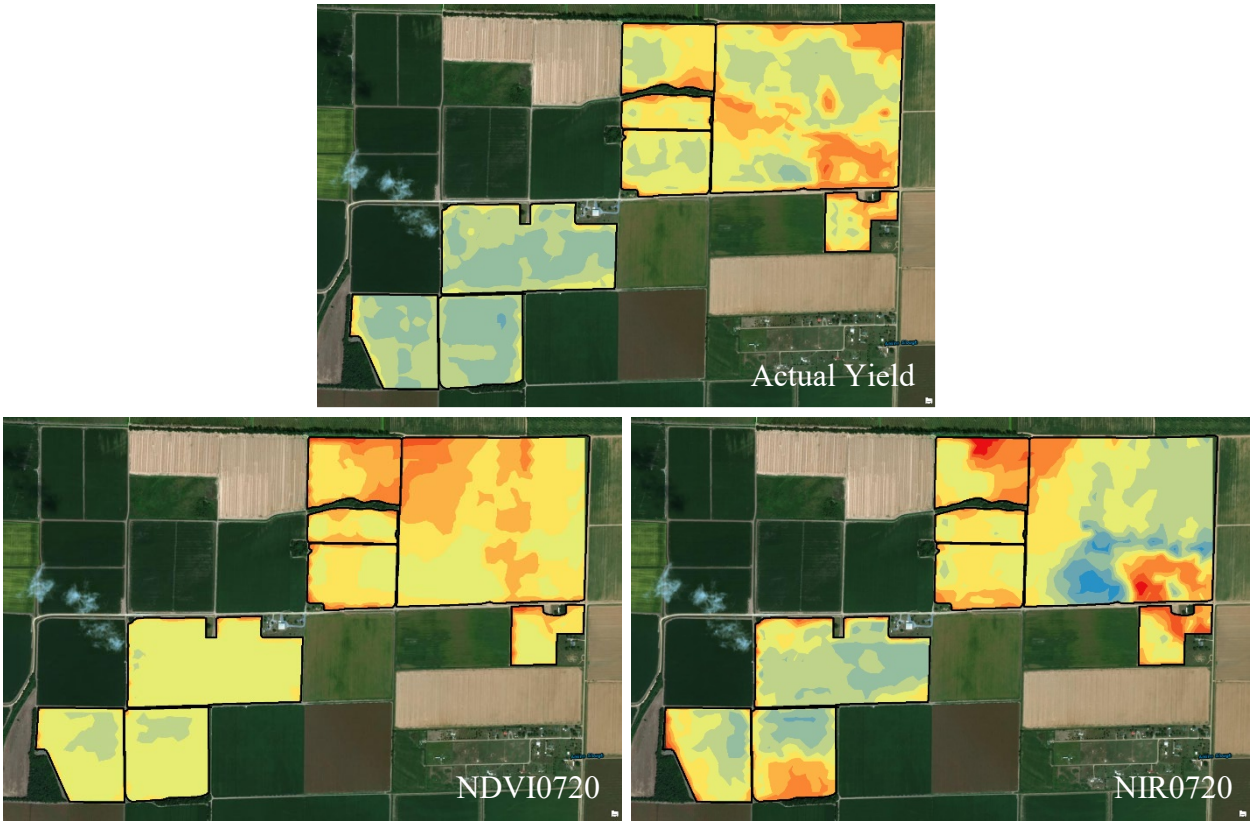

Figure 23. Interpolation of predicted yield using satellite normalized difference vegetation index (NDVI0720) and near infrared (NIR0720) images on 20 July 2017 of Robert 2 showed a significant correlation between the actual and predicted yield.

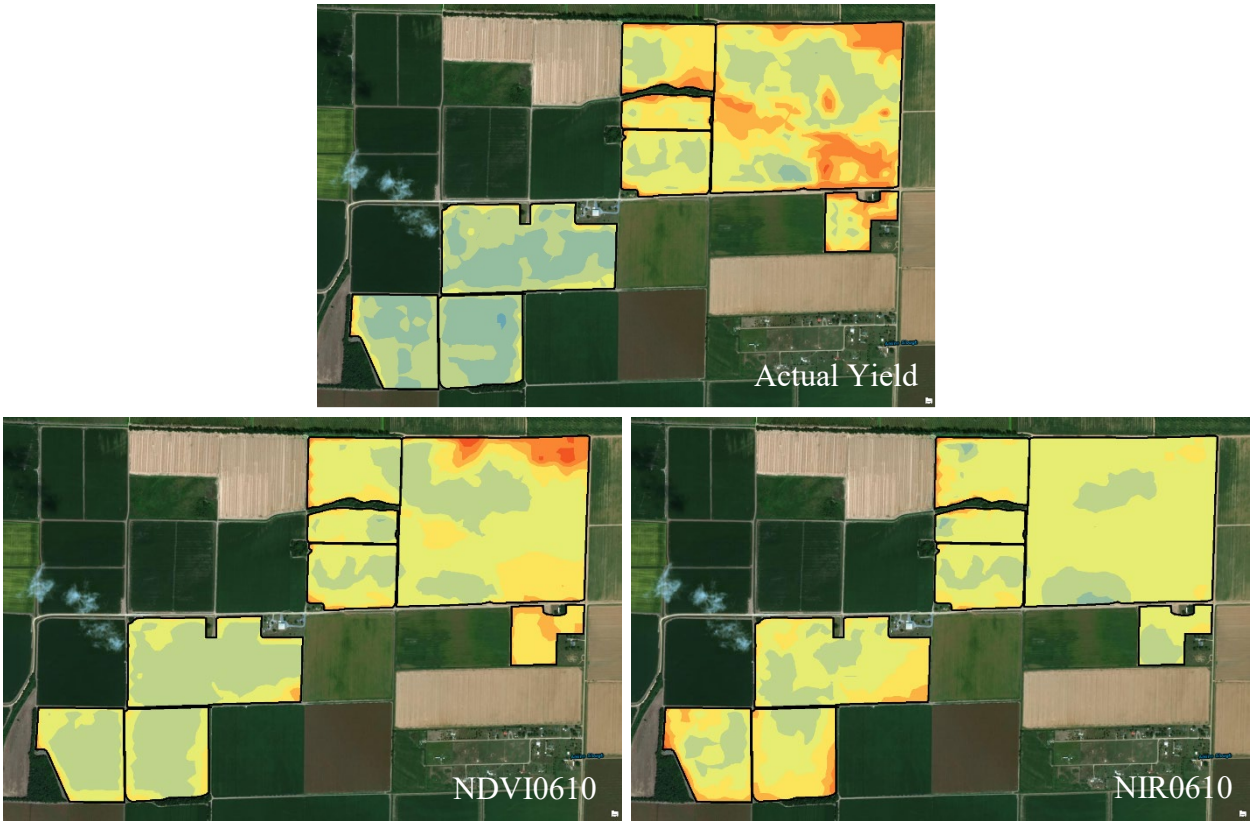

Figure 24. Interpolation of predicted yield using satellite normalized difference vegetation index (NDVI0610) and near infrared (NIR0610) images on 10 June 2017 of Robert 3 showed a significant correlation between the actual and predicted yield.

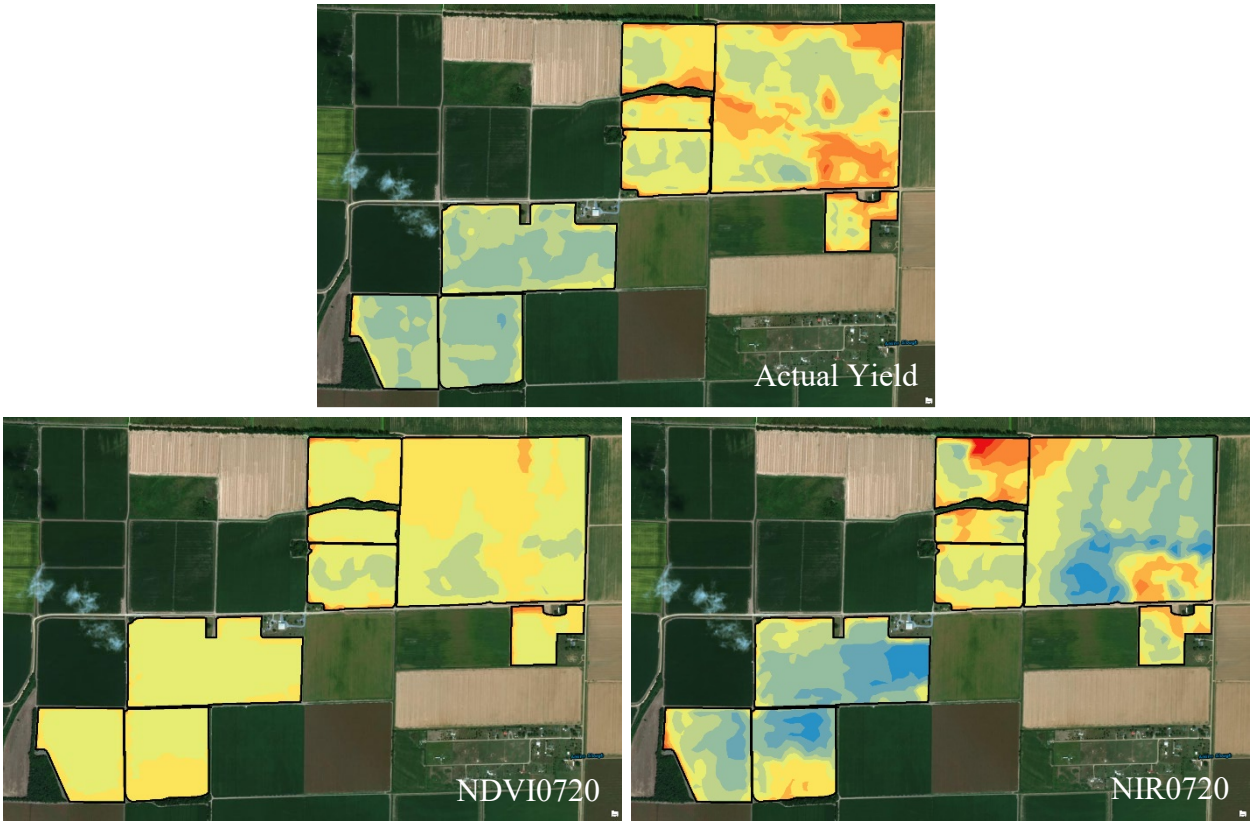

Figure 25. Interpolation of predicted yield using satellite normalized difference vegetation index (NDVI0720) and near infrared (NIR0720) images on 20 July 2017 of Robert 3 showed a significant correlation between the actual and predicted yield.

Conclusion

Site-specific management of *Meloidogyne incognita* using management zones and predicting crop damage areas using EC may offer grower and environmental, as well as economic, benefits when compared to field-wide 1,3-D fumigation applications. *Meloidogyne incognita* management strategies are limited for crop protection. Therefore, site-specific management strategies may be crucial for sustained and profitable soybean production in the Mid-South. With the average size of farms growing in the United states, field sampling may not adequately characterize spatial distributions of *M. incognita* in individual fields, because sampling can be labor-intensive and (or) cost-prohibitive. Accurate spatial and temporal detection of *M. incognita* can be questionable with classical sampling methods, while soil textural variability within fields can be estimated relatively accurately and easily by calculating EC with soil mapping equipment. The use of EC mapping technologies to predict soil texture variability within fields has been suggested to be an effective management tool for nematodes in cotton in the Mid-South. The use of EC values to establish management zones does not eliminate the need for understanding the spatial and temporal distribution of *M. incognita*. The use of verification strips should be an essential component in understanding the intensity of damage and should be extensively used by growers during each growing season to improve the efficiency of their pesticide program. Spatial data equipment, such as that of the Veris EC Mapping sensors, can be combined with aerial imagery, in relation to crop health, to allow growers to implement better management decisions. By utilizing this technology along with other spatial data layers, such as yield and aerial imagery, growers can make more economical and efficient management decisions.

Yield prediction from early or even mid-season parameters can help assist growers in making informed decisions regarding marketing, storage and transportation. Furthermore, creating

a yield prediction model based on historical data would help growers make future production decisions based on commodity prices and profitability. With the growing need of site-specific farm management, adequate understanding and interpretation of spatial analysis reports and production recommendations are crucial. Agronomists must be able to combine data from different sources, using different sample designs.

Precision agriculture can generate a tremendous amount of data, and each practice can have thousands of associated data points with many different properties for each one. Manipulating and analysis of this huge quantity of data requires the use of complex software and high computation power. Most often synthesis and analysis of this data are beyond the capabilities of most farmers, consultants, and retail agriculture professionals. In addition, outputs from many applications may not be universally compatible due to software proprietary concerns, making it impossible to exchange data. Because the concepts and technology that are associated with precision agriculture are relatively recent developments, not enough data has been collected to determine exactly what the results mean in certain scenarios.

The Food and Agriculture Organization predicts there will be 9.6 billion people in the world by the year 2050, which means food production needs to increase 70% despite the limited availability of arable land. To resolve the issue of future food demands, current production systems need to dramatically increase yields per hectare. Computer software will soon be able to create and perform management decisions based on field performance with little to no human intervention. However, this technological based farming will generate a tremendous amount of data. Often data management is complex, and each aspect will create thousands of data points that could include many different properties for each one. This huge amount of data requires the use of complex software and great computational power to manipulate and analyze the data. Further, the

outputs from specific software are likely not to be compatible with other software. The incompatibleness makes it impossible to exchange and share data, which makes the process even that much more complicated. Because of the complexity, the adoption of precision agriculture and site-specific management will be reliant on technologically trained agronomists and more data collection to determine its true value.